A Tissue-Engineered Blood Vessel Model for Vascular Aging

by

Ellen Elizabeth Salmon

Department of Biomedical Engineering
Duke University

Date:_____

Approved:

_____
George A. Truskey, Advisor

_____
Brenton Hoffman

_____
Joel Collier

_____
Christopher Kontos

_____
Thomas Povsic

Dissertation submitted in partial fulfillment of
the requirements for the degree of Doctor
of Philosophy in the Department of
Biomedical Engineering in the Graduate School
of Duke University

2021

ABSTRACT

A Tissue-Engineered Blood Vessel Model for Vascular Aging

by

Ellen Elizabeth Salmon

Department of Biomedical Engineering
Duke University

Date:_____
Approved:

_____
George A. Truskey, Advisor

_____
Brenton Hoffman

_____
Joel Collier

_____
Christopher Kontos

_____
Thomas Povsic

An abstract of a dissertation submitted in partial
fulfillment of the requirements for the degree
of Doctor of Philosophy in the Department of
Biomedical Engineering in the Graduate School of
Duke University

2021

Abstract

Clinical studies have identified a strong correlation between aging and the development of atherosclerosis. In particular, endothelial cell senescence, a state of dysfunction characterized by the inability of cells to replicate, is implicated in age-related changes in vasoreactivity. Oxidative stress is considered the primary source of endothelial cell (EC) senescence *in vivo*. EC senescence leads to abnormal proliferation of vascular smooth muscle cells, reduced vasoreactivity, enhanced vascular permeability, and greater adhesion of circulating monocytes and lipids. Endothelial senescence often occurs coincident with an inflammatory response within the endothelium. By specifically targeting endothelial cell senescence, we hope to develop a more robust *in vitro* model fo r atherosclerosis capable of modeling clinically observed changes in vasoreactivity and responding to drugs that specifically target senescence. Senolytics and senomorphics, drugs which specifically reduce the viability of and inflammation in senescent cells, are a rapidly growing class of drugs. Developing *in vitro* models of senescent tissues to evaluate their safety and efficacy would be advantageous for future preclinical trials and the development of novel drugs targeting senescence.

The Truskey lab developed tissue-engineered blood vessels (TEBVs) which recapitulate the structure and function of an arteriole or small artery *in vitro*. These vessels can be fabricated within a few hours, perfused immediately after fabrication, and

reach functional maturity after a week. Measurements of endothelium-mediated vascular function confirm the presence of a healthy endothelium in the vessels for several weeks after initial fabrication. This *in vitro* system allows more precise control over the cellular and structural components of blood vessels than is possible with *in vivo* experiments. Ultimately, the development of a more robust *in vitro* model for atherosclerosis will provide a platform for the evaluation of new drugs during preclinical trials. In this work, our goal was to determine the conditions under which TEBVs are suitable for such a model in three specific aims. After characterizing induction of senescence and inflammation after exposure to oxidative stress, TEBVs were exposed to lipids and monocytes to evaluate the degree to which senescence increased the initiation of atherosclerotic lesions within the intima. After identifying the conditions under which significant senescence and atherogenesis in the TEBVs, they will also be exposed to drugs targeting senescence to confirm that application of drugs can be used to reduce senescence and atherogenesis within the vessels.

In Specific Aim 1, I evaluated the functional effects of stress-induced senescence on TEBVs. Stress-induced senescence was induced *in vitro* by treatment with 100 μM hydrogen peroxide (H_2O_2). 2-D Cord-blood derived endothelial colony forming cells (CBECFCs), human neonatal dermal fibroblasts (hNDFs), and TEBVs were treated for 5 or 7 days with 100 μM H_2O_2 to model chronic oxidative stress. H_2O_2 treatment significantly increased senescence, measured by quantifying p21 positive nuclei, and

reduced NOS3 expression in CBECFCs. Although H_2O_2 treatment induced senescence in both the ECs and hNDFs, the functional effects on the vasculature were endothelium specific. Expression of VCAM-1 increased in the ECs and endothelium-dependent vasodilation in TEBVs was reduced. Vasoconstriction and endothelium-independent vasoreactivity were preserved in hNDFs. The results suggest that vascular cell senescence first leads to endothelial dysfunction.

In Specific Aim 2, I evaluated the capacity of stress-induced senescence to increase monocyte adhesion and foam cell formation in the TEBVs. Stress-induced senescence was generated by application of 100 μM H_2O_2 for 5 days. To develop an atherogenesis model, low density lipoprotein was enzymatically modified into a more inflammatory state which is often identified within atherosclerotic lesions. Introducing 50 μg/mL enzyme-modified low-density lipoprotein (eLDL) for the final 24 hours of 7 day 100 μM H_2O_2 treatment on 2-D CBECFCs further increased endothelial cell activation. There was a significant increase in the percentage of ICAM-1 positive cells when eLDL was applied to endothelial cells alongside H_2O_2 compared to H_2O_2 alone. Expression of VCAM-1 and E-Selectin, already significantly increased by 100 μM H_2O_2 was not further increased by co-treatment with 50 μg/mL eLDL. hNDFs absorbed and retained eLDL, even without H_2O_2 in the growth media. When TEBVs were exposed to a combination of eLDL, H_2O_2, and fluorescently-labeled U937 monocytes, endothelium-dependent vasoreactivity was significantly compromised. Lipid retention within the

stress-induced senescence in TEBVs increased VCAM-1, and E-selectin which produced increased adhesion of circulating monocytes and foam cell formation in the monocytes and medial hNDFs.

In Specific Aim 3, I built upon this senescence model to evaluate the drug-responsiveness of the senescent TEBVs when exposed to drugs that target senescence specifically, and quantified the resulting effects on vasoreactivity, monocyte adhesion, and foam cell formation. Development of a physiologically relevant model for vascular senescence can provide a valuable tool for evaluating the efficacy of drugs targeting atherosclerosis, particularly a new class of drugs in development called senolytics. Senolytics, and their sister drugs senomorphics, specifically target senescent cells and transiently disable the anti-apoptotic pathways that prolong their lives, reducing the burden of senescent cells within the tissue. Senomorphics target factors within the senescence-associated secretory pathway (SASP) to reduce cytokine production and inflammation. Dasatinib and quercetin, two senolytics, and tacrolimus, a senomorphic, were tested on CBECFCs growing in 2-D to see if they were effective at reducing the percentage of p21 positive (senescent) cells. Of the three drugs tested, tacrolimus was found to produce the most significant effect on both senescence and inflammation within the CBECFCs and used in TEBV trials. TEBVs treated with 10 nM tacrolimus for 48 hours after induction of senescence recovered significantly more endothelium-dependent vasoreactivity compared to vessels left to recover from H_2O_2 in normal

growth media without tacrolimus. Additionally, addition of 10 nM tacrolimus for the duration of hydrogen peroxide treatment significantly reduced adhesion of monocytes and foam cell formation compared to vessels without tacrolimus.

In summary, the work presented here demonstrates that a TEBV model of vascular senescence can be generated in under two weeks using near-physiological levels of hydrogen peroxide. This model can model atherogenesis by adding only eLDL and monocytes. We were also able to effectively use the senomorphic tacrolimus to mitigate the effects of senescence on monocyte adhesion and lipid uptake. This system could be used to investigate other senolytics or test the efficacy and toxicity of novel drugs still in development.

Dedication

This is dedicated to my son, Noah Salmon. In your eyes, I could do anything, and so I did.

Contents

List of Tables

List of Figures

Acknowledgements

I want to extend my sincere thanks to my first and best supporters, my family. My mother, Lenora Branham, and my father, Kevin Weburg, raised me to reach for the stars. They encouraged me to reach my full potential, even if that meant reaching for new and unfamiliar dreams. Their unwavering support of my journey helped me persevere when it would have been so easy to fall short.

To my husband, Matthew Salmon, I am forever grateful. The sacrifices he made to support me and our son Noah during my time at Duke made this dream possible. Thank you for lifting me up when I was weary, making sure I always had snacks while writing, and defending my accomplishments to those who felt I was doing "too much".

To Dr. Truskey, my thesis advisor, I offer sincere thanks for six and a half years of excellent mentorship. You helped me tackle new problems, pushed me as a scientist, and equipped me with the resources to succeed. I was especially lucky to have an advisor who allowed me to take two internships and ensured that I had access to every possible resource as a student mother. Dr. Truskey has been an excellent example of scientific integrity, a source of creativity, and an example of how to lead in the field with compassion and grace. I only hope that I can serve those under my care as well in my own career.

I extend sincere thanks to my entire thesis committee as well. Thank you for challenging me to deeply understand the science I study and contribute meaningfully to

new understanding. Your advice has strengthened not only this work, but my hunger for greater understanding and my ability to understand and solve complex scientific problems. In particular, I am grateful to Dr. Brenton Hoffman and Dr. Joel Collier for being truly excellent teachers and for allowing me, so many times, to show up unannounced at their office to discuss technical issues and new ideas for my research.

I also want to acknowledge the wonderful members of the Truskey lab, past and present, who have trained me, encouraged me, and continued this work after me. In particular, I want to thank Tracy Daubert, Brittany Davis, Cristina Fernandez, and Leigh Atchison for helping me learn key techniques and making the Truskey lab feel like home to a brand new graduate student. Catherine Oliver, you were the best office-mate I could have asked for. I want to thank Nadia Abutaleb, Anandita Ananthakumar, Ellery Jones, Xu Zhang, Qiao Zhang, Muath Bishawi, and Kevin Shores for advising me on experiments and making the lab a warm and inviting place to work. To my former and current undergraduate students, Akhil Bedapudi, Hannah Vaughan, Martha Davis, and Brad Foster, thank you for your hard work. It was a joy and a privilege to watch you develop your skills as scientists and move on to exciting things in your careers.

Finally, I want to thank all of the administrators, sanitation workers, healthcare workers, and graduate school officials who went to extraordinary lengths to ensure that Duke University could remain open during the COVID-19 pandemic. I would not have been able to complete this work without their heroic efforts to ensure our safety.

1. Introduction

1.1. Motivation and Significance

New strides in three-dimensional *in vitro* cell culture have given rise to human microphysiological systems (MPS), miniaturized tissues, usually containing multiple cell types, which better mimic the structure, cell composition, intercellular interactions, and function of native tissue. If human MPS are to make significant impact on the development of novel therapeutics, they must model both healthy and diseased states. MPS models exist for several diseases including inflammatory bowel disease, certain cancers, and even rare genetic diseases like Hutchinson-Gilford Progeria Syndrome[1,2].

Here, we focus on the use of a Tissue Engineered Blood Vessel (TEBV) model for cardiovascular disease. Cardiovascular diseases are the leading cause of death in the world and represent a significant area of pharmacological intervention and development[3]. Vascular pathologies manifest acutely, as ischemia, heart attacks, strokes, aneurysms[3], but they seldom arise spontaneously. Chronic inflammation, vascular stiffening, and other age-related phenomena contribute to dysfunction in the endothelium, leaving regions of the vasculature primed for disease. Endothelial cell (EC) senescence triggered by oxidative stress contributes to vascular dysfunction and sensitivity to atherogenic stimuli[4]. Endothelial cell permeability and inflammatory activation increase with senescence, resulting in greater retention of circulating lipids and monocytes, the initiation of atherosclerosis[5]. Furthermore, senescent cells are

identified within atherosclerotic lesions[5]. By specifically inducing senescence within a TEBV system, the atherogenic potential of the model is increased. Furthermore, the relevance of senescence as a therapeutic target can be better evaluated in such a model.

A TEBV model for cardiovascular disease captures key features of the most prevalent chronic health condition in the United States[6]. As such, a human MPS representative of cardiovascular disease can be used to study a large number of drugs currently available and in development. Given its prevalence, cardiovascular disease, many patients experience cardiovascular disease alongside other pathologies. A cardiovascular disease MPS can be created in series with other disease models to more fully replicate the pathology of patients living with multiple conditions. These multi-disease systems could be used to both confirm that treatments for other diseases do not exacerbate cardiovascular disease and also identify treatments with dual efficacy.

1.2. Atherosclerosis

Cardiovascular disease can lead to heart attack and stroke, killing roughly 17 million people worldwide[3]. The pathology of atherosclerosis is marked by the development of lipid-laden regions within the vasculature[7,8]. These lesions develop within the layers of vascular smooth muscle cells (vSMCs), just below the endothelial cells (ECs) lining the vessel interior. The cholesterol component within high density lipoprotein (HDL), apolipoprotein A-I (apoA-I) is atheroprotective and promotes cholesterol efflux[9,10]. Only in cases where the serum concentration of HDL is many times

normal or intracellular modification of the protein occurs does it have a deleterious effect.

Non-high density lipoproteins (nHDL), including very low, low, and intermediate density lipoproteins (vLDL, LDL, and iLDL respectively) are of particular import in the development of atherosclerotic plaques[11]. Esterase-modified LDL species contain apolipoprotein B-100 (apoB-100), the ligand responsible for receptor-mediated LDL uptake[12,13]. Within endothelial cells or the vascular intima, LDL is easily converted into a potent atherogenic molecule when modified into oxidized LDL (oxLDL) or enzyme-modified LDL (eLDL)[14]. *In vitro*, oxidation of LDL occurs when it is exposed to copper or other metal ions, though oxLDL is found in plaques more abundantly in the later stages of atherosclerosis than in early plaques[15]. Local free radicals generated by plasma or intracellular H_2O_2, NADPH oxidases, or inducible nitric oxide synthase (iNOS) overexpression can also oxidize LDL[16]. oxLDL is known to activate an inflammatory response in the endothelium, increasing expression of VCAM-1, ICAM-1, and E-Selectin. It prompts vascular smooth muscle cells (vSMCs) to transition from a quiescent, contractile state to a proliferative state wherein they deposit excess collagen and fibronectin that lend structure and stability to growing atherosclerotic plaques[17,12,18].

When early atherosclerotic lesions were excised and analyzed, eLDL was the primary lipid present within the lesions[9,19]. Enzyme-modification of LDL also transforms it into a potent inflammatory stimulus[20,21]. Hydrolysis by cholesterol esterases increases

retention of the eLDL within vSMCs and monocytes[16]. Unlike oxLDL, eLDL contributes to foam cell formation in both vSMCs and monocytes[22]. eLDL passes through, rather than resides in, endothelial cells, but it's presence within the vessel media and nearby foam cells evokes a strong inflammatory response, increasing cytokine secretion and presentation of leukocyte-adhesion molecules on the cell membrane[23]. eLDL increases expression of VCAM-1 and other immune cell adhesion molecules to a greater degree than oxLDL[16]. The increase in adhesion molecule expression results in greater monocyte recruitment to the site. Once they have migrated into the vessel media, they consume the trapped eLDL and become foam cells, unable to return to circulation[24,25].

As these lesions grow in size, the vessel lumen is partially occluded, reducing blood flow overall[26]. The core of this plaque may become necrotic, as nutrients are unable to fully penetrate the mass of lipids, foam cells, and ECM proteins[27]. These apoptotic and pre-apoptotic cells excrete inflammatory cytokines into the local environment. In many cases, the danger of a growing atherosclerotic lesion is not the occlusion of the vessel directly. Rather, it is the destabilization of the endothelial layer which can expose the thrombogenic material underneath leading to a clot *in situ* or one which detaches from the vessel wall and occlude blood flow to vital areas downstream[7,8].

Dyslipidemia is a crucial factor in the development of atherosclerosis, but it is by no means the only one. Atherosclerosis preferentially localizes to arterial bifurcations or

turns in the vasculature[28,29]. The low, oscillating shear stresses found here reduce endothelial nitric oxide synthase expression and thereby limiting endothelium-dependent vasoreactivity in the region[30]. These shear profiles can also increase apoptosis and can results in extracellular matrix remodeling that directly stimulates increased NF-κB expression, p21 expression, and can even cause apoptosis[30].Expression of adhesion molecules like ICAM-1 is also increased in areas of low and reversing shear stress[31,32]. These regions are more prone to oxidative stress and monocyte adhesion even absent elevated eLDL or oxLDL levels[33].

Inflammatory stimuli also cause vascular cells to release increased amounts of cytokines like TNF-α, IL-1, and IL-6[34,35]. Sufficiently high, sustained concentrations of TNF-α can cause senescence outright as well[36]. Inflammatory cytokines stimulate the NF-κB pathway which elevates the amount of membrane adhesion proteins, like VCAM-1 and ICAM-1, on the surface of the endothelium[35]. Adhesion molecule overexpression facilitates adhesion of circulating inflammatory cells and lipoproteins, directly contributing to the risk of vascular diseases like atherosclerosis[37,38]. The increased adhesion molecule expression caused by inflammation is referred to as endothelial "activation". Although usually helpful in eliminating pre-cancerous cells, the increased recruitment of monocytes to the vessel wall, particularly when coincident with hyperlipidemia, exacerbates atherogenic phenotypes and contributes to foam cell formation[39,25].

1.2.1. Endothelial Cell Senescence and Atherosclerosis

Senescence refers to a phenotype adopted by cells when their proliferative capacity has been exhausted due to either repeated cell division (replicative senescence) or telomere damage and oxidative stress (stress-induced senescence)[40]. The relative contribution of replicative senescence and stress-induced senescence to the overall population of senescent cells within the endothelium is unclear, but stress-induced senescence is most heavily implicated with atherosclerosis given the highly oxidative and genotoxic environment created[41,42]. Both senescent vSMCs and ECs were identified within excised atherosclerotic lesions, but the bulk of senescent cells were located on or near the vessel lumen[5].

Compared to healthy endothelial cells, senescent endothelial cells have a larger area and more permeable cellular membrane. Furthermore, and the mechanosensitive membrane complexes which govern endothelial cell response to shear stress are less prevalent, reducing endothelial cell shear responsiveness[40,43]. Senescent ECs have lower levels of endothelial nitric oxide synthase (eNOS) activity and greater cytosolic nitric oxide (NO) degradation[34,44]. Clinical data shows aging individuals exhibit decreased vasodilation in response to acetylcholine, which acts by stimulating a burst of nitric oxide production within endothelial cells that subsequently relaxes the smooth muscle cells[45]. In the light of *in vitro* data showing that NO production is reduced in senescent ECs, this clinical data suggests that an increase in endothelial cell senescence with

patient age can be estimated with minimally-invasive evaluations of vasoreactivity. Meanwhile vasodilation in response to papaverine, which relaxes vascular SMCs directly, was not significantly affected by patient age[45]. The maintenance of endothelium-dependent function and age-dependent loss of endothelium-dependent function further confirms the theory that the increase risk for and development of atherosclerosis is primarily mediated by the endothelium, rather than by vascular smooth muscle cells.

Vascular smooth muscle cells are more proliferative in NO-deprived environments and may invade areas of EC injury, further impairing normal vessel function[46]. Oxidative stressors also damage synthesized NO, converting it to a form which compromises endothelial nitric oxide synthase (eNOS) activity rather than NO, further depleting the intracellular NO supply[44]. Additionally, oxidative stress response proteins, like oxidases, exhibit age-dependent decreases in function. Although some cell replication occurs at sites of vascular injury or angiogenesis, there is minimal EC turnover in intact vasculature. Studies have identified increased p21 expression in vascular endothelial cells in the veins of older adults compared to younger individuals[47]. These studies did not specifically identify a source of senescence, but the most probable cause of this increased senescence is oxidative stress rather than cell replication. A reduction in senescence is also associated with improved function[47].

Cellular senescence can be measured by nuclear p21 staining. P21 is a cyclin-dependent kinase inhibitor that regulates cell cycle progression (Figure 1). It is a downstream effector of p53 activated in response to DNA damage, making it an ideal marker for evaluating cellular senescence. High levels of p21 cause the arrest of cellular replication. It has been used to quantify senescence *in vitro*, as well as in tissue sections[48].

Functional changes due to endothelial cell senescence are closely related to the development of atherosclerosis[47]. Increased production of inducible nitric oxide synthase (iNOS) contributes to an oxidative environment within the endothelium. The senescence-associated secretory phenotype (SASP) contributes significantly to the risk of atherosclerosis in regions of endothelial cell senescence[49,50]. Increasing senescence results in greater expression of p21 and downstream p65. Higher p65 levels decrease SIRT1 expression and increases NF-κB acetylation, increasing its binding efficiency as a promoter for IL-6 and IL-8[51,52]. The increase in production of IL-6, IL-8, and MCP-1, increases the expression of immune cell adhesion molecules like VCAM-1 and ICAM-1[41,53].

1.2.2. Senolytics & Geroprotective Therapies

Senolytics are a class of drugs which encourage apoptosis in senescent cells, which are normally protected by senescent cell antiapoptotic pathways (SCAPs, Figure 1). Some, like navitoclax, inhibit BCL-2 family proteins[54]. Inhibition or post-translational modification of BCL-2 increases apoptosis[55]. Dasatinib and Quercetin act upstream of

BCL-2, targeting PI3K directly[56] PI3K is responsible for Akt phosphorylation, increasing Akt activity and prolonging cell lifespan[57]. Dasatinib can also block ephrin receptor tyrosine kinase activity directly, mitigating the anti-apoptotic effects of receptor-ligand interactions[58]. Others, like resveratrol, inhibit NF-κB activity[59]. NF-κB has anti-apoptotic Still others direclty inhibit the activity of cell cycle arrest proteins like p21, allowing tradiitonal apoptotic machinery to proceed[60].

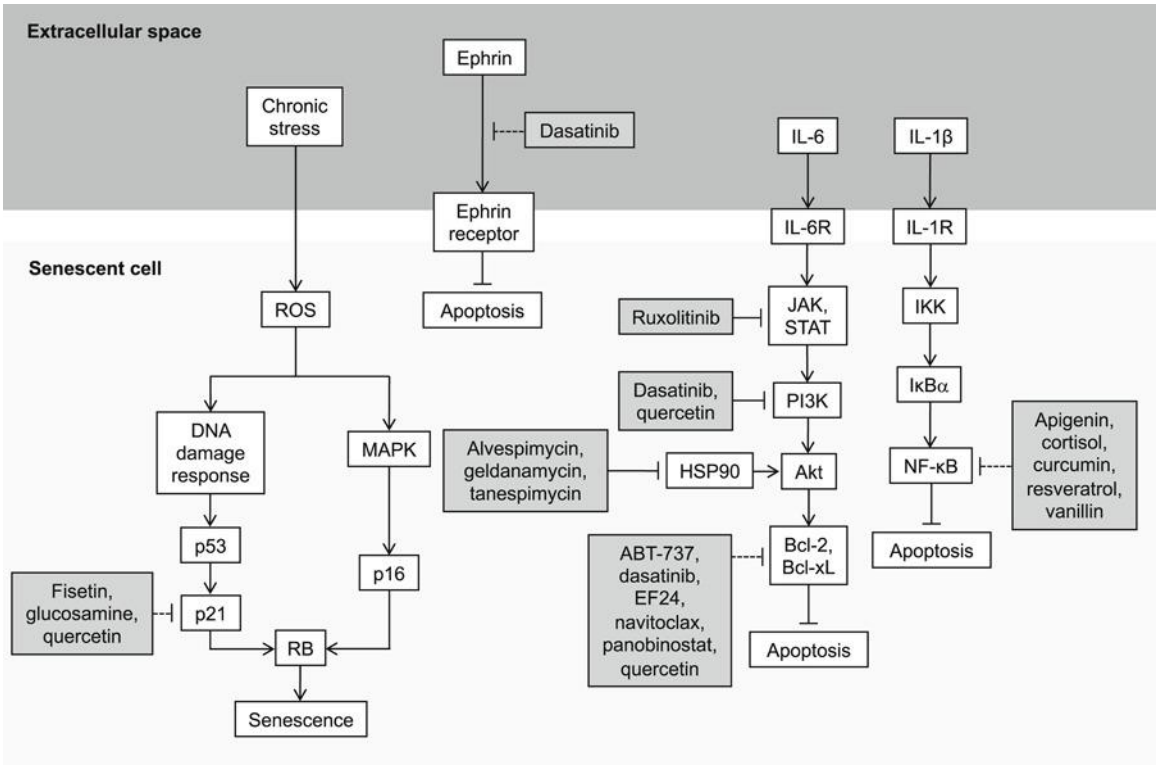

Figure 1: Senolytic Drugs Reduce the Accumulation of Cell Cycle Arrest Drugs and Inhibit Anti-Apoptotic Pathways to Reduce the Biological Burden of Senescent Cells

Adapted from Goy et al.[151]

Senomorphics target the SASP and other senescence-associated cellular pathologies without causing cell lysis. They are often broadly classed as immunosuppressive therapeutics which preferentially target the inflammatory

molecules activated by the SASP[50]. In this work we specifically focus on the senomorphic tacrolimus, which binds to FK-binding proteins to inhibit cacineurin-induced NF-κB activity[61]. Tacrolimus is also an inhibitor of the mTOR pathway, and in certain cell types is a more potent promoter of apoptosis than everolimus and other rapamycin analogs[62,63]

While these drugs represent an exciting advance, they may be difficult to apply broadly as the effect of a single drug may vary significantly by cell type. For example, tacrolimus broadly inhibits inflammation and promotes regrowth of healthy vascular endothelial and smooth muscle cells after damage[64], but can induce problematic degrees of apoptosis in brain and kidney cells[65]. Dasatinib and quercetin have different efficacy in different tissues, leading to them often being introduced simultaneously as a cocktail. For example, quercetin is minimally effective in adipocytes and dasatinib does not target senescent endothelial cells, although they target similar cellular mechanisms[56]. To reach the maximum number of cells, these can be administered as a cocktail.

Patients with atherosclerosis stand to benefit greatly from the administration of senolytics and other geroprotective therapies. Senescent cells, both vSMCs and ECs, have been found within atherosclerotic lesions. Preclinical trials in mice have found that removal of senescence cells with senolytics like navitoclax decreases plaque formation[66], reduces expression of inflammatory factors by suppressing the SASP, and stabilizes existing plaques[27]. They represent over a dozen ongoing clinical trials[67]. As new

senolytics are identified, the mechanisms by which they exert their geroprotective effects continue to grow.

1.3. Vascular Structure and Function

Blood vessels range in size and composition in proportion to their role in the vasculature. Large arteries, carrying blood at high velocity and pressure away from the heart, have thick walls consisting of many layers of smooth muscle cells supported by collagen, fibrin, and elastin. The elasticity of large arteries allows them to accommodate the highly pulsatile flow of blood near the heart and smooth blood flow as it transitions to the smaller vessels. Large arteries have a unique outer layer called the adventitia which contains a layer of extracellular matrix and fibroblasts that provide structural support for the vessel[17]. The adventitia also contains a network of capillaries and lymphatic vessels called the *vaso vasorum* which provides oxygen, nutrients, and fluid drainage for the arterial wall. Arterioles are thinner than arteries and lack some of their elasticity, serving as the primary regulators of blood flow in the body. They act as gateways to organs and groups of muscles, dilating or constricting to control blood pressure and flow to downstream tissues, muscle, and organ systems[17]. Capillaries are the smallest vessels, consisting of only a layer of endothelial cells supported by pericytes. The venous analogues to these vessels, venules, and veins, which return blood

flow to the heart, are similar in structure. However, veins have comparatively fewer layers of vascular smooth muscle cells for the same vessel diameter.

Blood vessels are composed of three distinct layers (Figure 2). The intima consists of a confluent monolayer of endothelial cells (ECs) called the endothelium, which regulate solute and fluid transport across the vessel wall and regulate the behavior of the surrounding smooth muscle cells (SMCs)[17]. The medial layer contains vascular SMCs embedded in a matrix of collagen, glycosaminoglycans, and a small amount of elastin. The media is the primary determinant of the overall mechanical properties of the vascular wall[68–70]. The outer layer, or adventitia, is found only in large and medium-sized arteries. It consists of mainly of collagen-family proteins and fibroblasts that provide structural support for the vessel[17]. In the largest vessels, the adventitia also contains its own capillary network, the vaso vasorum, which provides nutrients and oxygen to the outer layers of the vessel wall.

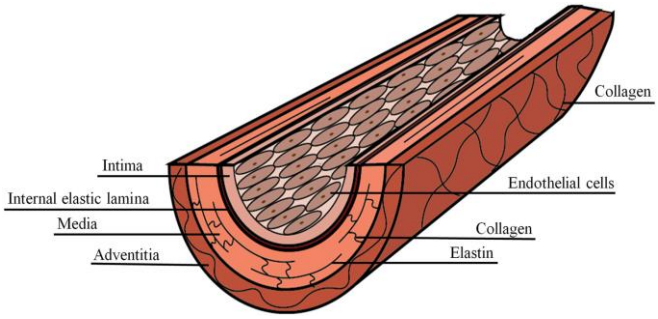

Figure 2. The Composite Structure of an Artery.

Arteries consist of three distinct layers, the adventitia, media, and intima. In arterioles, only the media and intima are present.

1.2.3. Vascular Smooth Muscle Cells

Vascular smooth muscle cells (vSMCs) are the predominant cell type within the walls of the vasculature. They align circumferentially in layers around the endothelial lumen. vSMCs are extremely responsive to external stimuli. Chronic stimuli produce epigenetic changes, as when prolonged exposure to NF-κB causes the cells to transition from a quiescent to proliferative state[71]. vSMCs are also able to rapidly respond to acute stimuli. This is critical to their role in regulating vessel diameter to direct blood flow to the appropriate organ systems in accordance with metabolic needs[71]. These signals can be the result of circulating factors conducted through the vessel wall, secreted factors from neighboring nerve or endothelial cells, or mechanical cues from blood pressure and strain on the vessel ECM proteins.

VSMCs ensure the vessel wall is structurally sound by depositing and organizing ECM proteins. When this fails due to injury or age, vSMCs can produce excess transglutaminase leading to calcification and vascular stiffening[72]. Excess matrix metalloproteinase production can hasten the degradation of elastin in the vessel wall, further stiffening the vessel wall. Dysfunctional vSMCs can also deposit fibronectin into the medial layer of the vessel, further contributing to inflammation in the vasculature[46].

1.2.4. Endothelial Cells

Endothelial cells form a confluent monolayer supported by a basement membrane on the lumen of all blood vessels[73]. In normal blood flow conditions, endothelial cells

preferentially align in the direction of blood flow and maintain vessel patency through secretion of anti-thrombogenic factors[74]. Abnormalities in paracrine signaling between ECs and SMCs can lead to hyper-proliferation of vascular SMCs[6]. More proliferative vascular smooth muscle cells deposit excess collagen and fibronectin causing arterial stiffening[10].

One of the most important EC-derived regulatory molecules is nitric oxide (NO), a soluble gas. NO causes vasodilation, inhibits smooth muscle cell proliferation, and limits platelet adhesion[76]. NO-mediated vasodilation after exposure to acetylcholine is used clinically as measure of vascular health[77]. Additional factors, like platelet derived growth factor (PDGF), limit the proliferation of vascular smooth muscle cells[78–80]. In instances of endothelial injury, production of PDGF will increase, leading to pathological smooth muscle cell proliferation[78] and, ultimately, arterial stiffening.

Arteries stiffen with both age and disease[81]. Vascular stiffening can occur through increased collagen deposition, collagen glycation, and deposition of stiffer ECM proteins like fibronectin[68,82]. This indirectly damages the vasculature by limiting availability of NO[18], leading to an increase in reactive oxygen species and NF-κB levels, as well as greater endothelial permeability[19]. The increase in substrate stiffness can also directly contribute to senescence of the endothelium[85].

1.4. Human Microphysiological Systems for Disease Modeling and Drug Development

The development of new drugs requires a significant investment of time and money, requiring an average of 10 years and over $2 billion from initial discovery to final clinical approval[86]. As many as 80% of drugs fail in stage I and II clinical trials due to lack of efficacy or unexpected toxicity, despite excellent performance in preclinical trials[87]. Identifying cytotoxic or ineffective drugs before costly clinical trials begin, streamlines the drug development pipeline and reduces the overall cost of bringing new treatments to market. Ultimately more funding can be allocated to the development of effective drugs and discovery of new therapeutic targets, as well as passing on potential savings to patients[88].

Two-dimensional monoculture *in vitro* models can be useful for identifying new drug candidates or therapeutically relevant biologics. However, these cells can have vastly different behavior than cells in a physiological environment. For example, many key functions of endothelial cells are activated by physiological shear stresses not present in static monocultures[89]. Human microphysiological systems (MPS) represent an exciting step forward in improving the fidelity of *in vitro* cultures to the native biology while maintaining some of the tunability and cost-effectiveness of standard *in vitro* cultures.

Disruption of proper vascular function, particularly in the endothelium, threatens homeostasis of the body as a whole. The vascular system is regularly exposed

to agents, like reactive oxygen species, which impair normal EC function and lead to senescent phenotypes. The resulting EC dysfunction increases sensitivity to stimuli implicated in vascular pathogenesis, specifically atherosclerosis. The development of a senescent TEBV model ***directly addresses the inadequacy of current in vitro models*** for studying the effects of stress-induced EC senescence on the circulatory system by ***developing a physiologically relevant in vitro model*** on which ***functional tests*** can be performed. It also offers significantly more precise control over the condition of the cells, i.e. the severity and mechanisms of EC senescence, than *in vivo* models.

The importance of endothelial cell function in atherogenesis is increasingly recognized. Endothelial cell senescence, and the resulting permeability are recognized risk factors. However, other aspects of the role of endothelial cell senescence are poorly understood. For example, fibronectin deposits are found in areas of hypertension and inflammation. Yet it is unclear if this is a result of inflammation and deposited by the nearby cells, or if this deposition is caused by an external stimulus. Clarifying these mechanisms will help identify the most fruitful therapeutic targets for drug development. The results of these experiments will provide greater mechanistic insight into the functional effects of EC senescence. The disease models developed can be used to investigate the mechanisms by which existing treatments work, as well as aid in the development of new treatments. These models can also be incorporated into the

"human-on-a-chip" project being developed, and aid in larger efforts to improve understanding of the physiological response to drugs, toxins, or other stimuli.

The system developed here, and similar systems, may have much to contribute to the development of new drugs. However, there are several improvements that need to be made to the systems to meet the necessary requirements to serve as tools for preclinical trials or use in personalized medicine. Currently these systems are very low throughput compared to animal trials used in preclinical studies. Currently, many are made with primary cells from individual donors, but either commercially available cell line, or a diverse library of primary cells would be necessary to ensure a robust number of cells in order to scale up simultaneous production of vessels. The number of simultaneous vessels that can be fabricated and maintained by an individual scientist are much lower than in animal studies of a similar nature with the protocols described herein. Further improvements to increase the statistical power and number of independent TEBVs and flow circuits that can be fabricated and maintained by a single analyst simultaneously. These methods will also have to pass necessary validation requirements to show that the results of the *in vitro* studies conducted have relevance to actual patient performance. This requires more robust vessel acceptance criteria comparing baseline vasoreactivity *in vitro* to vasoreactivity in young, healthy adults *in vivo*, as well as comparisons for individuals who are older and/or living with atherosclerosis. Clearly elucidating these parameters will provide more clarity in

determining the efficacy of new drugs in development or the optimal drug regimen for a particular patient.

1.5. Hypothesis and Specific Aims

The overall goal of this work was to develop a tissue-engineered blood vessel (TEBV) model for vascular aging. A TEBV model for vascular aging permits the study of the relative contributions of senescent endothelial cells and vSMC or contractile cells to vascular dysfunction. Furthermore, this model may be used to test the toxicity, dosing, and efficacy of drugs targeting atherosclerosis or senescence. By inducing senescence in the system, rather than applying supra-physiolgoical levels of pro-inflammatory stimuli, we hope to maximize the clinical relevance of our atherogenesis model. We hypothesized that a TEBV could be exposed to senescence-inducing stimuli and thereby sensitized to pro-atherogenic stimuli and used to evaluate the efficacy of senolytic and geroprotective drugs. This hypothesis was tested through the following aims:

Specific Aim 1: Evaluate the functional effects of stress-induced senescence on TEBVs. In this aim, we optimized the use of hydrogen peroxide to induce senescence and inflammation on TEBVs and the endothelium in particular. Initially, we explored the effects of H_2O_2 treatment on cord blood-derived endothelial colony forming cells (CBECFCs) in static culture. Different concentrations of H_2O_2 and durations of exposure were tested to determine the minimum concentration and exposure times necessary to induce a significant amount of senescence in the cells. Once identified these conditions

were also applied to human neonatal dermal fibroblasts (hNDFs), which induced senescence without affecting expression of contractile proteins. We then applied these conditions to TEBVs after their initial 7-day maturation period and the establishment of baseline vasoreactivity. We confirmed the H_2O_2 treatment affected vasoreactivity, and induced senescence and inflammation in the TEBVs. qRT-PCR was used to confirm that changes in gene expression matched the observed changes in vasoreactivity and inflammatory protein expression.

Specific Aim 2: Evaluate the capacity of stress-induced senescence to increase the monocyte adhesion and foam cell formation in the TEBVs. In this aim we focused on building on the first aim to develop a TEBV model for early-stage atherosclerosis relying on vascular aging to prime the system to lipid uptake and monocyte adhesion. Prior work has shown that monocyte adhesion could be prompted in healthy TEBVs with the addition of eLDL. In these studies a burst of TNF-α was used to further increase the degree of monocyte adhesion[90]. Instead, we focused on the use of stress-induced senescence in the TEBVs to induce senescence in the TEBVs rather than inflammation induced by low doses of TNF-α. Initial experiments were performed to confirm that continued exposure to both eLDL and H_2O_2 at the necessary concentrations did not reduce cell viability. Co-treatment with eLDL and H_2O_2 had no impact on endothelial cell senescence beyond what was caused by H_2O_2 alone. This co-treatment did increase overall endothelial cell activation, as measured by expression of the inflammatory

proteins VCAM-1, ICAM-1, and E-Selectin, compared to H_2O_2 alone. The effects on TEBVs were also evaluated by characterizing vasoreactivity before and after treatment, and quantifying senescence and activation within the vessel endothelium. The presence of lipids and monocytes within the vessel were also quantified.

Specific Aim 3: Evaluate the drug-responsiveness of the TEBV senescence model and the ability of geroprotective agents to reduce senescence-induced vascular dysfunction, monocyte adhesion, and foam cell formation. This aim focused on evaluating the drug-responsiveness of the model and testing the capacity of geroprotective therapeutics to reduce monocyte adhesion and foam cell formation. First, a number of senolytic and geroprotective therapeutics were identified that have had success in clinical trials or in the clinic. We tested three of these, tacrolimus, quercetin, and dasatinib, on CBECFCs in static culture at a wide range of concentrations and dosing regimens. Treating the cells prior to H_2O_2 exposure or introducing drug treatment alongside H_2O_2 produced inconsistent degrees of senescence and inflammation. However, adding these drugs, especially tacrolimus, briefly after the removal of H_2O_2 significantly reduced senescence in the CBECFCs. When applied to TEBVs after H_2O_2 treatment, endothelium-dependent vasoreactivity experienced almost complete recovery in only 48 hours, while spontaneous recovery of endothelium-dependent vasoreactivity was almost non-existent. Monocyte adhesion was reduced somewhat when tacrolimus was added alongside H_2O_2. However, tacrolimus had a

more pronounced effect on the reduction in foam cell formation, significantly reducing the amount of eLDL retained by hNDFs and monocytes within the TEBVs.

2. A Tissue Engineered Blood Vessel Model for Stress-Induced Endothelial Cell Senescence

Text and figures presented in this chapter have been previously published in the following form: Salmon, E. E., Breithaupt, J. J. & Truskey, G. A. Application of Oxidative Stress to a Tissue-Engineered Vascular Aging Model Induces Endothelial Cell Senescence and Activation. *Cells* **9**, (2020).[91]

2.1. Introduction

Complications due to cardiovascular disease increase dramatically with age[23]. In particular, a decline in the endothelium-dependent vasoreactivity occurs, even in healthy, low-risk individuals, which predisposes them to cardiovascular disease[92]. As we age vascular cells accumulate damage in a variety of ways. This damage results in cellular senescence, a phenotype in which cells that have exhausted their proliferative capacity, yet resist apoptosis[47,93]. For example, circulating lipoproteins damage and inflame the endothelium as well as accumulate within vascular smooth muscle cells. Periods of inflammation result in oxidative stress, reduced autophagy, and poor vasoreactivity[34].

Endothelial cells serve as key regulators of vessel tone and patency, blood flow, vessel permeability, immune response, and vSMC quiescence[17]. Senescent endothelial cells exhibit lower levels of endothelial nitric oxide synthase (eNOS) activity[89]. The increased presence of ROS causes significant degradation of cytosolic nitric oxide (NO)

[83,89,94]. The resulting limited NO bioavailability leads to reduced vasoreactivity and increased vSMC proliferation[76]. This contributes to clinically observed reductions in endothelium-dependent vasodilation in older individuals[45]. Additionally, endothelial cell senescence increases secretion of inflammatory signals, like TNF-α, resulting in increased NF-kB expression[39,95]. The resulting increase in expression of VCAM-1, ICAM-1, and other cellular adhesion markers facilitates the adhesion of circulating monocytes, directly contributing to the development of atherosclerosis. Furthermore, senescent endothelial cells have been identified inside atherosclerotic plaques[5].

Vascular smooth muscle cells (vSMCs), which comprise the arterial wall, are also affected by cellular senescence. Senescence-associated β-Galactosidase and p21 positive vSMCs have been identified within the intima of advanced atherosclerotic plaques[96]. The presence of senescent vSMCs also increases plaque area and the necrotic core within the vessel intima[27]. However, vSMC-dependent vasoreactivity is preserved in older patients[97]. H_2O_2 has been used in many studies to examine the effects of oxidative stress or stress-induced senescence on endothelial cells *in vitro*. In some studies, H_2O_2 is applied at a high dose, often in excess of 250 μM H_2O_2 for less than 12 hours[98]. While this significantly increased the senescence of the endothelial cells, this dose of H_2O_2 is nearly eight times the highest estimated plasma concentrations of H_2O_2[99]. Other studies have treated mouse brain microvascular endothelial cells with 50 μM H_2O_2, but a treatment

period of 10 days was necessary for any significant increase in endothelial cell senescence[100].

There are numerous models to study cardiovascular disease study ranging from *ApoE* knockout mice to microvascular endothelial networks and cell culture monolayers. While animal models are advantageous because they permit long term studies and use of clinically relevant measures to quantify outcomes, the utility of these systems to study senescence specifically is limited. *In vitro* models offer greater tunability, facilitating more precise applications of stressors to specific cell types rather than looking at systemic effects. Key aspects of endothelial cell behavior, like nitric oxide synthesis and TFG-β production are shear-mediated, limiting the utility of monolayer culture[29]. Notch and paracrine signaling between endothelial cells and vascular smooth muscle cells have potent effects on vessel behavior, necessitating a co-culture approach[101]. Tissue engineered blood vessels (TEBVs) overcome these limitations by recreating a complete blood vessel *in vitro* within an optically clear perfusion system[102]. Their functionality has been well characterized and they are responsive to treatment with TNF-α and statins[103]. They provide an ideal foundation for the development of a three-dimensional *in vitro* vascular senescence model. In this study, we developed a TEBV model of vascular senescence and examined the relative influence of endothelial cell and smooth muscle cell senescence on vasoreactivity.

2.2. Methods

2.2.1. Cell Culture

Human cord blood derived endothelial colony forming cells (CBECFCs) were isolated as previously described[104]. Isolation and culture protocols for CBECFCs were approved by the Duke University Institutional Review Board. Human umbilical cord blood samples were obtained from the Carolina Cord Blood Bank. Patient identifiers were removed prior to receipt.

After receipt, blood is diluted 1:1 with Hanks Buffered Salt Solution (HBSS, Invitrogen). The diluted blood sample is layered slowly atop an equal volume of room temperature Histopaque 1077 (Sigma) and centrifuged at 740 g for 30 minutes. Buffy coat mononuclear cells were removed and washed with Endothelial Cell Growth Medium (Cell Applications) containing 1% penicillin/streptomycin solution (Gibco). The mononuclear cells are centrifuged at 515 g for 10 minutes and resuspended in endothelial cell culture media three times and plated on TCPS six-well plates coated with 50 μg/mL rat tail collagen I. Media is changed daily for the first 7 days of culture and every 48 hours after. Colony formation is visible after 7-10 days of culture. Flow cytometry is used to confirm purity of the resulting endothelial cell population (Supplement Table 1). Cells are harvested at P4 – P6. After resuspending cell samples in 10% goat serum, 5 μL of the appropriate antibody is added to a 95 μL sample containing

500,000 cells. Cells are then fixed with 0.5% PFA, rinsed, and resuspended in DPBS. 9,000 events per sample are recorded.

Human neonatal dermal fibroblasts (hNDFs) are purchased from Lonza. They are grown in high glucose Dulbecco's modified eagle medium (Invitrogen) supplemented with 10% vol/vol heat inactivated fetal bovine serum (Gibco), 1% penicillin/streptomycin (Gibco), 1% MEM non-essential amino acids (Gibco), 1% sodium pyruvate (Gibco), 1% GlutaMAX (Gibco), and 0.1% β-Mercaptoethanol (ThermoFisher). Media is changed every 48 hours.

2.2.2. Tissue Engineered Blood Vessel (TEBV) Fabrication

Tissue engineered blood vessels (TEBVs) were made as previously described[103]. Rat tail collagen I (BD Biosciences) is diluted to a concentration of 2.05 mg/mL in 0.6% acetic acid comprising 80% of the total volume of the TEBV solution. 10X serum-free Dulbecco's Modified Eagle's Medium (DMEM, Sigma) was added to make up 10% of the total TEBV volume. The mixture is then titrated to a pH of 8.5 with 5M NaOH. A solution of hNDFs at a concentration of 5×10^6 cells/mL is added comprising the final 10% of the TEBV volume and leading to a final density of 0.5×10^6 hNDFs/mL in the TEBV. After mixing, the gel solution was poured into a 3 mL luer-lok syringe (BD Biosciences) stoppered with a closed two-way stopcock. To create a tubular collagen scaffold, an 810 μm diameter steel mandrel is inserted into the center of the syringe

mold and held in place with parafilm. The solution gels at room temperature over 30 minutes.

After gelation is complete, the gel and mandrel are removed from the syringe mold and laid on a 0.8 μm pore Nylon membrane filter (Whatman) atop 10 autoclaved Kim Wipes. The TEBV rests there for 8-10 minutes until ~90% of the water has been removed. The nylon filter and TEBV are then transferred to a 150 mm petri dish filled with sterile PBS to facilitate easier removal of the filter and lubricate the PBS for removal from the mandrel. Next, the TEBV is mounted in an acrylic chamber with hollow grips (0.711 μm outer diameter, McMaster-Carr) on each end of the vessel to allow perfusion of the vessel lumen. Black silk sutures hold the TEBV in place on the grips (Figure 3A). Next, a solution of 500,000 ECFCs suspended in endothelial cell growth media is slowly pushed through the vessel lumen. The vessel is rotated for 60 minutes at a speed of 10 rph to ensure uniform monolayer adhesion. TEBVs are perfused with TEBV growth media at a flow rate of 0.5 mL/min for the first 24 hours after fabrication, then the flow rate is increased to 2 mL/min for the remainder of the experiment (Figure 3B). This results in a laminar shear stress of 6.8 dynes/cm^{2}[103]. TEBV perfusion media contains low glucose DMEM, 1% penicillin/streptomycin, 1% MEM non-essential amino acids, 0.1%

β-Mercaptoethanol, and 3.7% heat-inactivated fetal bovine serum for the first week of culture. After one week of culture, 2mg/mL ε-aminocaproic acid was added to pres

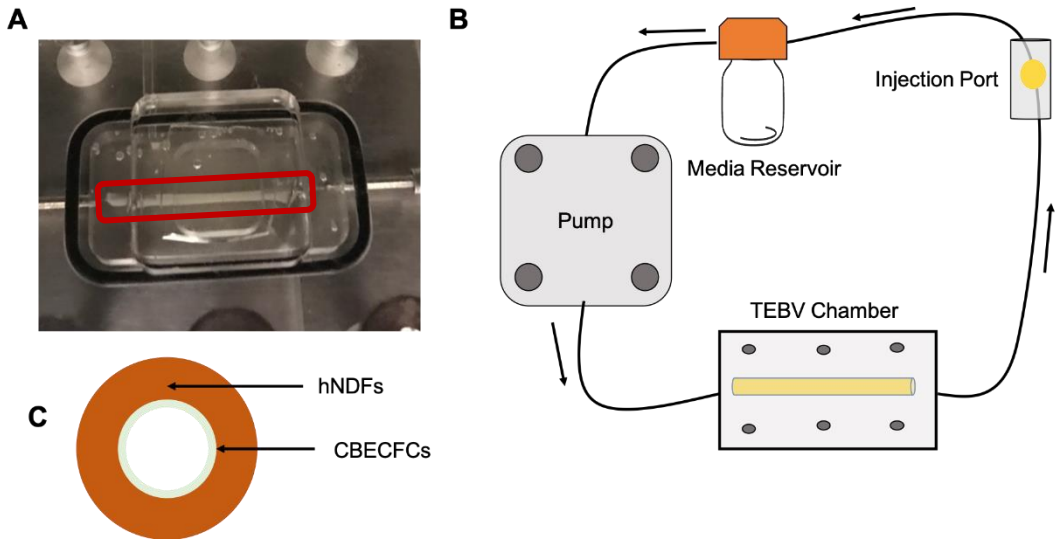

Figure 3: TEBV Perfusion System and Cell Types.

A: TEBV sutured in place within a TEBV chamber filled with optically clear cell culture media. A small black O-ring maintains a water-tight seal between the top and bottom portions of the chamber. A red box is used to identify the TEBV. B: Schematic showing the components of the TEBV perfusion circuit. Media flows out of the reservoir, through the pump and into the TEBV chamber. Injected drugs are added between the TEBV chamber and the reservoir to avoid bubbles entering the chamber and obscuring the viewing window. C: Cross-sectional representation of the cell types within the TEBV. hNDFs in a collagen matrix form the media, with an endothelial monolayer on the inner wall of the vessel.

TEBV vasoreactivity is quantified in response to phenylephrine, acetylcholine, and sodium nitroprusside. 1 mM stock solutions of each drug are prepared by diluting lyophilized powders in sterile DPBS without calcium or magnesium. This 1 mM solution is injected into the reservoir of the TEBV flow circuit via a silicone injection port

integrated into the perfusion tubing. A 1 μL/mL dilution is used, resulting in a dose of 1 μM in the flow circuit. These doses are expected to elicit about half the maximum vasodilation or vasoconstriction of the TEBVs. TEBV diameter equilibrates after introduction of phenylephrine for five minutes. Next, acetylcholine is injected, and the diameter change is quantified after five minutes. Finally, sodium nitroprusside is added to the flow circuit and the diameter change is quantified after 8 minutes. Diameter changes are recorded on video with a stereo microscope equipped with a 0.5x magnification lens using ISCapture (Meiji Technology). Still shots are selected from these videos at the time points described above (300 seconds after phenylephrine injection, 300 seconds after acetylcholine injection, and 480 seconds after sodium nitroprusside injection). The diameter at the time of phenylephrine injection is used as a baseline. The still images are quantified using the line tool in ImageJ. Five points evenly spaced along the TEBV are randomly selected to measure the diameter. The same points along the TEBV are used to measure the diameter change in response to each drug. A typical TEBV has a baseline diameter of 1500-2000 μm corresponding to about 150-250 pixels in ImageJ.

TEBV vasoreactivity is first quantified 7 days after fabrication to evaluate baseline vasoreactivity and confirm appropriate function of the TEBV. For this initial test of vasoreactivity, only phenylephrine and acetylcholine are used. If vasoconstriction and vasodilation do not exceed -1% and 1% respectively, the vessel is not used for further

study. In the data presented here, this test is called "Day 0" and further tests of vasoreactivity are described using the number of days after this initial test of vasoreactivity, rather than the total number of days since vessel fabrication. H_2O_2 is added after a vessel passes this initial test of vasoreactivity on Day 7 and vasoreactivity is measured again on Day 5 or Day 7 of H_2O_2 treatment with acetylcholine, phenylephrine, and sodium nitroprusside.

2.2.3. Hydrogen Peroxide Treatment

ECFCs or hNDFs are plated at a density of 5,300 (controls) or 7,900 cells/cm^2 (H_2O_2 treated) in 24-well plates. The lower seeding density of the control cells is necessary to reduce over-crowding of the cells within the wells due to the higher growth rate of the cells in the absence of H_2O_2. All cells are allowed 18-24 hours to firmly adhered to the plate before H_2O_2 is introduced to cell culture media. H_2O_2 is diluted from a 30% stock solution (9.77 M) to 50 or 100 μM in the appropriate cell culture growth medium. Media is changed every 48 hours until the cells are fixed on the seventh day of treatment. TNF-α is diluted from a 200 U/μL stock to 100 U/mL in the appropriate cell culture and added with media containing H_2O_2 for the final 24 hours of cell culture.

The degradation of H_2O_2 in the media was estimated using a fluorometric hydrogen peroxide assay kit (Sigma MAK165). H_2O_2 stocks were made according to assay protocols and rested in the cell culture incubator for 24 or 48 hours before analysis.

At the appropriate time point, samples are diluted along a standard curve ranging from 0.1-10 μM H_2O_2 in assay buffer. Fluorescence at 590 nm is measured using a Perkin-Elmer Victor^3 1420 Multilabel Counter. 24- and 48-hour samples were compared to freshly prepared H_2O_2 stocks.

2.2.4. Immunofluorescence

Cells in well plates are fixed with 10% formalin for 10 minutes at room temperature. Cells are permeabilized with 0.1% Triton-X and then blocked with 10% goat serum (Gibco) in DPBS. Primary antibodies for P21 and VCAM-1 (Abcam) were diluted 1:250 in 10% goat serum. Primary antibodies for E-Selectin and ICAM-1 (SCBT) were diluted 1:200 in 10% goat serum. After staining overnight at 4°C, samples were rinsed 3 times with DPBS. Goat anti-rabbit Alexa-Fluor 594 or goat anti-mouse Alexa-Fluor 488 secondary antibodies were added at a dilution of 1:500 in 1% Goat serum with 1 μL/mL Hoechst 33342 for 1 hour at room temperature. Samples were rinse an additional 3 times in DPBS and imaged immediately. 2-D samples were imaged at 20X on a Nikon Eclipse TE2000-U. TEBV sections were mounted on slides with Fluor Save, covered with a cover slip, and imaged on a Zeiss 510 inverted confocal microscope at 20X magnification.

For TUNEL staining, TEBVs were fixed on Day 14 (after 7 days of 0 or 100 μM H_2O_2) in 10% formalin and cut into 1 cm sections. Sections were embedded in O.C.T. (Tissue-Tek) and frozen at -80°C. 10 μm sections were cut using a Leica CM 1950 and

mounted on Superfrost Plus slides (VWR). After mounting, sections were permeabilized with Proteinase k and stained using an Alexa-Fluor 594 TUNEL kit (ThermoFisher). 30-minute DNase I treatment (Thermo) was administered to sections after permeabilization to provide a positive control. After TUNEL staining, sections were blocked with 3% BSA in 1X PBS. Sections were then stained for α-SMA in 10% goat serum at 4°C overnight and labeled with Alexa Fluor 488 secondary antibodies. A 1X solution of Hoechst 33342 was used to stain nuclei. Three sections from each vessel were imaged for analysis.

2.2.5. qRT-PCR

RNA was extracted from the TEBVs using an RNeasy Mini Kit (Qiagen) and a slightly modified version of the manufacturer's protocol. Briefly, TEBVs were submerged in 150 µl Buffer RLT with 10 µl/ml β-mercaptoethanol and vortexed for 2 minutes to disrupt tissue. 295 µl RNase/DNase free water and 15 µl proteinase K (Qiagen) was added and the solution was incubated at 55°C for 10 minutes. The solution was centrifuged at 10,000 × g for 3 minutes and the supernatant was used for further extraction. 225 µl of RNase/DNase free 98% ethanol was added and 700 µl of this solution was added to an RNeasy spin column. This was centrifuged at 10,000 x g for 15 seconds. The column was washed with the remaining RNeasy mini kit buffers as per manufacturer protocol and eluted in 40 µl of RNase/DNase free water. RNA purity and concentration were assessed using a NanoDrop spectrophotometer. Reverse transcription of RNA into cDNA was performed with 250 ng of TEBV RNA using the

iScript cDNA Synthesis Kit (BioRad). RT-PCR was performed using iQ SYBR Green Supermix (Bio-Rad) and the CFX96 Connect Real-Time PCR Detection System (Bio-Rad). Housekeeping gene primers were glyceraldehyde 3-phosphate dehydrogenase (GAPDH) primers (VHPS-3541, RealTime Primers). The gene of interest primers were custom made (Integrated DNA Technologies). Sequences used were eNOS (NOS3) Fwd: 5′-CATCTTCAGCCCCAAACGGA-3′ and Rev: 5′-ACGGGATTGTAGCCTGGAAC-3′, inducible nitric oxide synthase (NOS2) Fwd: 5′-CCCCCAGCCTCAAGTCTTATTTC-3′ and Rev: 5′-CAGCAGCAAGTTCCATCTTTCAC-3′, Nf-κB p65 (RELA) Fwd: 5′-AGCTCAAGATCTGCCGAGTG-3′ and Rev: 5′-ACATCAGCTTGCGAAAAGGA-3′, Sirtuin 1 (SIRT1) Fwd: 5′-TGCTGGCCTAATAGAGTGGCA-3′ and Rev: 5′-CTCAGCGCCATGGAAAATGT-3′, NOX4 Fwd: 5′-GCAGGATCCGTCATAAGTCATCCCTCAGA-3′ and Rev: 5′-GCTGTTAACGTCGACTCAGCTGAAAGACTCTTTAT-3′, von Willebrand factor (vWF) Fwd: 5′-GCAGTGGAGAACAGTGGTG-3′ and Rev: 5′-GTGGCAGCGGGCAAAC-3′, prolyl-4-hydroxylase β (P4HB) Fwd: 5′-GGACGTGGAGTCGGACTCTG-3′ and Rev: 5′-GGCTGTCTGCTCGGTGAACT-3′, fibroblast specific protein-1 (FSP-1) Fwd: 5′-GATGAGCAACTTGGACAGCAA-3′ and Rev: 5′-CTGGGCTGCTTATCTGGGAAG-3′. Fold change from reference RNA was calculated as previously described[105].

2.2.6. Statistical Analysis

Statistical analyses were performed using JMP Pro 15 (SAS Institute). One-way or two-way ANOVA with post-hoc Dunnett's test were used to compare means for all immunofluorescence quantification. A repeated measures ANOVA with post-hoc Tukey's test was used to compare means for all TEBV vasoreactivity data. P values less than 0.05 were considered significant. All data shown graphically represent mean ± SEM. N represents the number of independent experiments.

2.3. Results

2.3.1. H_2O_2 Treatment Causes Senescence and Inflammation in Cord Blood Derived Endothelial Colony Forming Cells (CBECFCs)

To examine H_2O_2 degradation in the cell culture media, 100 μM H_2O_2 was prepared in assay buffer and stored at 37°C for up to 48 hours. Results indicate that the concentration of H_2O_2 in the media degrades significantly in 48 hours (Figure 4). While these concentrations are lower than the concentration applied to the CBECFCs, we expect the relative degradation is comparable, with 20-40% of the potency of the H_2O_2 lost after 48 hours diluted in working solution, rather than the concentrated stock solution designed for long-term stability. These cyclic fluctuations in the concentration of H_2O_2 should not negate its ability to produce a significant effect on the treated cells.

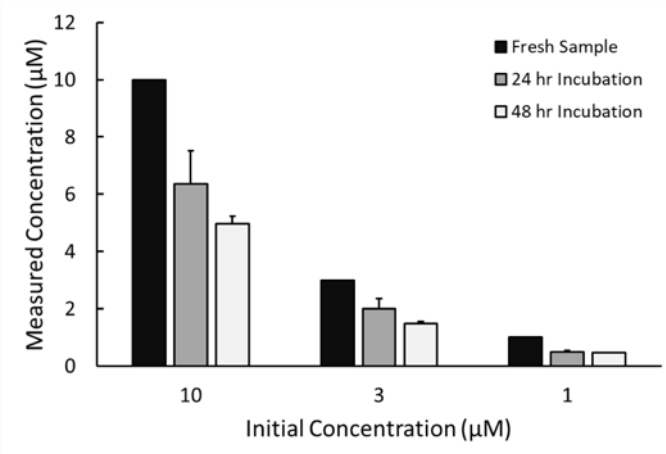

Figure 4: Degradation of H_2O_2 over time.

100 μM H_2O_2 was prepared in assay buffer and assayed up to 48 hours after initial preparation then diluted to concentrations within the functional range of the assay for analysis. Data represented as mean ± SEM. N = 3.

Senescence in CBECFCs was measured by immunofluorescence of the cell-cycle inhibitor p21[48] and quantification of p21 positive nuclei as a percentage of total nuclei. 5-day treatment with either 50 or 100 μM H_2O_2 did not affect the percentage of senescent cells (Figure 5A). Treatment with 100 μM H_2O_2 for 7 days caused a significant increase in the percentage of senescent CBECFCs (Figure 5). Treatment for 5 days, rather than 7 days, or use of 50 μM H_2O_2 rather than 100 μM H_2O_2 failed to cause an increase in the percentage of p21-positive nuclei. A small percentage of CBECFCs are P21-positive on Day 5 and Day 7 even without application of H_2O_2. P21 expression has not been measured on Day 0, but we believe this reflects the baseline senescence for these cell lines. There is no significant increase in senescence between Day 5 and Day 7 in the control cells.

H_2O_2 treatment at any concentration had no effect on expression of ICAM-1 (Figure 6A,D). Introduction of 100 U/mL TNF-α significantly increased ICAM-1 expression, but H_2O_2 did not affect ICAM-1 levels alone or in combination with TNF-α (Figure 6A). VCAM-1 expression was minimally affected by treatment with 100 U/mL TNF-α, although there was a significant interaction effect between TNF-α treatment and 100 μM H_2O_2 (Figure 6B,D). 5-day treatment with H_2O_2 did not significantly affect VCAM-1 expression unless co-treated with 100 U/mL TNF-α. 7-day treatment with 100 μM H_2O_2 caused a significant increase in VCAM-1 expression (Figure 6B). Treatment with 100 μM H_2O_2 for 7 days caused a significant increase in E-Selectin expression that was comparable to TNF-α induced E-Selectin expression in controls (Figure 6C,D). Treatment with 100 U/mL TNF-α also caused significant E-selectin expression in ECFCs cultured for 7 days, regardless of H_2O_2 concentration (Figure 6C,D). Of note, E-selectin expression in cells treated for 5 days with 100 μM H_2O_2 and given 100 U/mL TNF-α was

higher than cells treated with other concentrations of H_2O_2 for5 days (Figure 6C). A higher percentage of cells expressed VCAM-1 than E-Selectin.

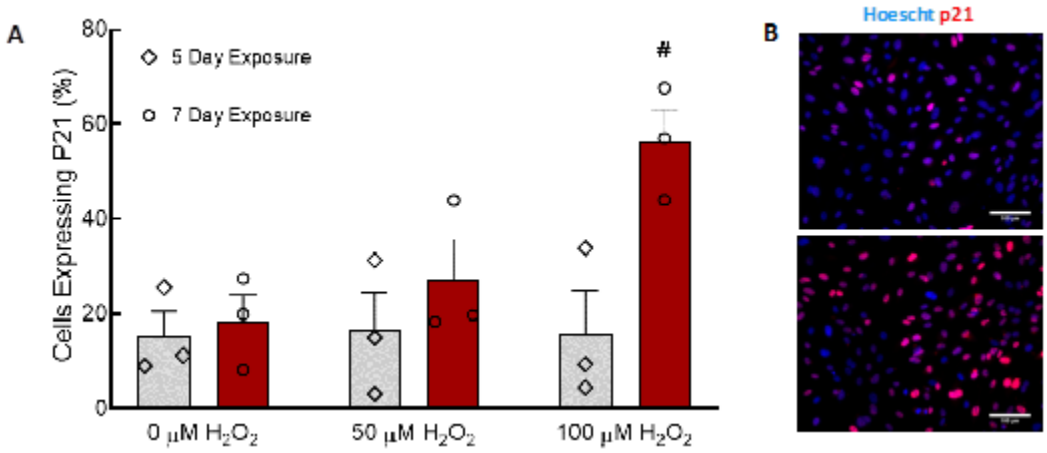

Figure 5: Treatment of CBECFCs with 100 μM H_2O_2 for 7 days induces CBECFC senescence.

A) The number of senescent (p21 positive) ECFCs was quantified after treatment for 5 or 7 days with H_2O_2. H_2O_2 concentration has a significant effect on p21 expression ($p < 0.05$). Treatment with 100 μM H_2O_2 for 7 days caused a significant increase in senescence compared to the 0 μM control (# $p < 0.01$). Bar graphs represent as mean ± SEM, individual points overlaid. N =3-4. B) **Control ECFCs exhibit minimal p21 expression, while ECFCs treated with 100 μM H_2O_2 for 7 days have high levels of nuclear p21 staining. Scale bars represent 100μm.**

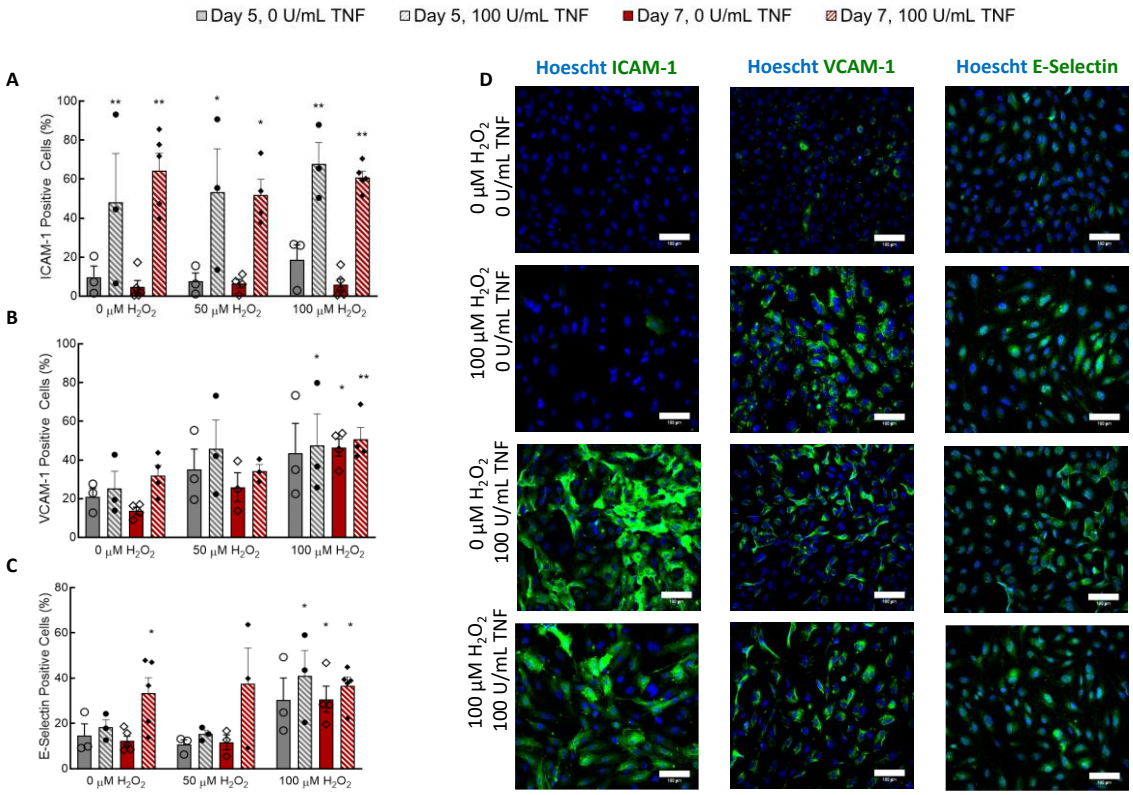

Figure 6: H2O2 treatment induces VCAM-1 and E-selectin expression in ECFCs.

A) TNF-α increased ICAM-1 expression ($p < 0.0001$), but H_2O_2 treatment did not affect ICAM-1 expression. B) Both TNF-α and H_2O_2 affect VCAM-1 expression ($p < 0.05$). Post-hoc analysis shows that 7-day treatment with 100 μM H_2O_2 with or without TNF-α causes a significant increase in VCAM-1 expression. 5-day treatment with H_2O_2 causes a significant increase in VCAM-1 expression when combined with a 24-hour dose of TNF-α. C) Both TNF-α and H_2O_2 affect E-Selectin expression ($p < 0.05$). 7-day treatment with 100 μM H2O2 causes a significant increase in E-Selectin expression with or without TNF-α treatment. D) Immunofluorescence was used to obtain the results present in A-C. Images show cells imaged on Day 7. Scale bars represent 100 μm. *$p < 0.05$ compared to 0 μM H_2O_2 and 0 U/mL TNF-α for each day. ** $p < 0.005$ compared to Day 5 0 μM H_2O_2 and 0 U/mL TNF-α. N = 3-5. Bars represents mean ± SEM.

2.3.2. Effects of H_2O_2 on hNDFs

Nuclear expression of p21 in hNDFs treated with 100 μM H_2O_2 for 7 days was increased (Figure 7A). Expression of calponin and α-SMA appear unaffected by treatment with 100 μM H_2O_2 (Figure 7). Quantification of these immunofluorescent images confirms that, while the senescence of the hNDF population increases considerably, the percentage of cells expressing the contractile proteins calponin and α-SMA are unaffected (Figure 7B). Treatment with 50 μM H_2O_2 and 5-day treatment durations were not tested.

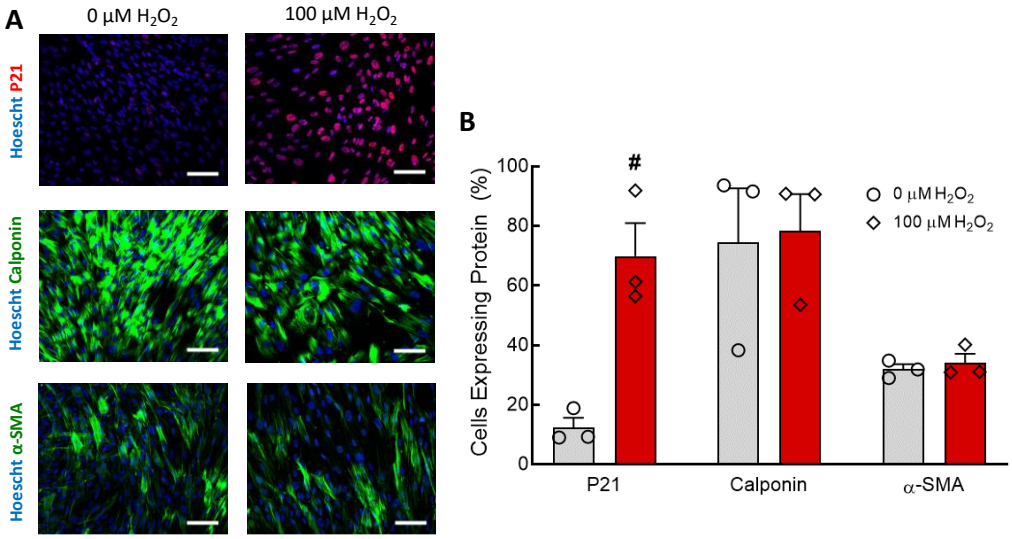

Figure 7: 7-day 100 μM H_2O_2 treatment increases senescence in hNDFs but does not affect contractile protein expression.

A) hNDFs were stained for P21, Calponin, and α-SMA. P21 expression is higher in hNDFs treated with 100 μM H2O2. Scale bars represent 100 μm. B) Quantification of p21, calponin, and α-SMA immunofluorescent staining. 7-day treatment with 100 μM H2O2 caused a significant increase in hNDF senescence compared to 0 μM controls (# $p < 0.001$). Expression of calponin and α-SMA was not affected by 100 μM H2O2. N = 3. Bars represent mean ± SEM.

2.3.3. Endothelium-Dependent Vasoreactivity is Compromised in TEBVs Treated with H_2O_2

To identify baseline vasoreactivity in the absence of a functional endothelium, vessels were made without an endothelial lumen and matured for 7 days. In these vessels, endothelium-independent vasoreactivity was robust. Constriction in response to phenylephrine was robust, as was dilation in response to sodium nitroprusside. In the absence of a functional endothelium, the acetylcholine response is blunted, with only mild vasoconstriction occurring (Figure 8).

Figure 8: Vasoreactivity of TEBVs fabricated without an endothelium.

TEBVs were fabricated with hNDFs as the medial cells without endothelializing. TEBVs exhibited vasoconstriction in response to phenylephrine and dilation in response to sodium nitroprusside. In the absence of an endothelium, acetylcholine does not induce vasodilation. Data represented as mean ± SEM. N = 3.

As described in the methods, all TEBVs are matured in normal growth media for 7 days with a flow rate that produces a shear stress of 6.8 dynes/cm^2 on the endothelium. As described in the methods, vasoreactivity is tested after this initial maturation and denoted as "Day 0". Then, TEBVs are treated with 0 or 100 μM H_2O_2 for 5 or 7 days (Figure 9).

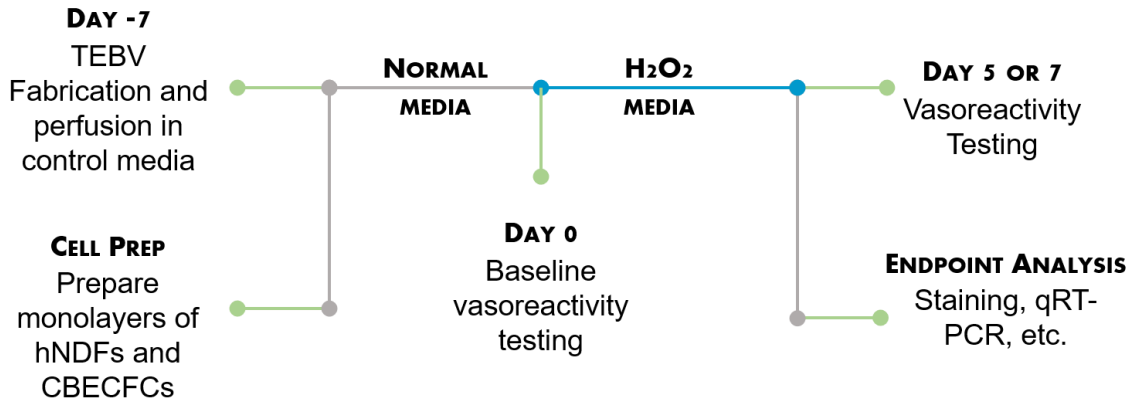

Figure 9: Timeline of TEBV H2O2 Treatment and Analysis

100 μM H_2O_2 treatment did not affect vasoconstriction in response to 1 μM phenylephrine compared to controls (Figure 10A). In contrast, TEBVs treated with 100 μM H_2O_2 for 5 days exhibited a significant reduction in endothelium-dependent vasodilation compared to the 0 μM H_2O_2 controls (Figure 10B). To assess whether the loss of endothelium-dependent vasodilation was the result of endothelial dysfunction specifically, on Day 12 or Day 14 TEBVs were also dosed with 1 μM sodium nitroprusside. In vessels treated with 100 μM H_2O_2 for 5 days there is a corresponding increase in their vasodilation in response to sodium nitroprusside. TEBVs matured in control media dilated in response to 1 μM acetylcholine but exhibited no change in their

diameter in response to subsequent introduction of sodium nitroprusside. This suggests that the maximum dilatory capacity of the vessel for these drug doses has been reached. The endothelium-independent vasodilation caused by sodium nitroprusside in H_2O_2-treated TEBVs was not significantly different from the endothelium-dependent vasodilation observed in controls. This indicates that treatment with 100 μM H_2O_2 only causes significant dysfunction in the CBECFCs, but not the hNDFs.

When TEBVs are treated with 100 μM H_2O_2 for a full 7 days, endothelium-dependent vasodilation is further reduced, and vasoconstriction in response to acetylcholine is reduced in several cases (Figure 10D). This is to be expected, as acetylcholine triggers constriction in the hNDFs in the absence of endothelial cells (Figure 8). Conversely, endothelium-dependent vasodilation improves slightly in vessels matured in control media. The endothelium-independent dilation of TEBVs treated with 100 μM H_2O_2 for 7 days is comparable to the endothelium-dependent dilation observed in TEBVs matured in only 0 μM H_2O_2 (Figure 10D). Vasoconstriction in response to phenylephrine remains consistent (Figure 10C).

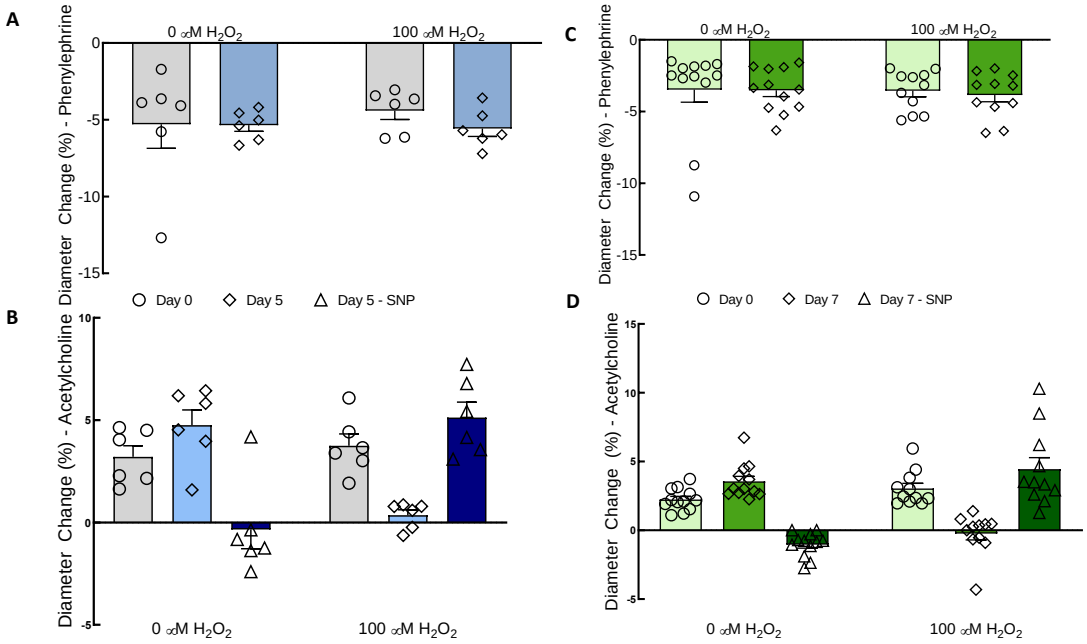

Figure 10: Treatment with 100 μM H2O2 for 5 or 7 days eliminates endothelium-dependent vasodilation, but not endothelium-independent vasoreactivity in TEBVs.

For all conditions, TEBVs were perfused for 7 days following fabrication before start of the experiment with or without 100 μM H_2O_2 and perfusion. Day 0 thus represents 7 days of perfusion. A) **Vasoconstriction in response to 1 μM phenylephrine is not affected by H_2O_2.** B) **Vasodilation in response to 1 μM acetylcholine is reduced by H_2O_2 ($p < 0.01$), and the effect of time (i.e. date tested) is H_2O_2 dependent ($p < 0.001$). There is a significant difference between the acetylcholine response of 0 and 100 μM H_2O_2 TEBVs ($p < 0.005$). Sodium nitroprusside (SNP) mediated vasodilation in vessels treated with 100 μM H_2O_2 is not significantly different from acetylcholine-mediated vasodilation in vessels matured in 0 μM H_2O_2.** C) **Vasoconstriction in response to phenylephrine is not affected by H_2O_2 concentration or timepoint, even when H_2O_2 treatment is extended from 5 to 7 days.** D) **Vasodilation in response to acetylcholine is reduced by H_2O_2 ($p < 0.0001$). Vessels treated with 100 μM H_2O_2 from Day 0 to Day 7 constrict in response to acetylcholine, rather than dilate. Sodium nitroprusside-mediated vasodilation in TEBVs matured in 100 μM H_2O_2 is not significantly different from acetylcholine-mediated vasodilation in control vessels. Note that Day 0 reflects a timepoint immediately before introduction of 0 or 100 μM H_2O_2, but is 7 days after vessel fabrication to ensure vessel maturity. N = 7 (A,B). N = 12 (C,D). Bars represent mean ± SEM.**

2.3.4. H_2O_2 Causes Endothelial Cell Senescence and Inflammation in TEBVs

Analysis of immunofluorescent stained TEBV segments cut *en face* was used to confirm that the endothelium was both present and senescent, and that contractile protein expression in the hNDFs was maintained. Immunostaining showed that expression of p21 was significantly increased in the hNDFs encapsulated within the vessel wall after 7 days of treatment with 100 μM H_2O_2 (Figure 11A,B). Expression of calponin and α-SMA in the vessel wall was not significantly affected (Figure 11A,B). H_2O_2 exposure also significantly increased the senescence of the ECFCs lining the vessel wall (Figure 11A,C). The expression of VCAM-1 in the endothelium was also significantly increased in vessels treated with 100 μM H_2O_2 compared to 0 μM controls (Figure 11A,C). It is worth noting that the number of ECFCs identified (e.g. vWF positive area coverage) has no observable differences after 7-day treatment with 100 μM H_2O_2. Furthermore, cross-sectional TUNEL staining confirms that treatment with 100 μM H_2O_2 for 7 days did not affect the proportion of apoptotic cells in the TEBVs (Figure 12). These data further confirm that the observed changes in vasoreactivity after 100 μM H_2O_2 treatment are the result of endothelial cell senescence, not the removal or death of the seeded endothelium.

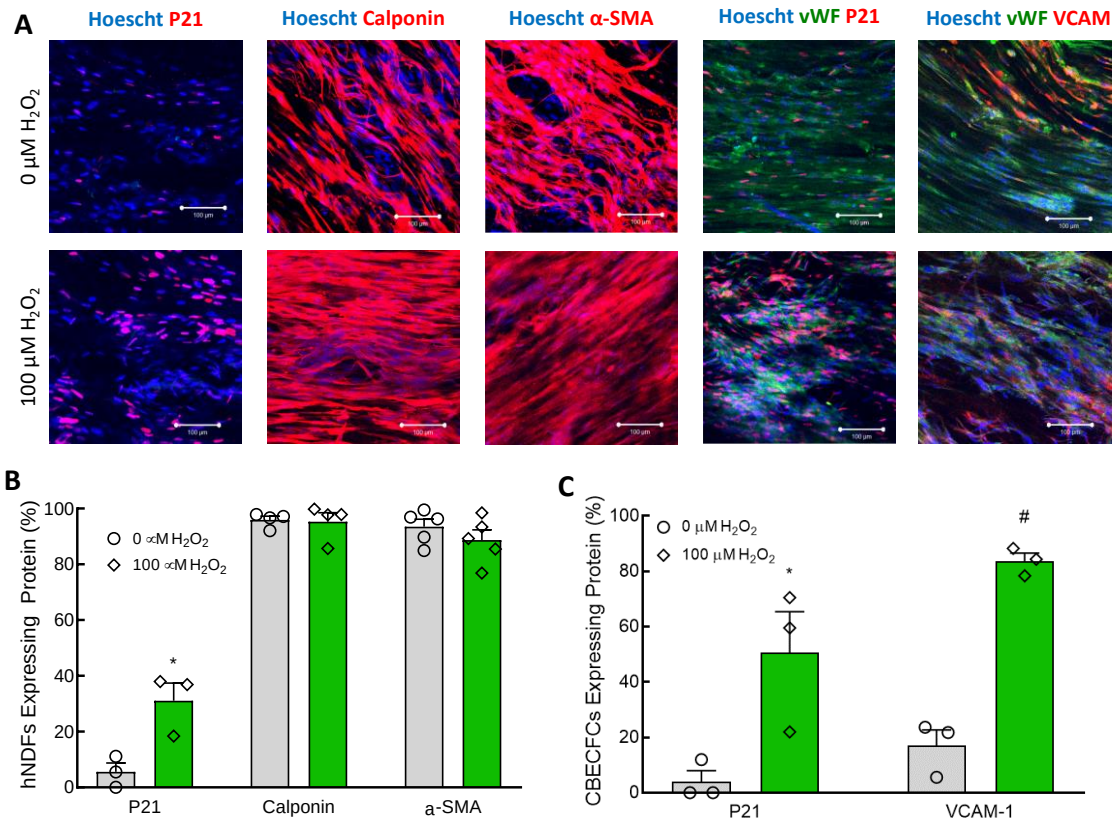

Figure 11: 7-day treatment of TEBVs with 100 μM H2O2 causes senescence in the embedded hNDFs and ECFCs, as well as an increase in endothelial VCAM-1 expression.

The treatment regime is the same as described in Figure 4. A) **Immunofluorescence was used to evaluate the expression of p21, calponin, α-SMA, and VCAM in the appropriate cell types within the TEBVs. Expression of p21 and VCAM-1 is increased in TEBVs treated with 100 μM H_2O_2 for one week. Scale bars represent 100 μm.** B) **Quantification of immunofluorescent images confirms that hNDFs encapsulated in TEBVs experience a significant increase in p21 expression (* $p < 0.05$) with 100 μM H_2O_2 treatment, but expression of calponin and α-SMA are not affected. Values represent mean ± SEM. N = 5.** C) **Quantification of immunofluorescent images confirms that treatment of TEBVs with 100 μM H_2O_2 significantly increases the expression of p21 and VCAM-1 in the CBECFC monolayer (# $p < 0.005$). Bars represent mean ± SEM. N = 3-5.**

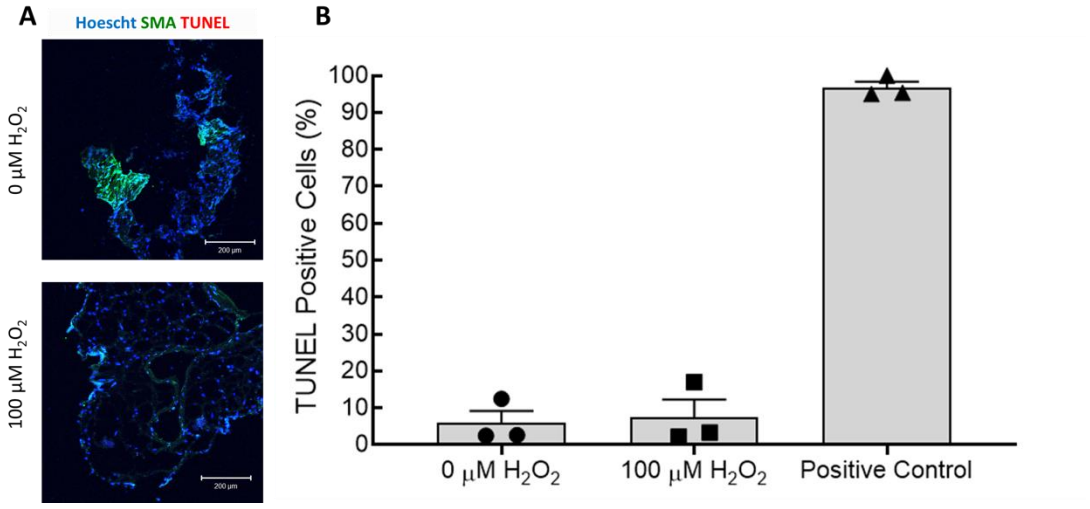

Figure 12: TUNEL Staining confirms that 7 day treatment of TEBVs with 100 μM H2O2 does not cause apoptosis.

As in figure 4, treatment began after maturation of TEBVs for 7 days under flow. A) **TEBV cross-sections were stained for α-SMA and DNA strand breaks (TUNEL stain). There is no observable difference in the degree of apoptosis between TEBVs treated with 100 μM H_2O_2 and controls. Scale bars represent 200 μm.** B) **Quantification of immunofluorescence shows that there is no significant increase in the number of TUNEL positive (apoptotic) cells in TEBVs treated with 100 μM H_2O_2. Bars represent mean ± SEM. N = 3.**

Next, we examined gene expression in TEBVs on Day 14 of maturation and compared those that had been treated with 100 μM H_2O_2 for 7 days to those matured only in control media. Relative to controls, 100 μM H_2O_2 treatment decreased mRNA expression of NOS3 (1.35±0.23 vs. 0.19±0.10, p=0.002), the gene which codes for endothelial nitric oxide synthase (eNOS). Conversely, expression of NOS2, the gene for inducible nitric oxide synthase (iNOS), was increased (1.26±0.15 vs. 6.2±1.96, p=0.04) (Figure 13A). Treatment had no effect on mRNA expression of RELA (1.28±0.20 vs. 0.42±0.14, p=0.008) indicating no difference in expression of the p65 subunit of nuclear

factor-κB (Nf-κB). Interestingly, SIRT1 mRNA, which produces the anti-aging sirtuin 1, was doubled (1.08±0.04 vs. 2.12±0.44, p=0.05) after H_2O_2 treatment (Figure 13A). NOX4, the gene for ROS producing 6 NADPH oxidase-4 was decreased by exogenous H_2O_2 (1.24±0.12 vs. 0.50 ±0.25, p=0.03). The relative expression of CBECFC-specific genes (vWF) is not significantly different in TEBVs treated with 100 μM H_2O_2 for 7 days (1.27±0.15 vs. 1.97±0.57, p=0.27) (Figure 7B). There is also a significant increase in the expression of the hNDF-specific genes P4HB (1.34±0.24 vs. 3.00±0.64, p=0.04) and FSP-1 (1.15±0.09 vs. 6.74±1.52, p=0.006) (Figure 13B).

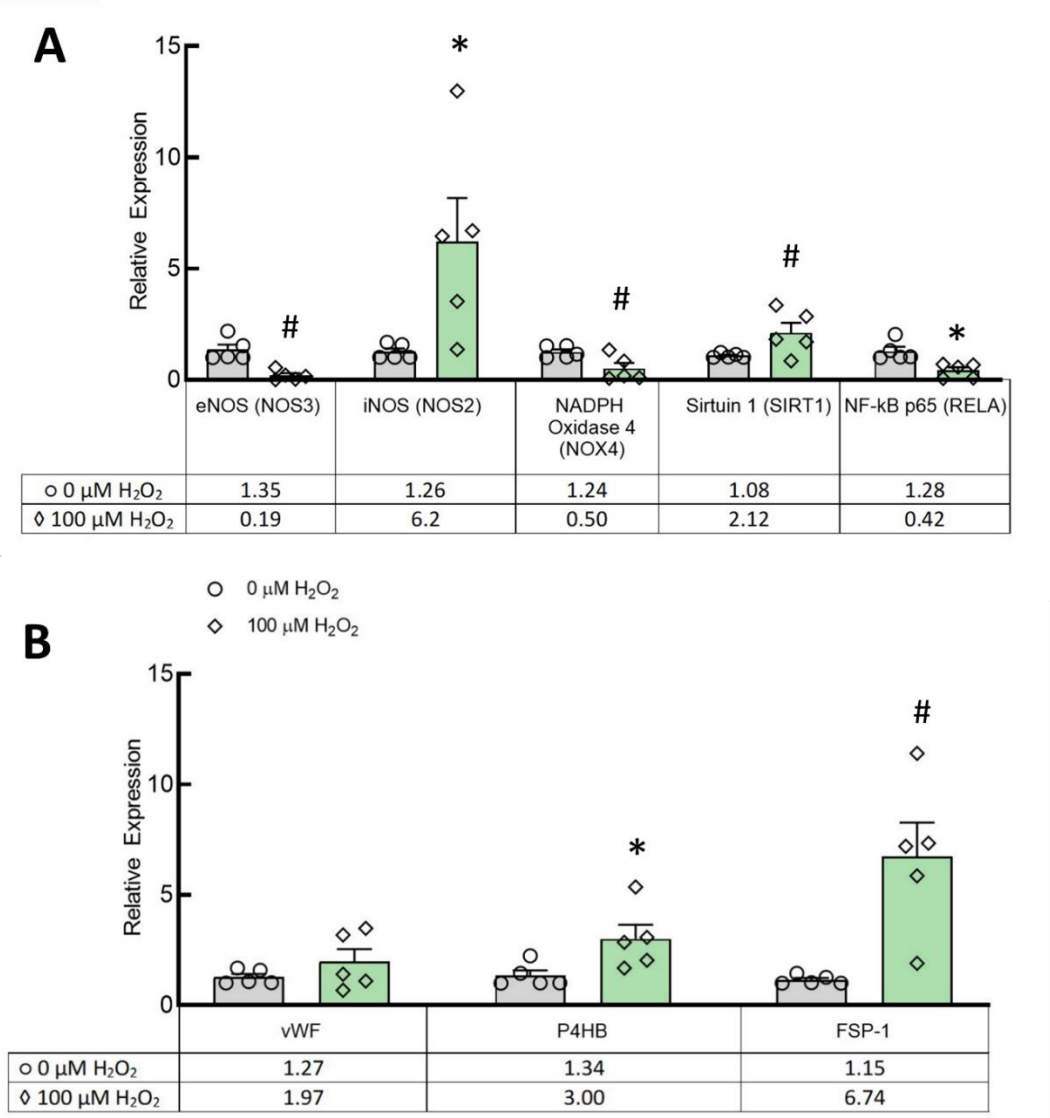

Figure 13: qRT-PCR of TEBVs shows SIRT1 expression increases significantly in TEBVs treated with 100 μM H2O2 and a reduction in CBECFC-specific protein expression.

A) eNOS levels decrease significantly, but iNOS expression increases nearly threefold in response. NOX4 expression also decreased significantly with H_2O_2 treatment. NF-κB expression was unaffected. B) Expresion of vWF, specific to the CBECFCs is decreased in TEBVs treated with 100 μM H_2O_2 compared to controls. The relative expression of hNDF-specific proteins, P4HB and FSP-1, are increased in treated vessels compared to controls. N = 5. Bars represent mean ± SEM. # indicates $p < 0.01$. * indicates $p < 0.05$.

2.4. Discussion

We developed a TEBV model of vascular senescence and showed that treatment of TEBVs with 100 μM H_2O_2 for 5-7 days diminishes endothelium-dependent vasodilation, while preserving endothelium-independent vasoreactivity (Figure 10), consistent with findings *in vivo*[45]. This study is the first to develop a tissue engineered blood vessel model for senescence. Furthermore, this model is able to be analyzed using a non-destructive, clinically relevant metric of vascular health. We explored the relative contributions of endothelial cells and vascular smooth muscle cells to overall vasoreactivity. 100 μM H_2O_2 is used to induce senescence in the TEBVs. This dose exceeds physiological plasma H_2O_2 concentrations[99]. This slightly higher concentration of H_2O_2 allows us to accelerate the timeline along which senescence is induced without causing apoptosis or acute cellular damage.

In both 2D cell culture and the TEBVs, 100 μM H_2O_2 treatment for 7 days caused significant senescence in CBECFCs and hNDFs (Figure 5). Although H_2O_2 treatment did cause a significant increase in hNDF senescence, expression of calponin and α-SMA is unaffected (Figure 7). When 100 μM H_2O_2 is applied to the TEBVs, endothelium-dependent vasoreactivity is significantly reduced, while endothelium-independent vasoreactivity is preserved (Figure 10). The robust sodium nitroprusside response confirms that the dilatory capacity of the vessels has not been reduced, indicating that the observed loss of dilation is based on the effects of the endothelium specifically,

rather than the hNDFs. Interestingly, TEBVs experienced a significant reduction in endothelium-dependent vasoreactivity after 5-day exposure to 100 μM H_2O_2, even though this was not long enough to produce a significant increase in endothelial cell senescence in 2D cultures. TEBV sections were stained for p21 and vWF, confirming that 7-day treatment with 100 μM H_2O_2 causes a significant increase in the number of senescent ECs, as well as hNDFs. Additionally, expression of eNOS was decreased in treated TEBVs. This suggests that the loss of endothelium-dependent vasodilation is the result of endothelial cell senescence rather than effacement of the endothelium. TUNEL staining also confirms that 7-day treatment with H_2O_2 does not induce apoptosis in either the hNDFs or the ECs (Figure 12). Expression of calponin and α-SMA was unaffected by H_2O_2 treatment in the TEBVs, just as seen in 2-D cultures. This is consistent with the robust hNDF-dependent vasoreactivity of the TEBVs regardless of H_2O_2 concentration.

The endothelium also expresses the adhesion molecules VCAM-1 and E-Selectin after treatment with H_2O_2, confirming that this model also captures the pro-inflammatory effects of senescence on the vasculature (Figure 11). Of note, ICAM-1 expression was not increased by H_2O_2 treatment in 2D (Figure 6). Overall, the level of stress-induced E-selectin expression, though significantly higher than controls, was less than the amount of stress-induced VCAM-1 expression. When HUVECs are treated with 50 U/mL TNF-α or IL-1, E-selectin expression peaks 4-6 hours after treatment, and

remains only slightly above baseline after 48 hours [106,107]. Conversely, ICAM-1 and VCAM-1 expression increases during a 24-hour exposure and remains high after 48 hours[106]. This explains the lower expression of E-selectin compared to VCAM-1 and ICAM-1 in the TNF-α treated positive controls (Figure 6), since these are measured 24 hours after initiation of treatment. The absence of oxidative stress-induced ICAM-1 expression in the CBECFCs suggests it is not activated by H_2O_2 treatment, rather than that expression is low due to a transience in activation. ICAM-1 and VCAM-1 are both targets of NF-κB, the primary signaling molecule governing endothelial cell activation[7]. However, expression of the two adhesion molecules can be differentially regulated despite their shared upstream effector[106].

VCAM-1 expression in the TEBV endothelium is significantly increased after treatment with 100 μM H_2O_2 (Figure 11). RELA was significantly decreased, unexpected given the increase in VCAM-1 expression. However, this is accompanied by an increase in SIRT1 expression, which itself limits NF-κB activity. This is typically the result of pro-apoptotic signaling, but there was no observable difference in vWF positive area identified within the TEBVs. Post-translational processing and modulation of Nf-κB activity is not measured in this study. Sirtuin 1 is associated with DNA repair and cellular health. In HUVECs, H_2O_2 treatment has decreased SIRT 1 expression[108]. It is unclear whether the bulk of SIRT1 mRNA in the present model is from hNDFs or ECFCs.

Treatment with 100 μM H_2O_2 did not affect vasoconstriction in response to 1 μM phenylephrine in the TEBVs (Figure 10A, C). In contrast, human saphenous vein samples show a reduction in vasoconstriction *ex vivo* when treated with as little as 10 μM H_2O_2 for 16 hours[109]. It is important to note that this data was obtained using a much higher concentration of noradrenaline (100 μM) as a vasoconstrictor, rather than the low dose of phenylephrine (1 μM) used here. It is possible that application of a higher dose of phenylephrine to the TEBVs could reveal a slight difference in the vasoconstriction with 100 μM H_2O_2 treatment. Furthermore, the saphenous vein is comprised of both vSMCs and perivascular fibroblasts, while the TEBVs used here contain only hNDFs within the vessel wall[110]. The presence of the vSMCs may add greater oxidative stress sensitivity to the endothelium-independent measures of vasoreactivity.

Several cell types could be used for the mural cells of TEBVs (vSMCs, mesenchymal stem cells (MSCs, and hNDFs), as well as for the endothelium (HAECs or ECFCs). While primary vSMCs seem ideal to maximize physiological relevance, they have limited proliferative capacity after isolation. Donor availability is also limited, and the quality of cells varies significantly from donor to donor[111]. If vSMCs from elderly donors are used, cell quality deteriorates even further[112]. MSCs are a more attractive cell type since they are more proliferative than vSMCs and differentiate to express vSMC proteins. However, TEBVs fabricated with hNDFs are significantly more contractile than those fabricated from MSCs[103], and still express the key proteins calponin and αSMA.

While HAECs are readily available commercially, CBECFCs proliferate more quickly. These two cells are also functionally equivalent as characterized by expression of nitric oxide, cellular adhesion in co-cultures, and shear-responsiveness[113]. CBECFCs are easily obtained with high yields per donor, and donor-to-donor variability is minimal, making them an ideal source of primary ECs for use in the TEBVs. TEBVs were made with hNDFs and CBECFCs to maximize the functional capacity of the TEBVs in their "healthy" state. This allows the greatest sensitivity when analyzing vasoreactivity for loss and reduction of function.

Endothelial cells play a significant role in maintenance of vascular health. As the endothelium grows dysfunctional, the risk of developing atherosclerosis increases significantly. The role of endothelial cell senescence in promoting an atherogenic phenotype in the vasculature is recognized. An optimal *in vitro* model of vascular aging will facilitate the development of novel treatments, like senolytics, that specifically target the effects of cellular aging on vascular health. This study demonstrates the utility of tissue engineered blood vessels (TEBVs) in generating an atherogenic environment. In future studies, the atherogenic potential of this model will be further explored by introducing monocytes and lipids to the TEBV perfusion circuit. It will also be used to investigate the effects of drugs specifically targeting senescence (i.e. senolytics) on the atherogenic potential of H_2O_2-treated TEBVs.

2.5. Chapter-Specific Acknowledgments

We thank Jason Breithaupt for assistance qRT-PCR analysis on several TEBV samples. This work was funded by NIH grant (UH3), CBTE, and NSFGRFP. **Need to insert relevant grant numbers and full funding information.

3. The Use Stress-Induced Senescence to Enhance Monocyte Adhesion and Foam Cell Formation in TEBVs

Figure 15, Figure 19, and some text in this chapter were published previously in the following form: Zhang, X. *et al.* Modeling early stage atherosclerosis in a primary human vascular microphysiological system. *Nat. Commun.* 11, (2020)[90].

3.1. Introduction

The pathology of atherosclerosis involves the accumulation of lipoproteins (specifically low-density lipoproteins) and monocytes within the arterial wall, ultimately thickening the vessel wall intima, sometimes to the point of near occlusion[114]. More dangerously, these legions can lead to destabilization of the arterial wall and rupture, exposing thrombogenic material that can clot *in situ*[115]. Risk factors like diet and age, or genetic predisposition to hyperlipidemia, create an oxidative environment that promotes legion formation[116].

Oxidative stress activates the vascular endothelial cells (ECs), resulting in increased expression of endothelial adhesion molecules (e.g. VCAM-1, ICAM-1, etc.), reduced shear responsiveness, and reduced vasodilation in response to changes in blood flow and circulating chemical signals[117–120]. Circulating low-density lipoproteins (LDL) can be enzymatically modified by plasma proteins to increase its inflammatory properties and increase retention in the vessel intima[117]. Circulating monocytes adhere in these areas where they, along with any native macrophages, consume the nearby enzyme-modified LDL (eLDL) in an unregulated fashion and transition into foam cells,

making it more difficult to for them to leave the intima[118,121]. eLDL can also accumulate in the vascular smooth muscle cells (vSMCs). Inflammation in the endothelium, as well as accumulation of eLDL in the vSMCs increases the proliferation of vSMCs in the intima[122].

Inflammation is one of the key events in the development of atherosclerotic lesions. Atherosclerosis occurs at higher rates in those with autoimmune diseases, like rheumatoid arthritis[123–125]. Anti-inflammatory therapies, like antibody therapies against IL-1β, reduces the incidence of adverse cardiovascular events[122,126]. In the previous chapter, we demonstrated that, while stress-induced senescence significantly increased expression of E-Selectin and VCAM-1 expression, it does not fully activate the endothelium. ICAM-1 expression is not affected by H_2O_2 exposure. We hypothesize that stress-induced senescence and inflammation activate complementary pathways to increase the overall inflammatory phenotype in the cell[42,127].

Aside from measures of vasoreactivity or vessel diameter that can be measured non-invasively in clinical settings, the initiation and progression of atherosclerosis have largely been studied in animal models like *Apoe*$^{-/-}$ mice[31]. While these animal models are useful, there are important differences in the nature of disease progression compared to humans, as well as the limited tunability of these systems and the difficulty of isolating specific factors that can be closely interwoven *in vivo*[128–130]. Human microphysiological systems are filling the gap by providing greater fidelity to native biology while

maintaining much of the tunability of *in vitro* models[131,132]. Tissue-engineered blood vessels (TEBVs) contain both intimal and medial layers, permitting the study of the interactions between endothelial cells and medial cells in an atherogenic environment[133].

In the previous chapter we found that oxidative stress-induced senescence increases VCAM-1 and E-Selectin expression within the endothelium. In this study we hypothesize that oxidative stress increases monocyte adhesion within TEBVs treated with H_2O_2. Introduction of enzyme-modified low-density lipoprotein (eLDL) alongside H_2O_2 is expected to further increase the expression of monocyte adhesion proteins expressed by the endothelium, resulting in even greater monocyte adhesion. Introduction of eLDL also permits the evaluation of foam cell formation within the TEBVs in an oxidative stress environment.

Based on the results presented in Chapter 2, TEBVs were treated with 100 μM H_2O_2 for 5 days to induce senescence and inflammation in the endothelium. Monocytes and eLDL were added during the H_2O_2 treatment period. Independently H_2O_2 serves as a sensitizing agent to increase monocyte adhesion and lipid uptake in the TEBVs in place of other inflammatory stimuli like TNF-α that have been used in prior studies[90,134]. Monocytes and lipids were fluorometrically labeled to quantify their accumulation in the vessel as well as foam cell formation. Future work will focus on the capacity of drugs to reverse or prevent this uptake.

3.2. Methods

3.2.1. Cell Culture

Human cord blood derived endothelial colony forming cells (CBECFCs) were isolated as previously described[104]. Isolation and culture protocols for CBECFCs were approved by the Duke University Institutional Review Board. Human umbilical cord blood samples were obtained from the Carolina Cord Blood Bank. Patient identifiers were removed prior to receipt.

After receipt, blood is diluted 1:1 with Hanks Buffered Salt Solution (HBSS, Invitrogen). The diluted blood sample is layered slowly atop an equal volume of room temperature Histopaque 1077 (Sigma) and centrifuged at 740 g for 30 minutes. Buffy coat mononuclear cells were removed and washed with Endothelial Cell Growth Medium (Cell Applications) containing 1% penicillin/streptomycin solution (Gibco). The mononuclear cells are centrifuged at 515 g for 10 minutes and resuspended in endothelial cell culture media three times and plated on TCPS six-well plates coated with 50 μg/mL rat tail collagen I. Media is changed daily for the first 7 days of culture and every 48 hours after. Colony formation is visible after 7-10 days of culture. Flow cytometry is used to confirm purity of the resulting endothelial cell population. Cells are harvested at P4 – P6. After resuspending cell samples in 10% goat serum, 5 μL of the appropriate antibody is added to a 95 μL sample containing 500,000 cells. Cells are then

fixed with 0.5% PFA, rinsed, and resuspended in DPBS. 9,000 events per sample are recorded.

Human neonatal dermal fibroblasts (hNDFs) are purchased from Lonza. They are grown in high glucose Dulbecco's Modified Eagle Medium (Invitrogen) supplemented with 10% vol/vol heat inactivated fetal bovine serum (Gibco), 1% penicillin/streptomycin (Gibco), 1% MEM non-essential amino acids (Gibco), 1% sodium pyruvate (Gibco), 1% GlutaMAX (Gibco), and 0.1% β-mercaptoethanol (ThermoFisher). Media is changed every 48 hours.

Monocytes used are the human U937 cell line (Sigma). Cells are maintained in RPMI-1640 containing 1% L-Glutamine (Sigma) supplemented with 10% Heat-Inactivated Fetal Bovine Serum (HI-FBS, Gibco). Media is changed every 48-72 hours.

3.2.2. TEBV Fabrication

Tissue engineered blood vessels (TEBVs) were made as previously described[103]. Rat tail collagen I (BD Biosciences) is diluted to a concentration of 2.05 mg/mL in 0.6% acetic acid comprising 80% of the total volume of the TEBV solution. 10X serum-free Dulbecco's Modified Eagle's Medium (DMEM, Sigma) was added to make up 10% of the total TEBV volume. The mixture is then titrated to a pH of 8.5 with 5M NaOH. A solution of hNDFs at a concentration of 5×10^6 cells/mL is added comprising the final 10% of the TEBV volume and leading to a final density of 0.5×10^6 hNDFs/mL in the TEBV. After mixing, the gel solution was poured into a 3 mL luer-lok syringe (BD

Biosciences) stoppered with a closed two-way stopcock. To create a tubular collagen scaffold, an 810 μm diameter steel mandrel is inserted into the center of the syringe mold and held in place with parafilm. The solution gels at room temperature over 30 minutes.

After gelation is complete, the gel and mandrel are removed from the syringe mold and laid on a 0.8 μm pore Nylon membrane filter (Whatman) atop 10 autoclaved Kim Wipes. The TEBV rests there for 8-10 minutes until ~90% of the water has been removed. The nylon filter and TEBV are then transferred to a 150 mm petri dish filled with sterile PBS to facilitate easier removal of the filter and lubricate the PBS for removal from the mandrel. Next, the TEBV is mounted in an acrylic chamber with hollow grips (0.711 μm outer diameter, McMaster-Carr) on each end of the vessel to allow perfusion of the vessel lumen. Black silk sutures hold the TEBV in place on the grips (Figure 3A). Next, a solution of 500,000 ECFCs suspended in endothelial cell growth media is slowly pushed through the vessel lumen. The vessel is rotated for 60 minutes at a speed of 10 rph to ensure uniform monolayer adhesion. TEBVs are perfused with TEBV growth media at a flow rate of 0.5 mL/min for the first 24 hours after fabrication, then the flow rate is increased to 2 mL/min for the remainder of the experiment (Figure 3B). A laminar shear stress of 6.8 dynes/cm^2 is generated across the endothelium[103]. TEBV perfusion media contains low glucose DMEM, 1% penicillin/streptomycin, 1% MEM non-essential amino acids, 0.1% β-Mercaptoethanol, and 3.7% heat-inactivated fetal bovine serum for

the first week of culture. After one week of culture, 2mg/mL ε-aminocaproic acid was added to preserve the long-term integrity of the TEBV.

Perfusion circuits for these experiments were made using L/S 13 tubing (MasterFlex) and a reservoir with a maximum capacity of 30 mL. The total volume in the flow circuit and TEBV chamber during the first week of perfusion is 20 mL This volume is reduced to 13 mL total while monocytes and enzyme modified low-density lipoprotein is added to the perfusion circuit.

3.2.3. Hydrogen Peroxide Treatment

H_2O_2 is diluted from a 30% stock solution (9.77 M) to 100 μM in the ε-aminocaproic acid-supplemented TEBV growth medium. Media is changed 24 hours after the first time adding H_2O_2 to media, and every 48 hours thereafter until TEBVs are fixed. Solutions are prepared fresh from the 9.77 M stock every time.

3.2.4. Preparation and Enzyme Modification of Low-Density Lipoproteins

Human plasma LDL (Sigma) is prepared for storage and use by first quantifying protein concentration with the Lowry Assay (Lee Biosolutions). The solution is diluted to a concentration of 10 mg/mL in 10% sucrose (w/v) saline solution (150 mM NaCl, 0.24 mM EDTA, pH 7.4) for use or storage at -80˚C[135]. Methods for enzyme modification were adapted from Chelian et al[136]. Aliquots of LDL are first dialyzed against a saline solution (150 mM NaCL, 0.24 mM EDTA, pH 7.4) for approximately 24 hours, refreshing the buffer after 3 and 6 hours after the beginning of the dialysis. After confirming the new

concentration of protein in the solution, trypsin is added at a concentration of 7 μg/mg LDL for 6 hours at 37°C. 12 μg cholesterol esterase (per mg LDL) is then added at 37°C for 10 hours. Next, 24 μg/mg trypsin is added for 6 hours at 37°C. Finally, 29 μg/mg cholesterol esterase is added for 48 hours at 37°C. This final solution is dialyzed against 1X DPBS (pH 7.4) for at least 24 hours. Particle uniformity is confirmed with a ZetaSizer particle analyzer to confirm enzyme modification has occurred for the entire solution. The solution is then passed through a 0.2 μm filter to sterilize and the final protein concentration is quantified using the Lowry Assay once more. The solution must be used within two weeks to avoid spontaneous oxidation of the LDL.

3.2.5. Oil Red O staining

At the conclusion of the experiment, cells are fixed in 10% formalin for one hour and then rinsed 3 times in DI water. A working solution of Oil Red O is made by dissolving lyophilized Oil Red O in isopropanol and diluting to an appropriate concentration in a mixture of isopropanol and DI water which is filtered before use. Before adding the Oil Red O stain, the cells are covered with a small volume of isopropanol for 5 minutes. Then diluted Oil Red O solution is added to fixed cells for 20-30 minutes. The wells are then rinsed with DI water 2-5 times until no visible stain remains. Hematoxylin is added for 1 minute to stain the nuclei, then rinsed 2-5 times with DI water until no visible stain remains again. PBS is added to the wells for imaging at 20X on a Nikon Eclipse TE2000-U.

3.2.6. Hydrogen Peroxide and eLDL Co-Treatment Toxicity Testing

CBECFCs were plated at a density of 15,000 cells/cm^2 and allowed to adhere for 24 hours in normal growth media. A solution of 50-100 μM H_2O_2 and 25-50 μg/mL eLDL is added to the cells. After 24, 48, or 72 hours of exposure the media is removed from the cells and they are stained for 40 minutes with 4 μM EthD-1 and 2 μM calcein-AM diluted in 1X DPBS without calcium and magnesium containing 1 μL/mL Hoechst 33432. Cells are then fixed with 10% formalin for 10 minutes and rinsed 3 times with 1X DPBS before imaging.

3.2.7. Fluorescent Labeling of Monocytes

Human U937 monocytes (Sigma) are harvested from suspension by centrifugation at 300 xg for 10 minutes. Cells are then resuspended in serum-free RPMI 1640 containing 1% L-glutamine at a concentration of 2 x 10^6 cells/mL and incubated with a 4.2 μM solution of CMPTX red in DMSO for 30 minutes. The cells are centrifuged again at 300 xg for 10 minutes and resuspended in normal growth medium to remove excess dye from the cells. Monocytes should be used within 48 hours after staining for maximum retention of fluorescence. Monocytes are introduced to perfusion media in 500 μL of TEBV growth media to produce a final concentration of 1 x 10^6 monocytes/mL in the total volume of the perfusion circuit.

3.2.8. Analysis of TEBV Vasoreactivity

TEBV vasoreactivity is quantified in response to phenylephrine, acetylcholine, and sodium nitroprusside. 1 mM stock solutions of each drug are prepared by diluting lyophilized powders in sterile DPBS without calcium or magnesium. This 1 mM solution is injected into the reservoir of the TEBV flow circuit via a silicone injection port integrated into the perfusion tubing. A 1 μL/mL dilution is used, resulting in a dose of 1 μM in the flow circuit. These doses are expected to elicit about half the maximum vasodilation or vasoconstriction of the TEBVs. TEBV diameter equilibrates after introduction of phenylephrine (PE) for five minutes. Next, acetylcholine (ACH) is injected, and the diameter change is quantified after five minutes. Finally, sodium nitroprusside (SNP) is added to the flow circuit and the diameter change is quantified after 8 minutes. Diameter changes are recorded on video with a stereo microscope equipped with a 0.5x magnification lens using ISCapture. Still shots are selected from these videos at the time points described above (300 seconds after phenylephrine injection, 300 seconds after acetylcholine injection, and 480 seconds after SNP injection). The diameter at the time of phenylephrine injection is used as a baseline for acetylcholine response, which is in turn used as a baseline for calculating the change in diameter in response to SNP. The still images are quantified using the line tool in ImageJ. Five points evenly spaced along the TEBV are randomly selected to measure the diameter. The same points along the TEBV are used to measure the diameter change in

response to each drug. A typical TEBV has a baseline diameter of 1500-2000 μm corresponding to about 150-250 pixels in ImageJ.

TEBV vasoreactivity is first quantified 7 days after fabrication to evaluate baseline vasoreactivity and confirm appropriate function of the TEBV. For this initial test of vasoreactivity, only phenylephrine and acetylcholine are used. If vasoconstriction and vasodilation do not exceed -1% and 1% respectively, the vessel is not used for further study. In the data presented here, this test is called "Day 0" and further tests of vasoreactivity are described using the number of days after this initial test of vasoreactivity, rather than the total number of days since vessel fabrication. H_2O_2 is added after a vessel passes this initial test of vasoreactivity on Day 7 and vasoreactivity is measured again on Day 5 or Day 7 of H_2O_2 treatment with acetylcholine, phenylephrine, and sodium nitroprusside.

3.2.9. Immunofluorescence

Cells in well plates are fixed with 10% formalin for 10 minutes at room temperature. Cells are permeabilized with 0.1% Triton-X and then blocked with 10% goat serum (Gibco) in DPBS. Primary antibodies for P21 and VCAM-1 (Abcam) were diluted 1:250 in 10% goat serum. Primary antibodies for E-Selectin and ICAM-1 (SCBT) were diluted 1:200 in 10% goat serum. After staining overnight at 4°C, samples were rinsed 3 times with DPBS. Goat anti-rabbit Alexa-Fluor 594 or goat anti-mouse Alexa-Fluor 488 secondary antibodies were added at a dilution of 1:500 in 1% Goat serum with

1 μL/mL Hoechst 33342 for 1 hour at room temperature. Samples were rinse an additional 3 times in DPBS and imaged immediately. 2-D samples were imaged at 20X on a Nikon Eclipse TE2000-U.

TEBVs are fixed before being removed from the chambers in 10% formalin for one hour at room temperature. The section of vessel between the two grips where a full endothelial layer is present is excised from the larger vessel and rinsed three times in DPBS. The vessel is then cut into smaller sections for each stain that is necessary before further processing. Vessel sections are transferred to a 48-well plate and permeabilized with 0.1% Triton-X and then blocked with 10% goat serum (Gibco) for 8 hours at room temperature. Primary antibodies for P21 (Abcam), VCAM-1 (Abcam), and von Willebrand Factor (vWF, Abcam) are diluted 1:100 in 1% goat serum. After incubating overnight at 4°C, samples are rinsed 3 times with DPBS waiting 5 minutes between rinses. Goat anti-rabbit Alexa-Fluor 594 and goat anti-mouse Alexa-Fluor 488 secondary antibodies were added at a dilution of 1:500 in 1% Goat serum with 1 μL/mL Hoechst 33342 for 1 hour at room temperature. Samples were rinse an additional 3 times in DPBS, waiting 10 minutes between rinses. TEBV sections were mounted on glass slides with Fluor Save, covered with a cover slip, and imaged on a Zeiss 510 inverted confocal microscope at 20X magnification.

3.2.10. Quantification of Lipids and Foam Cells in TEBVs

After fixation with 10% formalin, a section of the fixed TEBV is set aside for lipid staining. First, the sample is blocked in 10% goat serum (Gibco) for 1 hour at 37°C and rinsed with 1X DPBS. Then, a 3X solution of LipidSpot Lipid Droplet Stain (Biotium) diluted in PBS is applied for 30 minutes. Samples are transferred to a glass slide with 25 μL staining fluid without rinsing, covered with a cover slip, and imaged immediately on a Zeiss 510 Inverted Confocal Microscope.

3.2.11. Statistical Analysis

Statistical analyses were performed using GraphPad Prism 8. One-way or two-way ANOVA with post-hoc Dunnett's test were used to compare means for all immunofluorescence quantification. A repeated measures ANOVA with post-hoc Tukey's test was used to compare means for all TEBV vasoreactivity data. P values less than 0.05 were considered significant. All data shown graphically represent mean ± SEM. N represents the number of independent experiments.

3.3. Results

3.3.1. Simultaneous Treatment with eLDL and H_2O_2 is not Cytotoxic to CBECFCs

CBECFCs were exposed to 0, 50, or 100 μM H_2O_2 for a total of 7 days. For the final 24, 48, or 72 hours of H_2O_2 treatment, enzyme modified low-density lipoprotein (eLDL) was also added (Figure 14A). Analysis of the cells with a Live-Dead Assay found that there was no significant decrease in the percentage of live cells with eLDL treatment

alone, even for 72 hours (Figure 14B). When eLDL was added for the final 24-72 hours of 7-day H_2O_2 treatment there was not an effect on cell viability, even when administering 100 μM H_2O_2 with 50 μg/mL eLDL for 72 hours (Figure 14D).

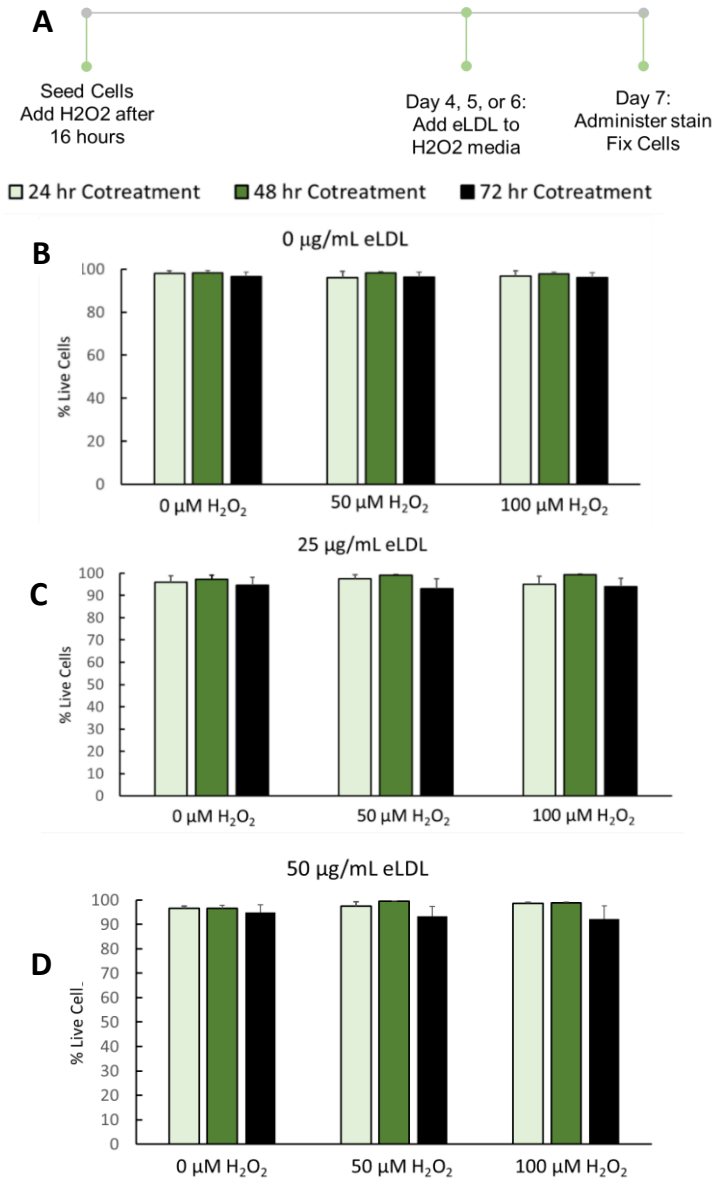

Figure 14: Simultaneous eLDL and H_2O_2 treatment does not compromise CBECFC viability.

CBECFCs treated with H_2O_2 and eLDL, added separately or together, do not have reduced viability. A: Schematic showing the timeline in which H_2O_2 and eLDL were introduced to the CBECFCs. B: H_2O_2 without eLDL introduced does not cause toxicity. B: Introduction of 25 µg/mL eLDL alongside H_2O_2 does not reduce cell viability. C: Introduction of 50 µg/mL eLDL does not significantly reduce cell viability alone or alongside 100 µM H_2O_2. N = 3. Data represents mean ± SEM.

3.3.2. eLDL Increases Activation in CBECFCs alone and with H_2O_2 Treatment

Enzyme-modified low-density lipoprotein (eLDL) was administered to CBECFCs at a concentration of 100 μg/mL for 24 hours to confirm that eLDL could induce an inflammatory response. 100 U/mL TNF-α for 4.5 hours was used as a positive control. PBS and unmodified LDL were used as negative controls. Endothelial activation was measured by evaluating expression of VCAM-1, ICAM-1, and E-Selectin (Figure 15A). As expected, unmodified LDL induced no increase in VCAM-1, ICAM-1, or E-Selectin expression, although there was some baseline E-Selectin expression identified. TNF-α treatment maximized expression of ICAM-1, VCAM-1, and E-Selectin. Enzyme-modified LDL treatment caused increased expression of ICAM-1, VCAM-1, and E-selectin as well, but not as much as TNF-α. This demonstrates that eLDL can be used to induce inflammation in the endothelium. VCAM-1 and E-selectin expression staining both exhibited high variability in the baseline and induced expression, making it difficult to objectively quantify the data. ICAM-1 staining had low background staining and a large, stimulus-dependent response facilitating quantification of ICAM-1 expression in response to PBS, LDL, eLDL, and TNF-α. The increase in response to eLDL is significant compared to PBS, and the increase due to TNF-α is significant compared to all conditions (Figure 15B). This illustrates that administration of an acute high dose eLDL alone can induce activation and inflammation in the endothelium.

Next, eLDL was administered at the conclusion of a 7-day H_2O_2 treatment to determine whether the combination treatment has an additive or synergistic effect compared to either solution individually.

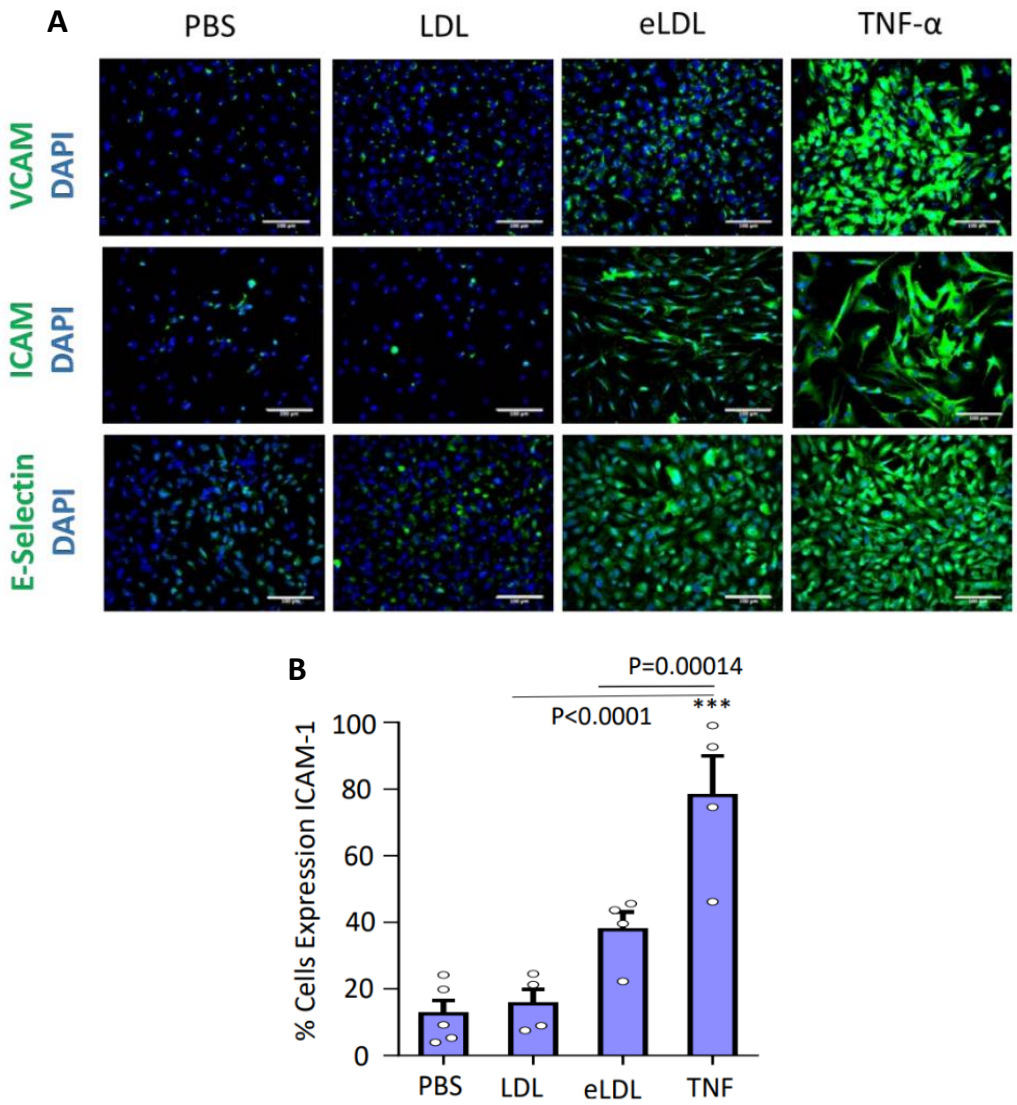

Figure 15: Endothelial Cell Activation in Response to eLDL Exposure.

A: CBECFCs were exposed to a solution of PBS, unmodified LDL, or enzyme-modified LDL for 24 hours. 100 U/mL TNF-α was administered for 4.5 hours as a positive control. Cells were stained for VCAM-1, ICAM-1, or E-Selectin. PBS and unmodified LDL both induced minimal response in the cells, although there was a small degree of baseline E-Selectin expression present. eLDL treatment caused a significant increase in the expression of VCAM-1, ICAM-1, and E-Selectin in all conditions. B: ICAM-1 expression was quantified for all conditions. 24 hour treatment with 100 µg/mL eLDL caused a significant increase in ICAM-1 expression. N = 4-5. Data represented as mean ± SEM with individual data points overlaid.

Endothelial cell activation when eLDL is administered for the final 24 hours of 7-day 100 μM H_2O_2 exposure was also evaluated. Only H_2O_2 concentration had a significant effect on the expression of VCAM-1 and E-selectin. There was no difference in VCAM-1 and E-Selectin expression in the 25 and 50 μg/mL conditions compared to the 0 μg/mL controls for each concentration of H_2O_2 (Figure 16). Ultimately, this was due to a high degree of variability in the degree of expression. Further replicates may help clarify the dominant trend. ICAM-1 expression was still unaffected by H_2O_2 concentration, but eLDL concentration was found to have a significant effect (2-way ANOVA, $p < 0.005$). Treatment with 50 μg/mL eLDL significantly increased ICAM-1 expression for each concentration of H_2O_2 tested (Figure 16, $p < 0.05$). No interaction effect between eLDL concentration and H_2O_2 concentration was identified.

P21 expression was also evaluated in the CBECFCs exposed to eLDL for the final 24 hours of a 7-day H_2O_2 treatment. eLDL exposure did not have a significant effect on the proportion of p21 positive (i.e. senescent) cells (Figure 17). The degree of senescence from 100 μM H_2O_2 and eLDL combined was comparable to the degree of senescence from 100 μM H_2O_2 alone (Figure 5). eLDL does not directly contribute to senescence in the endothelium, but complements endothelial activation induced by stress-induced senescence.

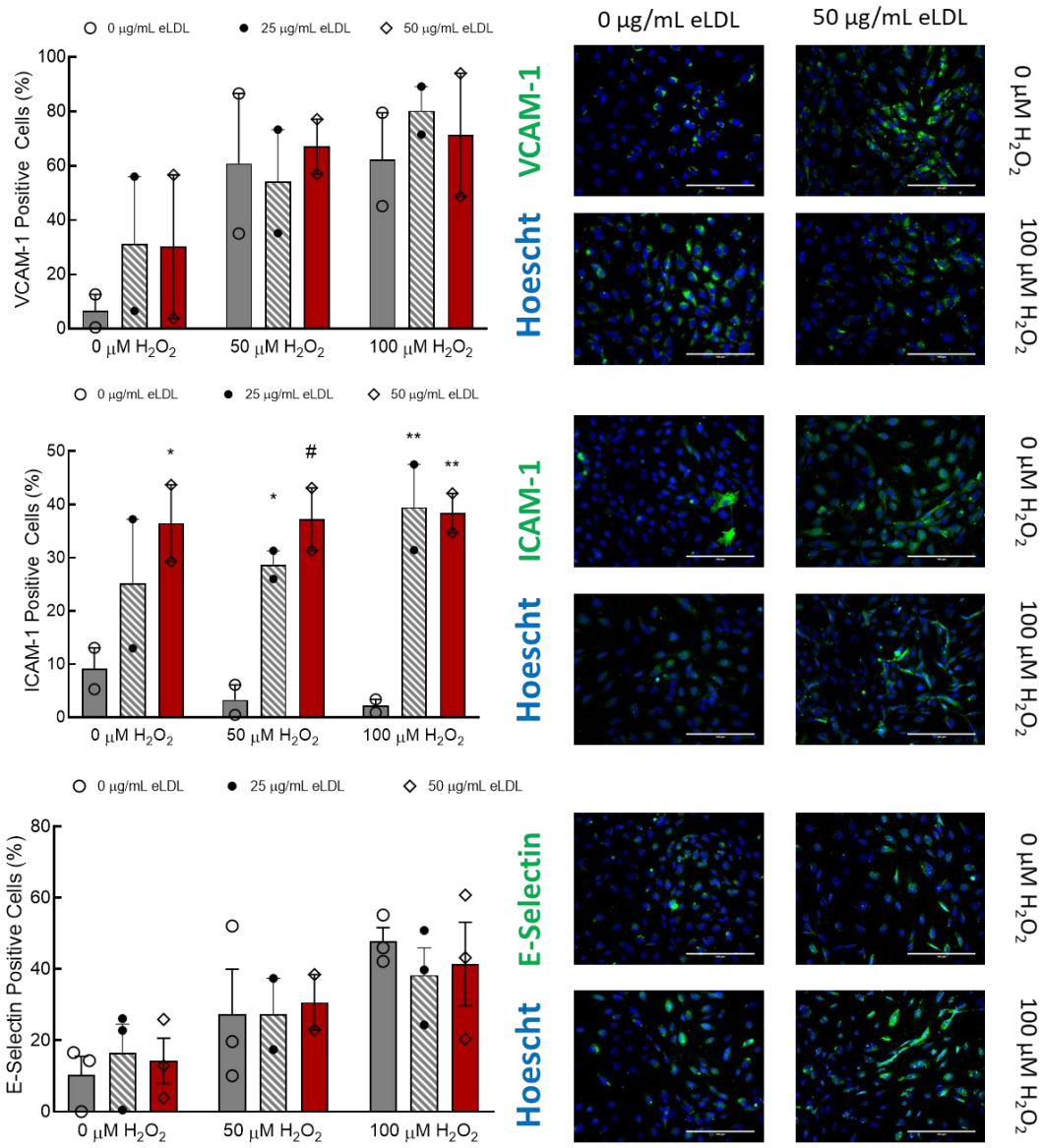

Figure 16: Treatment of CBECFCs with H_2O_2 and eLDL Maximizes Endothelial Cell Activation in 2D Cell Culture.

VCAM-1 expression was only significantly affected by H_2O_2 concentration. eLDL concentration did not increase VCAM-1 expression independently or additively with H_2O_2 treatment. ICAM-1 expression was significantly affected by eLDL only. H_2O_2 concentration did not interact with eLDL concentration to increase ICAM-1 expression additively or synergistically. E-Selectin expression was not affected by eLDL concentration. N = 2-3. Data represents mean ± SEM with individual data points overlaid. Scale bar represents 100 µm. * $p < 0.05$, # $p < 0.01$, ** $p < 0.005$ compared to 0 µg/mL for that H_2O_2 concentration.

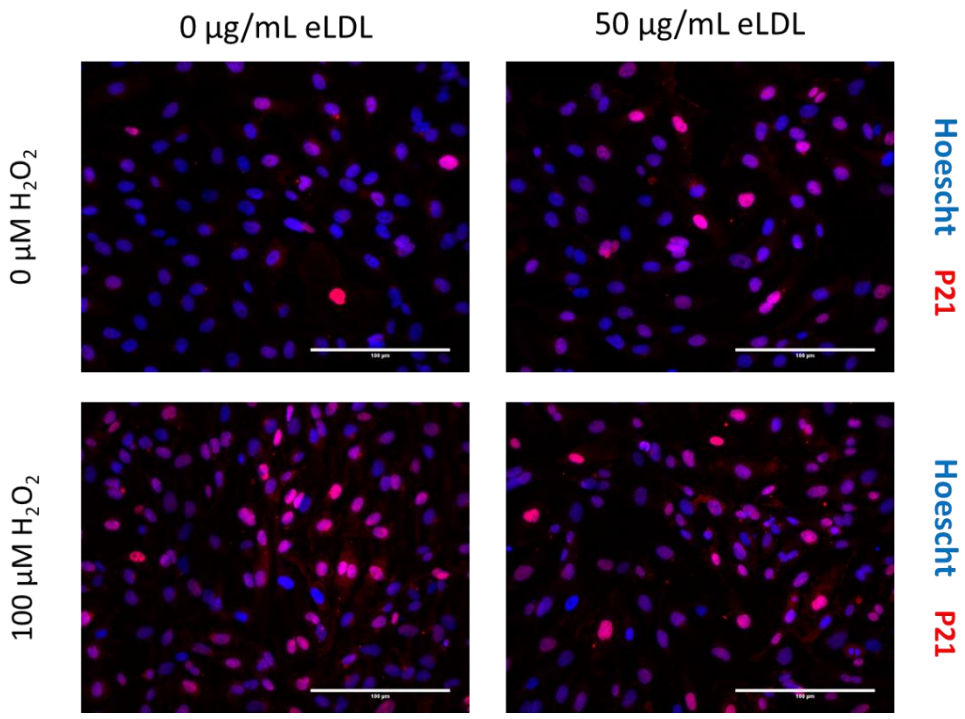

Figure 17: p21 Expression in eLDL and H_2O_2 co-treatment is Dominated by H_2O_2 Concentration.

2D CBECFCs were treated with 0 or 100 µM H_2O_2 for 7 days with 0 or 50 µg/mL eLDL during the final 24 hours of treatment. eLDL treatment didn't increase p21 expression with or without H_2O_2 treatment. Scale bar represents 100 µm.

3.3.3. hNDFs form Foam Cells After Exposure to eLDL

Low density lipoprotein was enzymatically modified to increase its inflammatory properties and increase its eventual retention within the vessel walls in TEBV experiments. Since the cells used for TEBV fabrication are hNDFs, rather than vSMCs, preliminary tests were conducted to confirm that they would accumulate eLDL in suspension. hNDFs were exposed to 0, 50, or 100 µg/mL eLDL in normal growth media for 24 hours and lipid uptake was quantified with an Oil Red O stain. hNDFs

readily absorbed both 50 and 100 μg/mL eLDL,with uptake being proportional to the concentration applied. This confirms that hNDFs are capable of retaining eLDL and that it should be possible to identify foam cell formation in the appropriate conditions within the TEBVs.

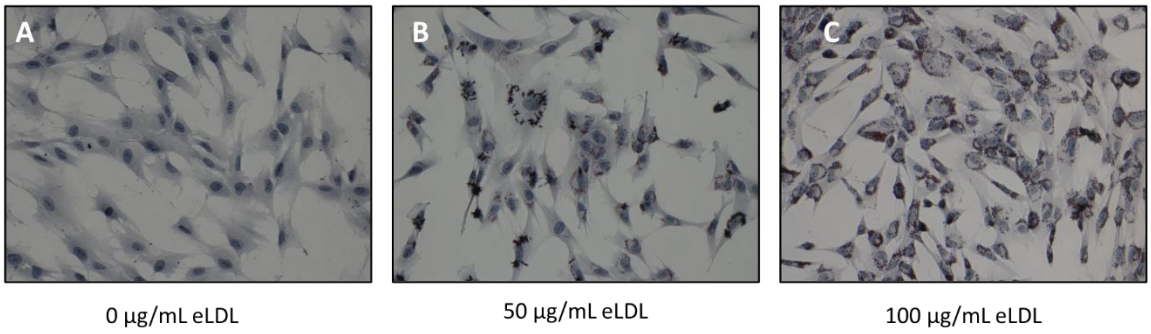

Figure 18: eLDL Uptake in hNDFs is Dose-Dependent.

hNDFs were treated with 0 (A), 50 (B), or 100 (C) μg/mL eLDL in normal growth media for 24 hours. Cells were rinsed thoroughly and then stained for lipids with Oil Red O. Uptake of eLDL occurred in both conditions, with a dose-dependent increase occurring with the higher concentration of eLDL.

3.3.4. Monocyte Adhesion is Increased in Senescent Tissue-Engineered Blood Vessels

TEBVs were matured for 7 days, then 100 μM H_2O_2 was added to the perfusion media for five days. U937 monocytes were added at a concentration of 1 x 10^6 cells/mL either for days 8-12 or days 9-12 after fabrication (Figure 19A). The control (free of eLDL, TNF, or H_2O_2), eLDL, and eLDL/TNFα conditions were perfused with monocytes for 72 hours The H_2O_2 ± eLDL conditions were perfused with monocytes for 96 hours. Monocytes were fluorescently labeled with CMPTX red for imaging after adhesion to the TEBV. Almost no monocytes adhered to the TEBV wall in the absence of pro-

inflammatory stimuli (Figure 19). When eLDL and/or TNF-α were included in the perfusion media with the monocytes, the number of monocytes adhering to the vessel wall significantly increases (Figure 19). These stimuli are pro-inflammatory, but they don't induce senescence.

To study the effect of senescence on this model specifically, monocytes were added 24 hours after introduction of 100 μM H_2O_2 to the TEBVs. TEBVs were treated with both 100 μM H_2O_2 and 1 U/mL for 96 hours (4 days), with a total of five days of H_2O_2 exposure as in prior experiments. U937 monocytes were fluorescently labeled for quantification of monocyte adhesion. Introduction of monocytes alongside 100 μM H_2O_2 increased monocyte adhesion beyond levels induced by eLDL and TNF-α (Figure 20). When eLDL is introduced alongside H_2O_2, adherent monocytes increase again. H_2O_2 alone increases expression of VCAM-1 and E-Selectin, but ICAM-1 expression is not increased unless eLDL is also administered. Increased expression oof the full spectrum of monocyte adhesion proteins within the endothelium when both H_2O_2 and eLDL are introduced is likely the reason for the increased uptake in this condition (Figure 16, Figure 20).

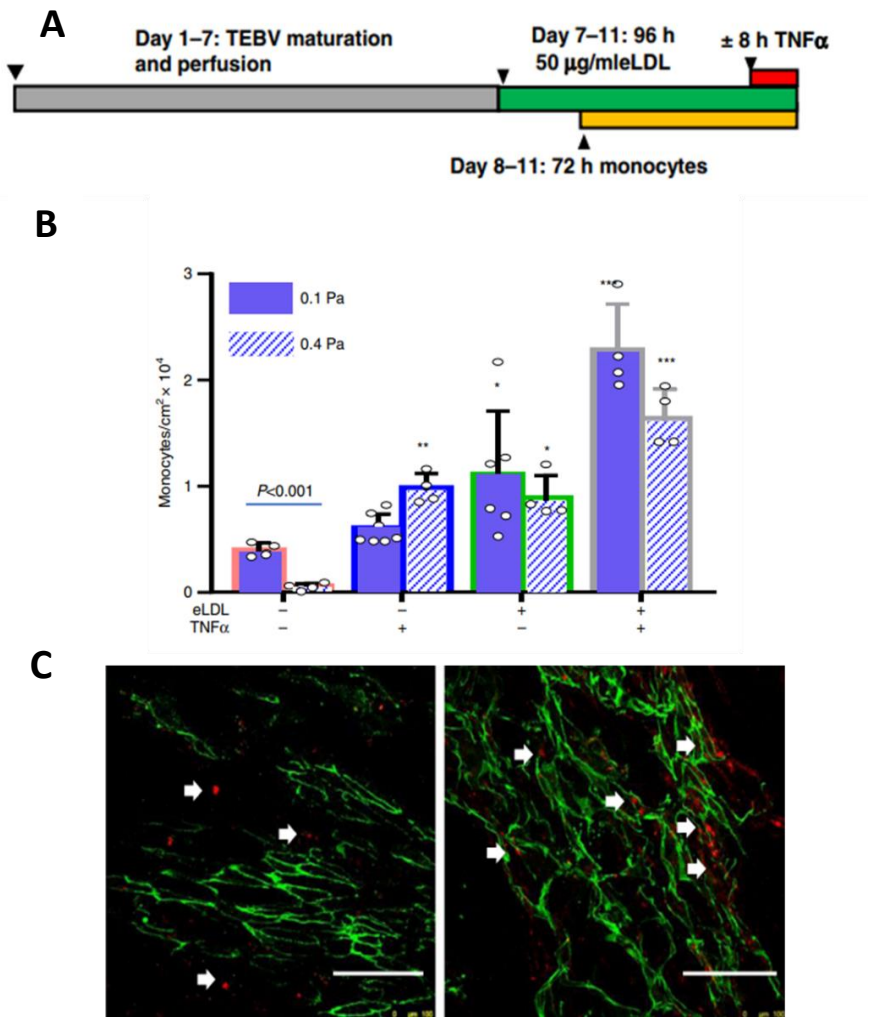

Figure 19: eLDL and TNF-α together can significantly increase monocyte adhesion in healthy TEBVs.

A: TEBVs were matured for one week then 50 µg/mL eLDL was added to the perfusion media for 4 days. Monocytes were added to the media the following day, with TNF-α added for the final 8 hours of perfusion. B: Vessels were perfused at 2 different flow rates to ensure maximal monocyte adhesion. Adhesion due to eLDL in the media was comparable to adhesion from TNF-α and combining the two had an additive effect on monocyte adhesion. C: Monocytes were fluorescently labeled with CMPTX-red Cell Tracker before introduction to the TEBV flow circuit. The endothelium is labeled with CD31 in green. Monocyte adhesion is increased when eLDL and TNF-α (C-right) than in negative controls (C-left). Scale bar is 200 µm. Data represented as mean ± SD with individual data points overlaid. N = 4-7. *P < 0.05 **P < 0.005, ***P < 0.0001 compared to -/- control.

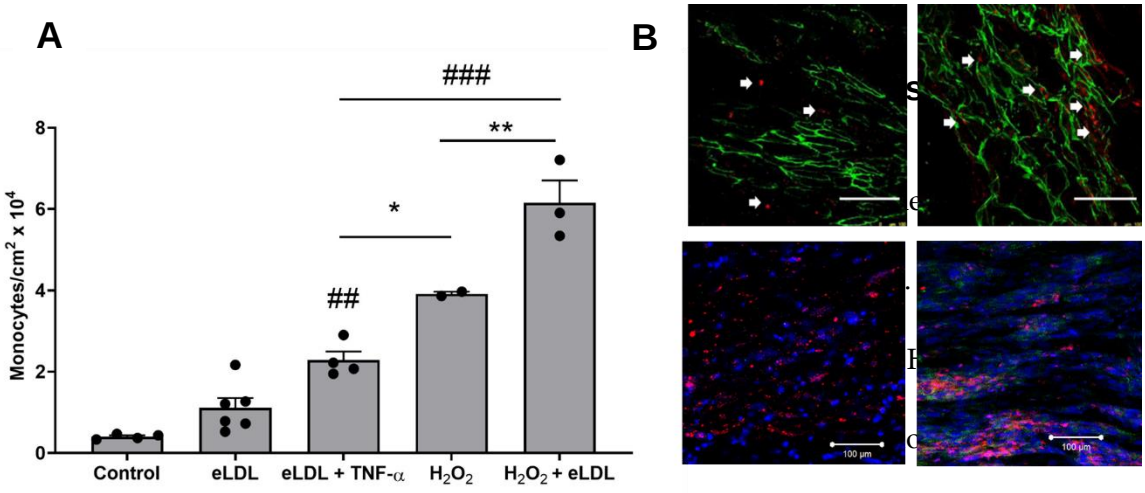

Figure 20: Monocyte Adhesion in TEBVs Treated with 100 µM H_2O_2 is Higher than in TEBVs Perfused with Control Media.

A: Control, eLDL, and eLDL + TNF-α TEBVs were exposed to 1 x 10^6 monocytes/mL for 72 hours alongside 0 or 50 µg/mL eLDL. TNF-α was added for the final 8 hours. H_2O_2 TEBVs were exposed to 100 µM H_2O_2 for a total of five days with 1 x 10^6 monocytes/mL included the final four days. The number of adherent monocytes in a given area is significantly increased compared to TEBVs not exposed to 100 µM H_2O_2. B: Representative images showing monocyte accumulation in TEBVs control conditions (top left), 50 µg/mL eLDL only (top right), 100 µM H_2O_2 (bottom left), and both 50 µg/mL eLDL and 100 µM H_2O_2 (bottom right). Red: Monocytes, Blue: Hoechst. Green: CD31. Scale bar represents 100 µm.

adhesion within the vessel wall compared to monocyte adhesion in the negative controls (Figure 19). TNF-α alone increased monocyte retention by a similar degree. Combining sustained eLDL exposure with an acute dose of TNF-α additively increased monocyte adhesion within the vessel wall (Figure 19). Foam cell formation was not quantified in TEBVs that were not treated with H_2O_2, they were stained for Oil Red O and sample images were taken to confirm a small degree of foam cell formation. The fluorescent LipidSpot Assay was used on vessels treated with 100 µM H_2O_2 and total fluorescent

area was quantified as an approximation of total foam cell formation within the vessel section. Background staining was minimal and a significant degree of lipid retention was found when eLDL was introduced to circulation (Figure 21).

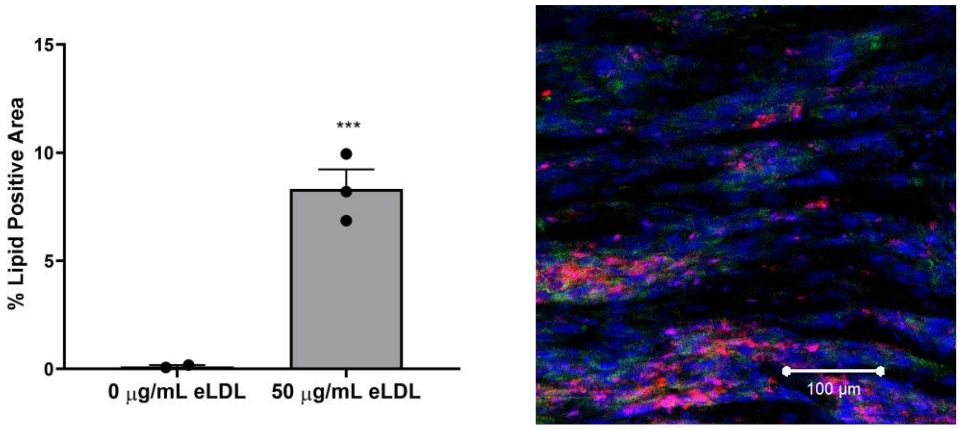

Figure 21: Monocyte Adhesion and Foam Cell Formation in TEBVs Treated with H_2O_2.

Mature TEBVs were treated with 100 μM H_2O_2 for five days. 50 μg/mL eLDL and 1 x 10^6 monocytes/mL were added for the final 4 days of H_2O_2 treatment. Adhered monocytes and foam cells were plentiful within the wall of the TEBV. eLDL-free vessels were used as a negative control to evaluate LipidSpot background staining. N = 2-3; *** P < 0.0005. Blue: Hoechst; Green: LipidSpot; Red: Monocytes. Scale bar represents 100 μm.

3.4. Discussion

In this chapter, we utilized the stress-induced senescence model previously developed to induce foam cell formation and monocyte adhesion in the TEBVs without the use of other pro-inflammatory cytokines like TNF-α. By introducing eLDL and U937 monocytes during H_2O_2 exposure the adhesion of monocytes within the vessel wall was maximized. A concentration of at least 50 μg/mL eLDL is necessary for significant lipid

uptake in the hNDFs in 24 hours (Figure 18). The increased duration of treatment when administered in TEBVs is expected to make up for the difference in initial uptake, so tests of cellular viability were performed using 50 μg/mL eLDL. Introduction of eLDL during 100 μM H_2O_2 exposure did not significantly reduce CBECFC viability, even when 50 μg/mL eLDL was added for 72 hours (Figure 14). Greater lipid uptake was observed when the concentration was increased to 100 μg/mL eLDL. However, this concentration of eLDL is likely to have a deleterious effect on the CBECFCs when administered for longer durations, particularly alongside H_2O_2. In preliminary experiments, 100 μg/mL eLDL reduced total endothelial cell number after 48 hours (data not shown). Other experiments found that combining 100 U/mL TNF-α with 100 μM H_2O_2 for 72 hours reduced total cell number as well (data not shown). Given the long exposure time necessary for robust monocyte adhesion and eLDL accumulation, using the lowest effective dose maximizes the chance that the system responses measured are due to endothelial cell senescence and inflammation, rather than outright apoptosis. 50 μg/mL eLDL and 100 μM H_2O_2 were found to be non-lethal when co-introduced for 72 hours, and total cell number was not affected by treatment (Figure 14).

eLDL was also confirmed to increase the activation of the endothelial cells, measured by expression of VCAM-1, ICAM-1, and E-Selectin, in addition to the inflammation that resulted from 100 μM H_2O_2 treatment alone. Unmodified LDL treatment caused no measurable increase in VCAM-1, ICAM-1, and E-Selectin

expression compared to the PBS control. Enzyme modification of the LDL increased its inflammatory properties significantly, though activation was still lower than acute TNF-α exposure. Expression of ICAM-1 was quantified and a significant increase compared to controls was confirmed (Figure 15).

100 μM H_2O_2 alone increased VCAM-1 and E-Selectin expression significantly but had no effect on ICAM-1 expression in 2-D cell culture (Figure 6). VCAM-1 expression was also increased within the TEBVs, but E-Selectin expression was not examined in TEBVs (Figure 11). Since eLDL increased expression of all adhesion molecules studied here, co-treatment with H_2O_2 should produce greater overall inflammation by fully activating expression of each adhesion molecule measured rather than only partially increasing expression of some of them. In particular, expression of ICAM-1 was significantly increased when both H_2O_2 and eLDL were present, compared to H_2O_2 concentration alone which had no effect on ICAM-1 expression (Figure 16). eLDL concentration did not have a significant effect on VCAM-1 or E-selectin expression (Figure 16). Expression of these adhesion molecules appears to have been maximized by 100 μM H_2O_2 exposure alone.

This was borne out in the degree of monocyte adhesion observed in the TEBVs treated with both eLDL and 100 μM H_2O_2 compared to those exposed to 100 μM H_2O_2 only. This suggests that VCAM-1 and E-Selectin expression is of similar importance to

ICAM-1 expression in determining monocyte adhesion, rather than one dominating adhesion more than the other.

TEBVs fabricated in an alternate vessel system accumulated very few monocytes within the vessel wall in the absence of 100 μM H_2O_2. Even the introduction of 100 μg/mL eLDL to the perfusion media for 48 hours failed to significantly increase monocyte adhesion. It was necessary to either expose these vessels to 50 μg/mL eLDL for 96 hours or use a combination of 50 U/mL TNF-α and 50 μg/mL eLDL to significantly increase monocyte adhesion in the vessel wall (Figure 19). In TEBVs treated with 100 μM H_2O_2, monocytes accumulated readily within the vessel wall without addition of any other pro-inflammatory stimuli. When eLDL was also introduced to the perfusion media, monocyte adhesion was increased even further.

Foam cell formation was also identified in vessels exposed to 100 μM H_2O_2, eLDL, and monocytes. To identify foam cells present, TEBV sections were stained with the LipidSpot solution and imaged immediately. Co-localization of lipids, nuclei, and CMPTX-labeled monocytes was used to identify formation of hNDF and monocyte foam cells within the vessel wall. From the 2-D pilot tests conducted, it is clear that hNDFs will consume nearby eLDL even in the absence of hydrogen peroxide (Figure 18). Further experiments will elucidate the degree to which the hNDFs present in the TEBV will spontaneously consume circulating eLDL in the absence of H_2O_2. The bulk of lipids identified by the LipidSpot stain were located within the hNDFs. This is most likely due

to the higher fraction of hNDFs comprising the vessel wall compared to a much smaller number of monocytes adhering to and migrating through the vessel wall. Lipid particles were found co-localized with both hNDFs and the adhered monocytes, indicating that foam cells of both cell types are present. The development of these lipid and monocyte rich regions within the vasculature indicates that early atherosclerotic lesions are forming within the systems after only 4 days of treatment with the full mixture of H_2O_2, eLDL and monocytes. In this time span, monocytes were able to disperse widely throughout the vasculature, although clear clusters are present. Similarly, lipids were distributed nearly homogenously throughout the vessel wall with the exception of some particularly dense clusters.

The atherosclerotic lesions formed in this model are in their infancy. They occupy a relatively small volume within the vessel wall. No signs of plaque are visible on the exterior of the vessel, aside from some discoloration in patches which did not seem to correspond to areas of greater monocyte and lipid staining when imaged microscopically. Since the toxicity of this atherogenic cocktail is estimated to be low, future experimentation could focus on prolonging exposure to create larger and more robust atherosclerotic lesions within the vessel wall. Changes in the diameter of the vessel lumen (i.e. experiments to check for occlusion) could be quantified non-destructively by examining differences in fluid velocity or flow rate upon exiting the chamber. This would also present the opportunity to identify whether this model is able

to replicate the increased presence of senescent cells within large, stabilized atherosclerotic plaques or if the degree of senescence throughout the endothelium is too high to identify a localized increased due to the H_2O_2 in the perfusion media.

3.5. Chapter-Specific Acknowledgments

We thank Hailee Patel, Jason Breithaupt, Ellery Jones, and Kevin Shores for aiding in preparing enzyme-modified LDL solutions. We thank Xu Zhang for his work in developing many protocols for administering LDL and monocytes to TEBVs and generating data that were used for baseline comparisons (seen in Figure 19) to data collected here. We also thank Varun Prasad for performing Oil Red O staining on hNDFs in 2-D to confirm eLDL uptake (seen in Figure 18).

4. Geroprotective Drugs Improve Vasoreactivity and Exhibit an Atheroprotective Effect on Senescent TEBVs

4.1. Introduction

The accumulation of senescent cells in tissues precipitates a variety of health conditions, atherosclerosis being one that affects a large portion of the global population[34]. Endothelial cell senescence is primarily the result of environmental stressors, rather than repeated cell replication as endothelial cells exist in a quiescent state absent other pathology[42,127]. For example, sustained hyperglycaemia can increase p21 and p53 expression within vascular endothelial cells, activating the SASP and leading to vascular inflammation[137]. This meta-inflammatory state often results in an accelerated atherosclerotic lesion growth in diabetic patients[138]. Inflammation itself can also be a cause of stress-induced senescence within the endothelium, a phenomenon known as cytokine-induced premature senescence (CIPS)[36]. Sustained exposure to as little as 10 ng/mL TNF-α can significantly increase the senescence of an endothelial cell population[36]. Here we focus on the use of reactive oxygen species (ROS) to induce oxidative stress-induced senescence within endothelial cells. H_2O_2 has been used to induce senescence in a number of endothelial cell lines and primary cells, including HUVECS and HAECs, as well as blood-derived endothelial colony forming cells used here[91,98]. Regardless of the exact source of senescence, it results in activation of the SASP and increased in expression of adhesion molecules like VCAM or ICAM[67]. This increases adhesion of circulating monocytes to the vessel lumen, followed by their migration into

the vessel intima. Circulating lipids also accumulate in the vessel intima where they are taken up by monocytes and vSMCs which then transition to foam cells[20,121].

Pharmaceutical intervention to reduce morbidity and mortality from atherosclerosis mainly target blood lipid levels (e.g. statins and cholesterol lowering drugs) or blood pressure (e.g. Ace inhibitors, β-blockers, etc.)[122]. More recently, anti-inflammatory drugs have been tested to reduce atherosclerotic lesion formation or stabilize plaques, as in a trial with an anti-IL-1β therapeutic that reduced the incidence of adverse cardiovascular events[126]. Despite their great potential, other anti-inflammatory treatments have proven marginally effective, if having an effect at all[139]. Given the evidence that stress-induced senescence has an effect on inflammation, and senescent cells have been found in large atherosclerotic plaques, geroprotective and senolytic drugs may help address the inadequacies of current anti-inflammatory treatments.

Senolytics encourage apoptosis in senescent cells which are otherwise resistant to apoptosis by disabling the pro-survival pathways that prolong their life[56,140]. Importantly, they don't cause apoptosis in non-senescent cells[141]. Dasatinib and quercetin were two of the first senolytics approved. They both target ephrin receptors which inhibit the PI3K pathway[57,62]. Unlike other treatments which focus on inhibiting inflammation directly, senolytics like dasatinib and quercetin have the potential to

reduce inflammation even after the drug has been fully metabolized by inhibiting the SASP and encouraging apoptosis of senescent cells[62].

Senomorphic or geroprotective drugs share common effectors with senolytics, but don't promote autophagy in the same way[142]. Chief among these is rapamycin which inhibit the mTOR pathway, resulting in decreased levels of IL-2 and improved cell viability[143,144]. Where senolytics transiently inhibit senescent cell anti-apoptotic pathways (SCAPs), rapamycin and similar geroprotective drugs inhibit both apoptosis and the SASP[67]. In this work, we explored treating the TEBVs with tacrolimus, a rapamycin analog which is used to suppress inflammation after organ transplantation and in drug-eluting stents[145]. Tacrolimus binds to intracellular FK-506, subsequently blocking the function of calcineurin and ultimately suppressing NF-AT-dependent cytokine gene transcription[146].

Senolytics and senomorphics have the potential to significantly improve the healthspan of patients living with atherosclerosis. In this work, we evaluated several dosing schemes for dasatinib, quercetin, tacrolimus, and a cocktail of dasatinib and quercetin on CBECFCs growing in 2-D during and after H_2O_2 treatment and evaluated the effect on senescence and inflammation within the cells. We then proceeded to treat TEBVs exposed to 100 μM H_2O_2 with tacrolimus during and after H_2O_2 exposure. Studying the application of these drugs in TEBVs exposed to oxidative stress allows us

to confirm that senolytics are effectively removing senescent cells from the vessel lumen. We can also confirm that this results in a reduction in adhesion molecule expression.

4.2. Methods

4.2.1. Cell Culture

Human cord blood derived endothelial colony forming cells (CBECFCs) were isolated as previously described[104]. Isolation and culture protocols for CBECFCs were approved by the Duke University Institutional Review Board. Human umbilical cord blood samples were obtained from the Carolina Cord Blood Bank. Patient identifiers were removed prior to receipt.

After receipt, blood is diluted 1:1 with Hanks Buffered Salt Solution (HBSS, Invitrogen). The diluted blood sample is layered slowly atop an equal volume of room temperature Histopaque 1077 (Sigma) and centrifuged at 740 g for 30 minutes. Buffy coat mononuclear cells were removed and washed with Endothelial Cell Growth Medium (Cell Applications) containing 1% penicillin/streptomycin solution (Gibco). The mononuclear cells are centrifuged at 515 g for 10 minutes and resuspended in endothelial cell culture media three times and plated on TCPS six-well plates coated with 50 μg/mL rat tail collagen I. Media is changed daily for the first 7 days of culture and every 48 hours after. Colony formation is visible after 7-10 days of culture. Flow cytometry is used to confirm purity of the resulting endothelial cell population. Cells are harvested at P4. After resuspending cell samples in 10% goat serum, 5 μL of the

appropriate antibody is added to a 95 μL sample containing 500,000 cells. Cells are then fixed with 0.5% PFA, rinsed, and resuspended in DPBS. 9,000 events per sample are recorded.

Human neonatal dermal fibroblasts (hNDFs) are purchased from Lonza. They are grown in high glucose Dulbecco's modified eagle medium (Invitrogen) supplemented with 10% vol/vol heat inactivated fetal bovine serum (Gibco), 1% penicillin/streptomycin (Gibco), 1% MEM non-essential amino acids (Gibco), 1% sodium pyruvate (Gibco), 1% GlutaMAX (Gibco), and 0.1% β-Mercaptoethanol (ThermoFisher). Media is changed every 48 hours.

Monocytes used are the human U937 cell line (Sigma). Cells are maintained in RPMI-1640 containing 1% L-Glutamine (Sigma) supplemented with 10% Heat-Inactivated Fetal Bovine Serum (HI-FBS, Gibco). Media is changed every 48-72 hours.

4.2.2. TEBV Fabrication

Tissue engineered blood vessels (TEBVs) were made as previously described[103]. Rat tail collagen I (BD Biosciences) is diluted to a concentration of 2.05 mg/mL in 0.6% acetic acid comprising 80% of the total volume of the TEBV solution. 10X serum-free Dulbecco's Modified Eagle's Medium (DMEM, Sigma) was added to make up 10% of the total TEBV volume. The mixture is then titrated to a pH of 8.5 with 5M NaOH. A solution of hNDFs at a concentration of 5×10^6 cells/mL is added comprising the final 10% of the TEBV volume and leading to a final density of 0.5×10^6 hNDFs/mL in the

TEBV. After mixing, the gel solution was poured into a 3 mL luer-lok syringe (BD Biosciences) stoppered with a closed two-way stopcock. To create a tubular collagen scaffold, an 810 μm diameter steel mandrel is inserted into the center of the syringe mold and held in place with parafilm. The solution gels at room temperature over 30 minutes.

After gelation is complete, the gel and mandrel are removed from the syringe mold and laid on a 0.8 μm pore Nylon membrane filter (Whatman) atop 10 autoclaved Kim Wipes. The TEBV rests there for 8-10 minutes until ~90% of the water has been removed. The nylon filter and TEBV are then transferred to a 150 mm petri dish filled with sterile PBS to facilitate easier removal of the filter and lubricate the PBS for removal from the mandrel. Next, the TEBV is mounted in an acrylic chamber with hollow grips (0.711 μm outer diameter, McMaster-Carr) on each end of the vessel to allow perfusion of the vessel lumen. Black silk sutures hold the TEBV in place on the grips (Figure 3A). Next, a solution of 500,000 ECFCs suspended in endothelial cell growth media is slowly pushed through the vessel lumen. The vessel is rotated for 60 minutes at a speed of 10 rph to ensure uniform monolayer adhesion. TEBVs are perfused with TEBV growth media at a flow rate of 0.5 mL/min for the first 24 hours after fabrication, then the flow rate is increased to 2 mL/min for the remainder of the experiment (Figure 3B). This results in a laminar shear stress of 6.8 dynes/cm^{2}[103]. TEBV perfusion media contains low glucose DMEM, 1% penicillin/streptomycin, 1% MEM non-essential amino acids, 0.1%

β-Mercaptoethanol, and 3.7% heat-inactivated fetal bovine serum for the first week of culture. After one week of culture, 2mg/mL ε-aminocaproic acid was added to preserve the long-term integrity of the TEBV.

Perfusion circuits for experiments exploring the effects of tacrolimus on recovery of endothelium-dependent vasoreactivity after H_2O_2 treatment were made using L/S 14 tubing (MasterFlex) and a reservoir with a maximum capacity of 50 mL. The total volume in the flow circuit and TEBV chamber during these experiments was 30 mL. Perfusion circuits for experiments containing eLDL and monocyte were made using L/S 13 tubing (MasterFlex) and a reservoir with a maximum capacity of 30 mL. The total volume in the flow circuit and TEBV chamber during the first week of perfusion is 20 mL. This volume is reduced to 13 mL total while monocytes and enzyme modified low-density lipoprotein is added to the perfusion circuit.

4.2.3. Hydrogen Peroxide Treatment

H_2O_2 is diluted from a 30% stock solution (9.77 M) to 100 μM in the ε-aminocaproic acid-supplemented TEBV growth medium. Media is changed 24 hours after the first time adding H_2O_2 to media, and every 48 hours thereafter until TEBVs are fixed. Solutions are prepared fresh from the 9.77 M stock every time.

4.2.4. Preparation and Modification of Low-Density Lipoproteins

Human plasma LDL (Sigma) is prepared for storage and use by first quantifying protein concentration with the Lowry Assay (Lee Biosolutions). The solution is diluted

to a concentration of 10 mg/mL in 10% sucrose (w/v) saline solution (150 mM NaCl, 0.24 mM EDTA, pH 7.4) for immediate use or storage at -80˚C[135]. Methods for enzyme modification were adapted from Chelian et al[136]. Aliquots of LDL are first dialyzed against a saline solution (150 mM NaCL, 0.24 mM EDTA, pH 7.4) for approximately 24 hours, refreshing the buffer 3 and 6 hours after the beginning of the dialysis. After confirming the new concentration of protein in the solution, trypsin is added at a concentration of 7 μg per mg LDL for 6 hours at 37˚C. 12 μg cholesterol esterase per mg LDL is then added at 37˚C for 10 hours. Next, 24 μg trypsin per mg LDL is added for 6 hours at 37˚C. Finally, 29 μg cholesterol esterase per mg LDL is added for 48 hours at 37˚C. This final solution is dialyzed against 1X DPBS (pH 7.4) for at least 24 hours. Particle uniformity is confirmed with a ZetaSizer particle analyzer to confirm enzyme modification has occurred for the entire solution. The solution is then passed through a 0.2 μm filter for sterilization and the final protein concentration is quantified using the Lowry Assay once more. The solution must be used within two weeks to avoid spontaneous oxidation of the LDL.

4.2.5. Administration of Senolytics

Tacrolimus (FK-506 monohydrate) is received as a lyophilized powder (Millipore Sigma). The lyophilized powder is dissolved in DMSO to a concentration of 10 mg/mL (12.15 mM). This solution is diluted to 1 mM in DPBS and filtered through a 0.2 μm pore filter to sterilize. This solution is aliquoted and stored at -20˚C for use up to 3 months

after dilution. This solution is diluted to a working concentration of 0.1 nM to 100 nM in endothelial cell growth media or endothelial growth media containing 100 µM H_2O_2 and added to CBECFCs growing in 2-D monoculture for 24 hours. To test for drug-responsiveness, TEBVs were treated with 10 nM tacrolimus for either the final 48 hours of 100 µM H_2O_2 exposure or for 48 hours after the removal of H_2O_2. It was also administered as a 10 nM dose for the duration of H_2O_2 exposure to evaluate its atheroprotective capacity.

Dasatinib is received at a lyophilized powder (Millipore Sigma). It is dissolved in DMSO at a concentration of 5 mM (2.44 mg/mL) and sterilized by passage through a 0.2 µm pore filter. This solution can be stored at -20˚C for up to six months after dissolution. The 5 mM stock is diluted to concentrations ranging from 0.1 nM to 10 µM in endothelial cell growth media and added to CBECFCs in 2-D monoculture for 24-48 hours. Dasatanib was added after removal of H_2O_2 to evaluate whether it can enhance recovery and during H_2O_2 treatment to explore its capacity to protect against stress-induced senescence.

Quercetin is received as a lyophilized powder (Millipore Sigma). It is dissolved to 30 mg/mL in pure DMSO and further dissolved to 1 mg/mL (3.30 mM) in a 1:4 DMSO:PBS solution. This solution is diluted to a treatment concentration of 0.1 nM – 100 nM and added to CBECFCs in 2-D monoculture for up to 48 hours. Quercetin was also

added in combination with Dasatinib. The quercetin solution is stable for 24 hours after preparation.

4.2.6. Analysis of TEBV Vasoreactivity

TEBV vasoreactivity is quantified in response to phenylephrine, acetylcholine, and sodium nitroprusside. 1 mM stock solutions of each drug are prepared by diluting lyophilized powders in sterile DPBS without calcium or magnesium. This 1 mM solution is injected into the reservoir of the TEBV flow circuit via a silicone injection port integrated into the perfusion tubing. A 1 μL/mL dilution is used, resulting in a dose of 1 μM in the flow circuit. These doses are expected to elicit about half the maximum vasodilation or vasoconstriction of the TEBVs. TEBV diameter equilibrates after introduction of phenylephrine for five minutes. Next, acetylcholine is injected, and the diameter change is quantified after five minutes. Finally, sodium nitroprusside is added to the flow circuit and the diameter change is quantified after 8 minutes. Diameter changes are recorded on video with a stereo microscope equipped with a 0.5x magnification lens using ISCapture. Still shots are selected from these videos at the time points described above (300 seconds after phenylephrine injection, 300 seconds after acetylcholine injection, and 480 seconds after sodium nitroprusside injection). The diameter at the time of phenylephrine injection is used as a baseline. The still images are quantified using the line tool in ImageJ. Five points evenly spaced along the TEBV are randomly selected to measure the diameter. The same points along the TEBV are used to

measure the diameter change in response to each drug. A typical TEBV has a baseline diameter of 1500-2000 μm corresponding to about 150-250 pixels in ImageJ.

TEBV vasoreactivity is first quantified 7 days after fabrication to evaluate baseline vasoreactivity and confirm appropriate function of the TEBV. For this initial test of vasoreactivity, only phenylephrine and acetylcholine are used. If vasoconstriction and vasodilation do not exceed -1% and 1% respectively, the vessel is not used for further study. In the data presented here, this test is called "Day 0" and further tests of vasoreactivity are described using the number of days after this initial test of vasoreactivity, rather than the total number of days since vessel fabrication. H_2O_2 is added after a vessel passes this initial test of vasoreactivity on Day 7 and vasoreactivity is measured again on Day 5 or Day 7 of H_2O_2 treatment with acetylcholine, phenylephrine, and sodium nitroprusside.

4.2.7. Fluorescent Labeling of Monocytes

Human U937 monocytes are harvested from suspension by centrifugation at 300 xg for 10 minutes. Cells are then resuspended in serum-free RPMI 1640 containing 1% L-glutamine at a concentration of 2×10^6 cells/mL and incubated with a 4.2 μM solution of CMPTX red in DMSO for 30 minutes. The cells are centrifuged again at 300 xg for 10 minutes and resuspended in normal growth medium to remove excess dye from the cells. Monocytes should be used within 48 hours after staining for maximum retention of fluorescence. Monocytes are introduced to perfusion media in 500 μL of TEBV growth

media to produce a final concentration of 1 x 10^6 monocytes/mL in the total volume of the perfusion circuit.

4.2.8. Immunofluorescence

Cells in well plates are fixed with 10% formalin for 10 minutes at room temperature. Cells are permeabilized with 0.1% Triton-X and then blocked with 10% goat serum (Gibco) in DPBS. Primary antibodies for P21 and VCAM-1 (Abcam) were diluted 1:250 in 10% goat serum. Primary antibodies for E-Selectin and ICAM-1 (SCBT) were diluted 1:200 in 10% goat serum. After staining overnight at 4°C, samples were rinsed 3 times with DPBS. Goat anti-rabbit Alexa-Fluor 594 or goat anti-mouse Alexa-Fluor 488 secondary antibodies were added at a dilution of 1:500 in 1% Goat serum with 1 μL/mL Hoechst 33342 for 1 hour at room temperature. Samples were rinsed an additional 3 times in DPBS and imaged within 24 hours. Samples were imaged on a Zeiss 510 inverted confocal microscope at 10X magnification.

TEBVs are fixed before being removed from the chambers in 10% formalin for one hour at room temperature. The section of vessel between the two grips where a full endothelial layer is present is excised from the larger vessel and rinsed three times in DPBS. The vessel is then cut into smaller sections for each stain that is necessary before further processing. Vessel sections are transferred to a 48-well plate and permeabilized with 0.1% Triton-X and then blocked with 10% goat serum (Gibco) for 8 hours at room temperature. Primary antibodies for P21 (Abcam), VCAM-1 (Abcam), and von

Willebrand Factor (vWF, Abcam) are diluted 1:100 in 1% goat serum. After incubating overnight at 4°C, samples are rinsed 3 times with DPBS waiting 5 minutes between rinses. Goat anti-rabbit Alexa-Fluor 594 and goat anti-mouse Alexa-Fluor 488 secondary antibodies were added at a dilution of 1:500 in 1% Goat serum with 1 μL/mL Hoechst 33342 for 1 hour at room temperature. Samples were rinse an additional 3 times in DPBS, waiting 10 minutes between rinses. TEBV sections were mounted on glass slides with Fluor Save, covered with a cover slip, and imaged on a Zeiss 510 inverted confocal microscope at 20X magnification.

4.2.9. Statistical Analysis

Statistical analyses were performed using GraphPad Prism 8. One-way or two-way ANOVA with post-hoc Dunnett's test were used to compare means for all immunofluorescence quantification. A repeated measures ANOVA with post-hoc Tukey's test was used to compare means for all TEBV vasoreactivity data. P values less than 0.05 were considered significant. All data shown graphically represent mean ± SEM. N represents the number of independent experiments.

4.3. Results

4.3.1. The Effects of Tacrolimus, Dasatinib, and Quercetin on Senescence and Inflammation in CBECFCs Recovering from Stress-Induced Senescence

One senomorphic, tacrolimus, and two senolytics, dasatinib and quercetin, were tested for efficacy at reversing senescence and inflammation in 2D cell culture. CBECFCs

were seeded in well plates and 100 μM H_2O_2 was added 24 hours after seeding. H_2O_2 exposure lasted a total of seven days. Tacrolimus, dasatinib, quercetin, or a combination of dasatinib and quercetin were added for 24 hours after the removal of H_2O_2. Cells were then evaluated for senescence and inflammation by immunofluorescent staining for p21 and VCAM-1. The effect of tacrolimus and quercetin when introduced during the final 24 hours of H_2O_2 were also evaluated. Concentrations ranging from 0.1 nM to 100 nM were tested to explore the widest range of treatment conditions that are likely to work.

Tacrolimus treatment resulted in a visible decrease in p21 expression when applied in a co-treatment scheme (i.e. introduced during the final 24 hours of H_2O_2 exposure). However, only p21 expression was decreased. VCAM-1 expression was high across all concentrations of tacrolimus (Figure 22A). When tacrolimus was applied after the removal of H_2O_2, the reduction in p21 positive cells was less pronounced. However, VCAM-1 expression did decrease noticeably in this treatment regime (Figure 22B).

The senolytic quercetin was also administered to CBECFCs in both a co-treatment and recovery dosing regime. Quercetin treatment also had a noticeable effect on p21 expression when administered alongside H_2O_2 during the final 24 hours of H_2O_2 exposure. VCAM-1 expression decreased slightly with treatment of any concentration of quercetin but did not increase with dose. Additionally, this manifested as a reduction in the intensity of VCAM-1 staining rather than a large decrease in the number of VCAM-1 positive cells (Figure 23A). When quercetin was administered during a 24-hour recovery

period, p21 expression was not noticeably reduced. However, VCAM-1 expression was decreased to a greater degree compared to the co-treatment condition for the same concentrations of quercetin (Figure 23).

Dasatinib was also administered to CBECFCs for 24 hours at the conclusion of a 7-day treatment with 100 μM H_2O_2 and p21 expression was evaluated. Many nuclei still stained positive for p21 even with 100 nM dasatinib treatment, indicating a high percentage of senescent cells still present (Figure 24). When dasatinib was administered alongside quercetin for 24 hours as CBECFCs recover from 7 day 100 μM H_2O_2, quercetin concentration dominated the degree of p21 expression. 10 nM quercetin reduced the number of p21 positive cells alongside 1 nM or 10 nM dasatinib (Figure 25). Since tacrolimus had the most consistent, significant effect on both senescence and VCAM-1 expression in the CBECFCs, it was selected as the drug to use in the following TEBV experiments. Further evaluation of the appropriate dosing scheme for a cocktail of quercetin and dasatinib is necessary before application to a TEBV model.

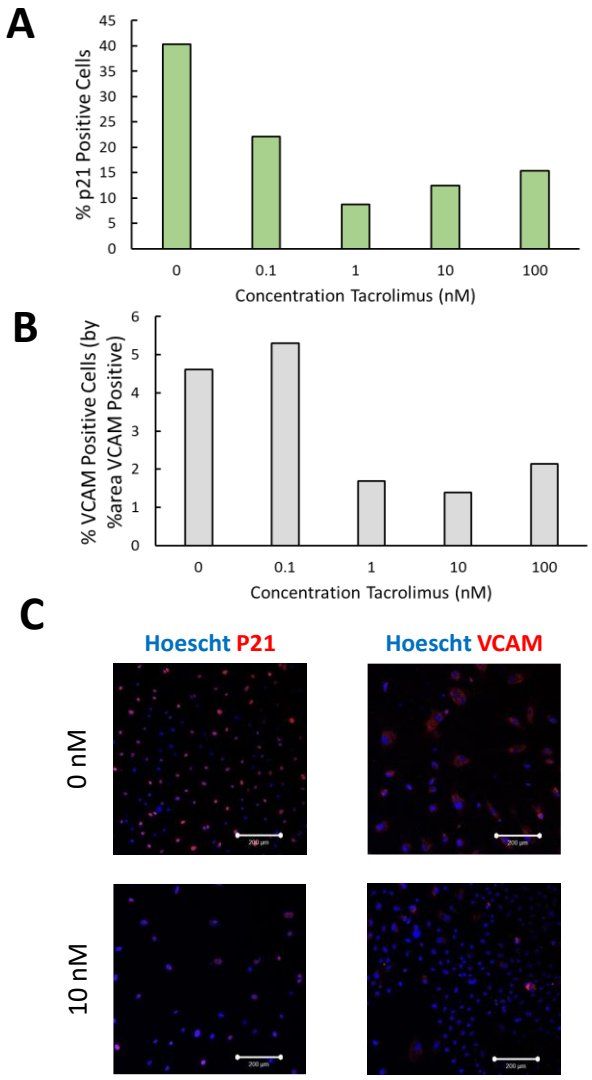

Figure 22: Tacrolimus Reduces the Number of Senescent and VCAM-1 Positive Cells After Oxidative Stress-Induced Senescence.

A: CBECFCs were treated with 100 μM H_2O_2 for a total of seven days, with tacrolimus being added to the media at the specified concentration for the final 24 hours of H_2O_2 exposure. P21 expression was noticeably reduced when concentrations of 1 nM or higher were used. However, VCAM-1 expression was not affected by tacrolimus treatment. B: CBECFCs were treated with 100 μM H_2O_2 for 7 days and then treated with the specified concentration of quercetin for 24 hours after removal of H_2O_2. In this treatment regime, p21 expression only decreased with concentrations of 10 nM or higher. VCAM-1 expression decreased with doses of 1 nM or higher. Scale bar indicates 200 μm.

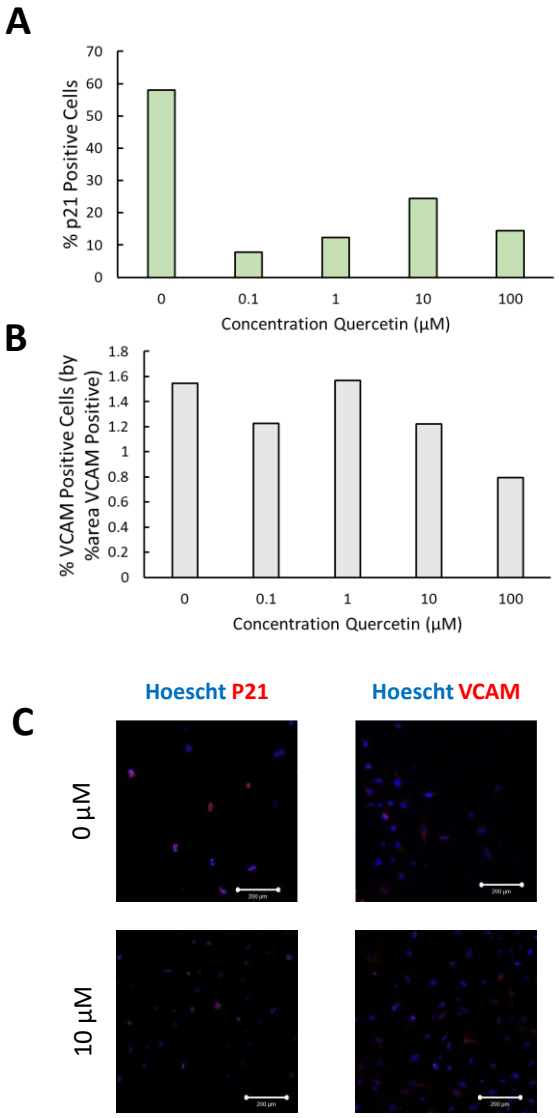

Figure 23: Quercetin Treatment Has Mixed Effects on Stress-Induced CBECFC Senescence and Inflammation.

A: CBECFCs were treated with 100 μM H_2O_2 for six days. Then they were exposed to 100 μM H_2O_2 and the specified concentration of quercetin for 24 hours and stained for p21 or VCAM-1. This co-treatment resulted in a decrease in p21 expression when 1 nM quercetin was used, but many cells still stained positive for VCAM-1. B: CBECFCs were treated with 100 μM H_2O_2 for 7 days and then treated with the specified concentration of quercetin for 24 hours after removal of H_2O_2. Neither p21 nor VCAM-1 expression were affected by the dose of quercetin applied. N = 1. Scale bar indicates 200 μm.

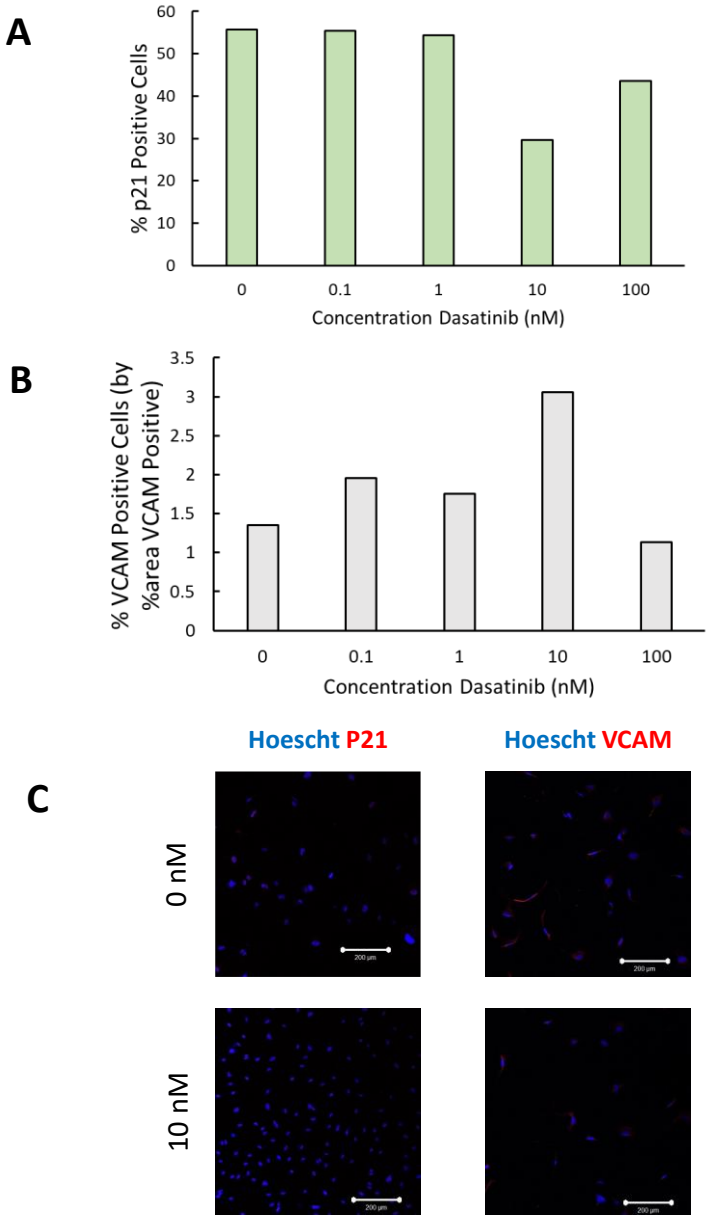

Figure 24: Dasatinib Treatment Minimally Effects CBECFC Inflammation and Senescence.

CBECFCs were treated with 100 μM H_2O_2 for 7 days to induce senescence and inflammation. Dasatinib was then added to the cells for 24 hours at the specified concentration. P21 and VCAM-1 expression were not significantly affected by dasatinib treatment. N = 1. Scale bar represents 200 μm.

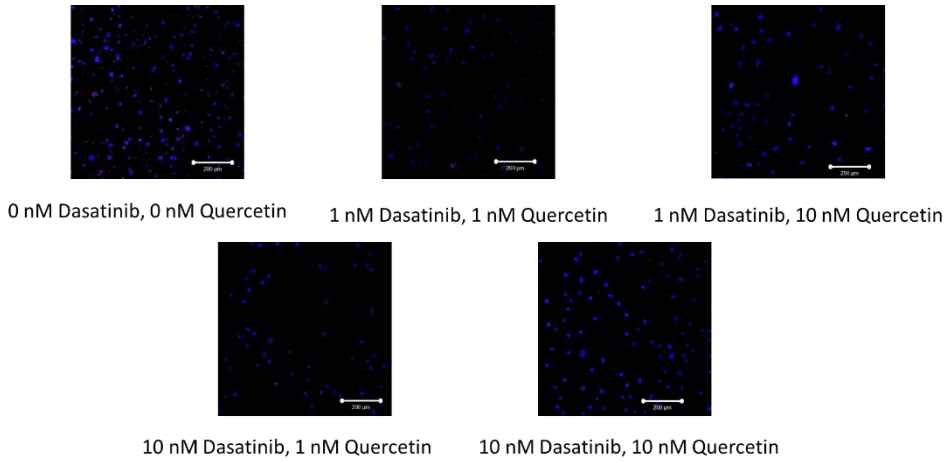

Figure 25: Treatment with a Dasatinib and Quercetin Cocktail Matches the Response of Quercetin Alone.

CBECFCs were exposed to 100 μM H_2O_2 for 7 days and then exposed to the specified concentrations of dasatinib and quercetin for 24 hours after removal of H_2O_2. Quercetin concentration had a dominant effect on the number of p21 positive cells. Dasatinib continued to have a negligible effect. Blue = Hoechst. Red = p21. Scale bar represents 200 μm.

4.3.2. Introduction of Tacrolimus After Removal of H_2O_2 Enhances Recovery of Endothelium-Dependent Vasoreactivity in TEBVs

TEBVs were matured for 7 days in normal growth media and then treated with 100 μM H_2O_2 on Days 7-12 after fabrication. After vasoreactivity testing on Day 12, vessels were either allowed to recover in control media (control recovery), given tacrolimus alongside continuing H_2O_2 treatment (co-treatment), or allowed to recover in media containing 10 nM tacrolimus (tacrolimus recovery). Final vasoreactivity testing is conducted on Day 14. A repeated measures ANOVA confirms that neither hydrogen peroxide, senolytic treatment, nor time affected vasoconstriction due to phenylephrine (Figure 26).

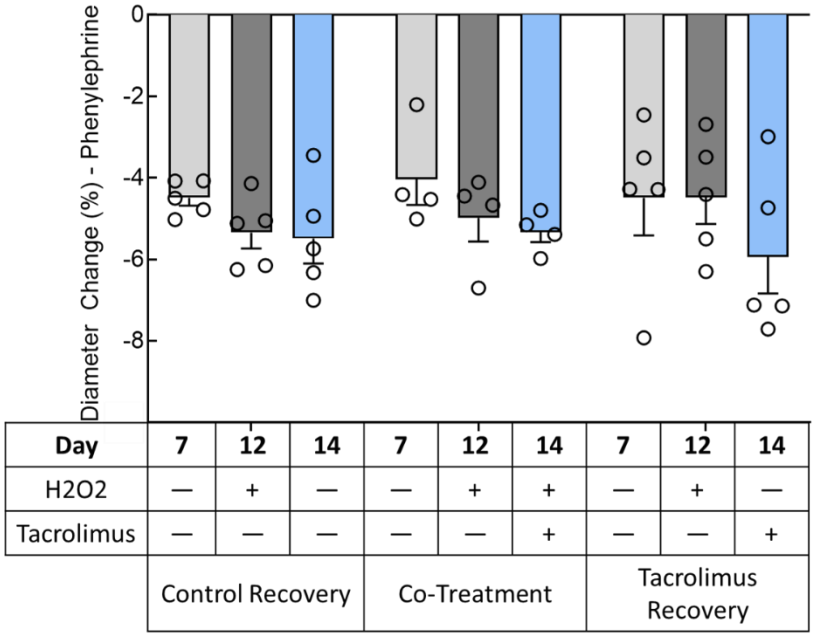

Figure 26: Vasoconstriction is Unaffected by Introduction of Tacrolimus in H_2O_2 Recovery Media.

TEBV Vasoreactivity is tested on Day 7, 12, and 14 after fabrication. Recovery conditions (control, co-treatment, and tacrolimus) does not affect endothelium-independent vasoconstriction in response to phenylephrine. N = 4-5. Data represented as mean ± SEM with individual data points overlaid.

Endothelium-dependent vasodilation was significantly affected by the presence of tacrolimus during the recovery period. As seen previously, 5-day treatment with 100 µM H_2O_2 ablated endothelium-dependent vasodilation. When vessels were allowed to recover for 48 hours in normal growth media, endothelium-dependent vasodilation in response to acetylcholine failed to return to the level seen before H_2O_2. Endothelium-independent vasodilation in response to sodium nitroprusside (SNP) was maintained. When tacrolimus and H_2O_2 were present during the 48 hour recovery period (labeled as

co-treatment), acetylcholine-response wasrecovered, but the effect was not significant compared to control recovery (Figure 27). When 10 nM tacrolimus was added to normal growth media during the recovery period (labeled as tacrolimus recovery), endothelium-dependent vasodilation was fully restored and significantly higher than control conditions (#, $p < 0.01$). The response of these vessels to sodium nitroprusside was correspondingly reduced compared to controls (** $p < 0.005$) (Figure 27). In cases

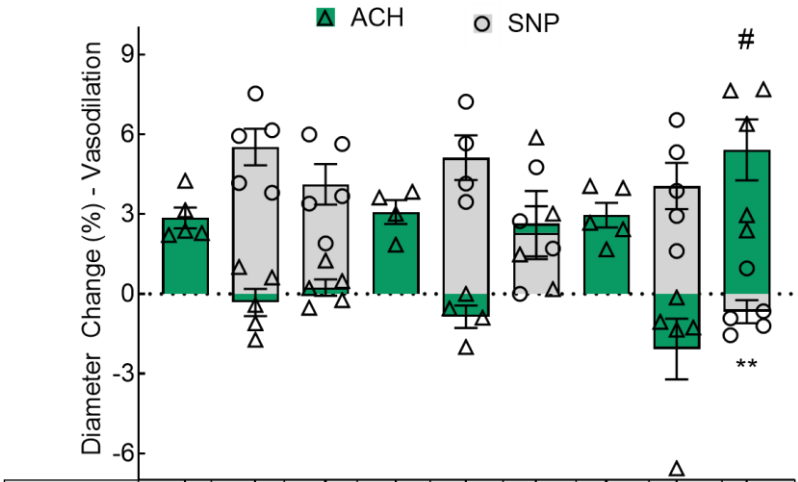

Figure 27: Introduction of Tacrolimus After Removal of H_2O_2 Restores Endothelium-Dependent Vasoreactivity.

TEBV vasoreactivity is tested on Days 7, 12, and 14 after fabrication for acetylcholine (ACH), with sodium nitroprusside (SNP) testing occurring on Days 12 and 14. Spontaneous recovery of endothelium-dependent vasoreactivity is minimal, shown by the dominance of SNP response in the control recovery condition. Co-treatment of tacrolimus and H_2O_2 for 48 hours leads to partial recovery of acetylcholine response. When vessels are allowed to recovery in media with tacrolimus without H_2O_2, acetylcholine response is restored. N = 4-5. Data represented as mean ± SEM with individual data points overlaid. #, $p < 0.01$. **, $p < 0.005$ compared to control recovery.

where robust acetylcholine response occurs, no further dilation is possible, thus the cchange in diameter in response to SNP is typically less than 0.5% reflecting only transient shifts in the vessel diameter rather than true change.

Furthermore, introduction of tacrolimus after the removal of 100 μM H_2O_2 reduced the expression of p21 and VCAM-1 within the TEBVs. In the cotreatment regime, p21 and VCAM-1 expression were reduced, but were still present at noticeable levels. In the recovery treatment scheme, p21 and VCAM-1 expression were comparable to levels in healthy vessels never exposed to H_2O_2 (Figure 28).

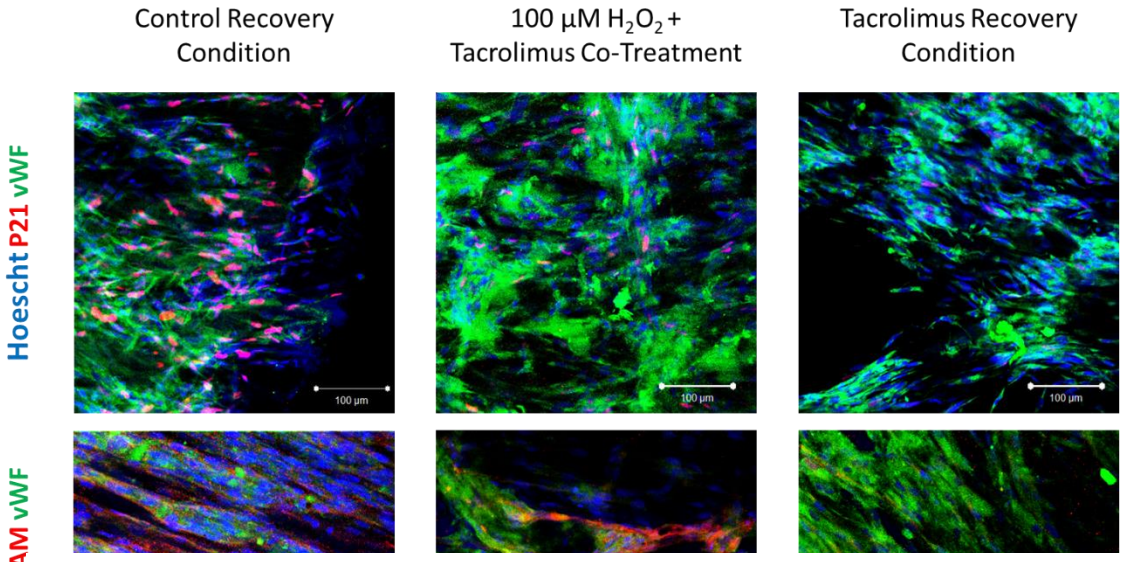

Figure 28: P21 and VCAM expression in TEBVs treated with Tacrolimus while recovering from 100 μM H_2O_2 exposure.

TEBVs exposed to 100 μM H_2O_2 express high levels of p21 and VCAM within the endothelium. When TEBVs recover for 48 hours in control media, p21 and VCAM expression remains high. When 10 nM tacrolimus is introduced alongside 100 μM H_2O_2 for 48 hours, expression of p21 and VCAM-1 are reduced considerably. When 100 μM H_2O_2 is removed and only 10 nM tacrolimus is present during recovery, p21 and VCAM-1 expression is returned to levels observed within healthy vessels never treated with 100 μM H_2O_2. Scale bar represents 100 μm.

4.3.3. Addition of tacrolimus reduces H_2O_2-induced accumulation of monocytes in TEBVs

In Chapter 3, we confirmed that the TEBVs treated with 100 μM H_2O_2 had greater numbers of adherent monocytes. Here, we used tacrolimus to reduce the number of adherent monocytes during H_2O_2 exposure. TEBVs were treated with 100 μM H_2O_2 for 5 days, beginning 7 days after their initial fabrication to ensure adequate maturation before inducing senescence. CMPTX-red labeled monocytes were introduced to the perfusion circuit at a concentration of 1 x 10^6 cells/mL perfusion media for 4 days beginning the day after H_2O_2 addition (i.e. days 8-12 after vessel fabrication). In TEBVs exposed to 100 μM H_2O_2 with and without 50 μg/mL eLDL, introduction of 10 nM tacrolimus for the duration of H_2O_2 exposure reduced monocyte adhesion by about 60-80% (Figure 29). The reduction in monocyte adhesion in vessels that were not exposed to eLDL was not significant due to the small number of experiments. A statistical power analysis suggests that 1-2 more replicate are needed to achieve statistical significance. Monocyte retention is still higher than in vessels where no H_2O_2 is present (Figure 19). However, it is important to recall that the controls in Figure 19 were obtained in an alternate TEBV system in which the total duration of monocyte exposure was shorter (72 hours vs. 96 hours) and that the difference between baseline and tacrolimus-induced monocyte adhesion is not statistically significant (Figure 21).

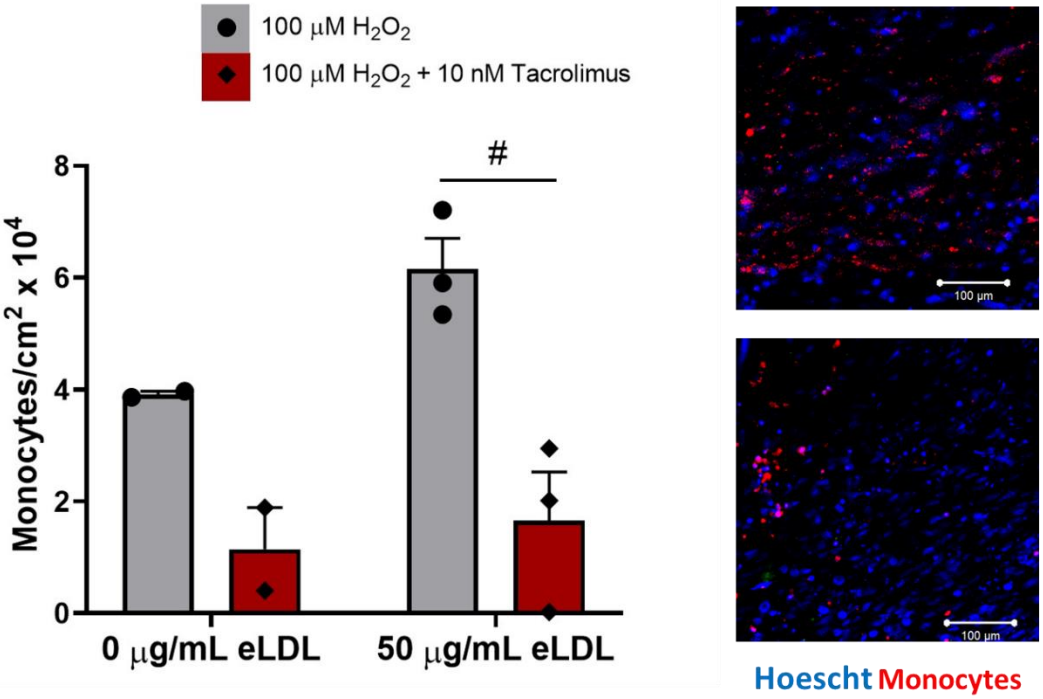

Figure 29: Tacrolimus Reduces Monocyte Adhesion in TEBVs treated with 100 μM H_2O_2

10 nM tacrolimus incorporated into the 100 μM H_2O_2 perfusion media significantly reduced monocyte adhesion in TEBVs exposed to 50 μg/mL eLDL. In vessels without eLDL, the reduction in monocyte adhesion was not significant. N = 2-3; # P < 0.01. Data represented as mean ± SEM with individual points overlaid. Scale bar represents 100 μm.

4.3.4. Tacrolimus protects endothelium-dependent vasoreactivity and reduces foam cell formation in TEBVs treated with H_2O

Tacrolimus improved endothelium-dependent vasoreactivity after removal of H_2O_2 but introducing it after significant foam cell formation may weaken its effect. Instead, it was introduced prior to the addition of eLDL and monocytes to explore its ability to protect against atherogenesis in an oxidative stress environment TEBVs were fabricated as normal and treated with 100 μM H_2O_2 on days 7-12 after fabrication. 50

μg/mL eLDL and 1 x 10^6/mL U937 monocytes were added on days 8-12 after fabrication. In treatment conditions, tacrolimus was added for the duration of H_2O_2 exposure (Figure 30A). When eLDL and monocytes are added alongside 100 μM H_2O_2, endothelium-independent vasoconstriction in response to phenylephrine is not different compared to vessels exposed only to 100 μM H_2O_2 (Figure 10). The addition of tacrolimus did not change vasoconstriction in response to phenylephrine compared to peroxide-treated vessels exposed to eLDL and monocytes (Figure 30B).

Similarly, the addition of monocytes and eLDL during 100 μM H_2O_2 exposure did not further reduce endothelium-dependent vasodilation in response to acetylcholine compared to 100 μM H_2O_2 alone. In these vessels, dilation only occurred in response to sodium nitroprusside which acts independent of the endothelium. When 10 nM tacrolimus was added alongside 100 μM H_2O_2, endothelium-dependent vasoreactivity was significantly higher (** $p < 0.005$, Figure 30C) and comparable to the acetylcholine response they had prior to H_2O_2 exposure as well as vessels 12 days after fabrication that were not treated with H_2O_2 at all (Figure 10). In vessels where tacrolimus was included the response to sodium nitroprusside was minimal.

These vessels were then stained with the LipidSpot lipid droplet detection assay to evaluate foam cell formation within TEBVs treated with eLDL, fluorescently-labeled monocytes, and H_2O_2. 10 nM tacrolimus reduced lipid retention within the vessel walls significantly (Figure 32). The degree of lipid accumulation was still significantly higher

than zero. Lipid accumulation was not quantified in vessels treated with eLDL in the absence of H_2O_2, and cannot be compared to eLDL accumulation in the presence of 100 μM H_2O_2 ± 10 nM tacrolimus.

The effect of 10 nM tacrolimus on p21 and VCAM-1 expression was also examined. Introduction of tacrolimus for the duration of 100 μM H_2O_2 exposure was also explored via immunofluorescence. Expression of both was significantly reduced when tacrolimus was included, even when eLDL was also included in perfusion media (Figure 31).

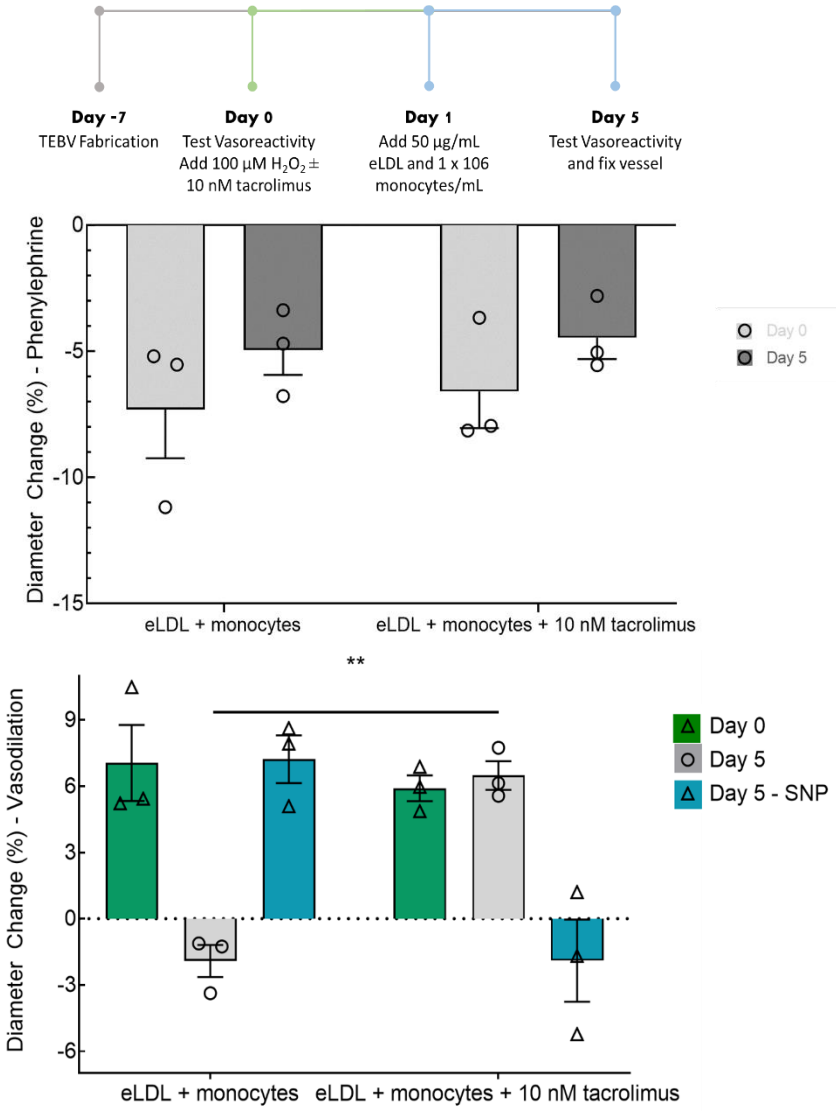

Figure 30: Tacrolimus protects endothelium-dependent vasoreactivity of TEBVs treated with H_2O_2, eLDL and monocytes.

A: Timeline of vessel fabrication and treatment. Initial vasoreactivity testing is 7 days after vessel fabrication ("Day 0"). 100 µM H_2O_2 ± 10 nM tacrolimus are added after vasoreactivity testing. The following day 50 µg/mL eLDL and 1 x 10^6 monocytes/mL perfusion media are added. Final vasoreactivity testing occurs on the 5th day of H_2O_2 exposure (the 4th day of eLDL and monocyte exposure). B: Vasoconstriction in response to phenylephrine is unaffected by introduction of tacrolimus. C: Tacrolimus protects endothelium-dependent vasodilation in TEBVs treated with H_2O_2, monocytes, and eLDL. Data represented as mean ± SEM with individual data points overlaid. ** $p < 0.005$.

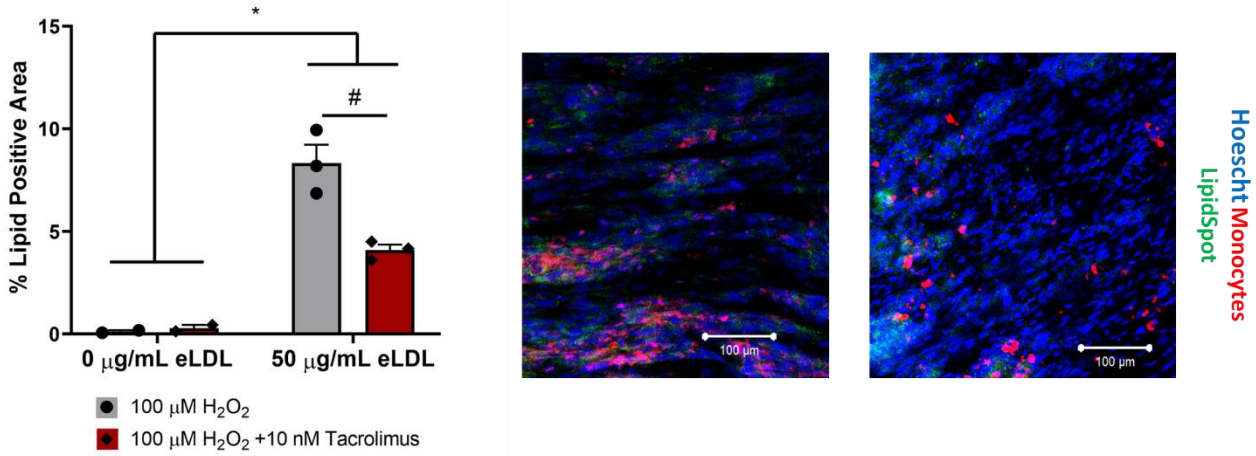

Figure 32: Lipid Retention is Reduced in TEBVs treated with 10 nM Tacrolimus.

Introduction of 10 nM Tacrolimus significantly reduced lipid retention within TEBVs treated with 100 μM H_2O_2. The degree of lipid retention was still higher than in lipid-free controls. N = 2-3. Data represented as mean ± SEM with individual data points overlaid. * $p < 0.05$; # $P < 0.01$. Scale bar represents 100 μm.

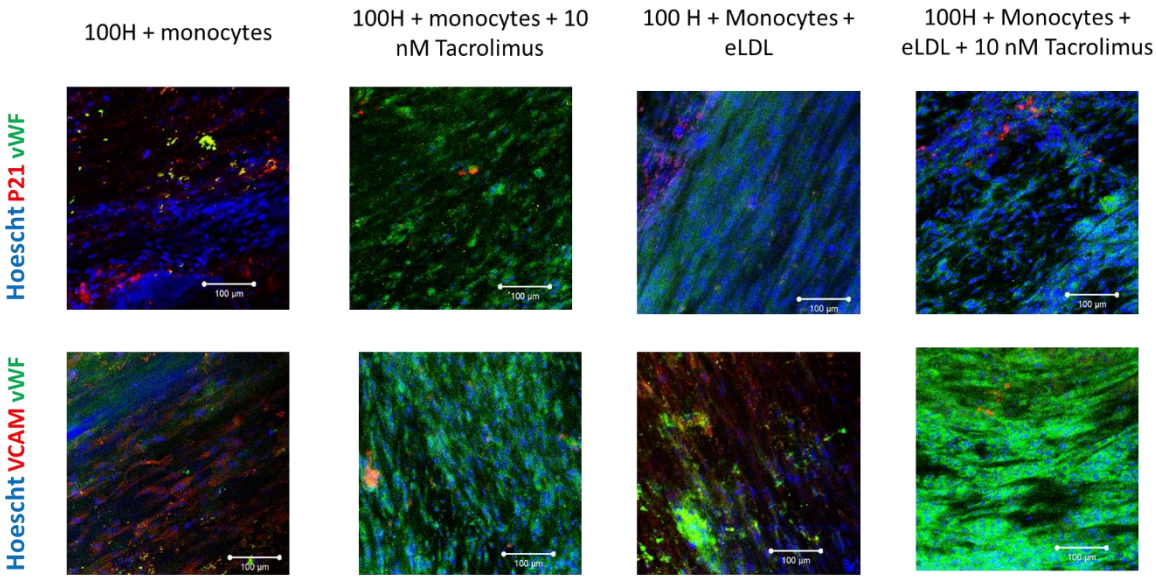

Figure 31: Tacrolimus Reduces p21 and VCAM-1 Expression in TEBVs when added for the duration of H_2O_2 Exposure.

P21 and VCAM-1 expression are high within the endothelium of TEBVs treated with 100 μM H_2O_2 and remains high when monocytes and/or 50 μg/mL eLDL are added simultaneously. Introduction of tacrolimus reduces the expression of p21 and VCAM-1 in TEBVs. Scale bar represents 100 μm.

4.4. Discussion

Two senolytics, dasatinib and quercetin, as well as the senomorphic drug tacrolimus, were tested on CBECFCs treated with 100 μM H_2O_2 for seven days either for the final 24 hours of H_2O_2 exposure (co-treatment) or for 24 hours after removal of H_2O_2 (recovery). Tacrolimus effectively reduced both p21 and VCAM-1 expression in the recovery and co-treatment schemes at concentrations of 1-10 nM. Anti-inflammatory effects of tacrolimus were more pronounced when it was added after the removal of H_2O_2 (Figure 22). Since H_2O_2 treatment increases VCAM-1 expression it is possible that this counteracts the anti-inflammatory properties of VCAM-1. It's also possible that introduction of VCAM-1 so late after the initiation of H_2O_2 exposure reduces its effectiveness. Adding tacrolimus from the initiation of 100 μM H_2O_2 exposure may increase the effectiveness of the treatment.

Dasatinib and quercetin had less potent efficacy compared to the tacrolimus. Quercetin successfully reduced p21 expression in CBECFCs when administered during the final 24 hours of H_2O_2 treatment. It had a more muted effect on inflammation, only slightly decreasing VCAM-1 expression (Figure 24). Dasatinib had no discernible effect on either senescence or inflammation (Figure 24). This is not surprising as data suggests that dasatinib does not target endothelial cells *in vivo*[56]. It is often administered in tandem with quercetin because the two target complementary cell types. A dasatinib and quercetin cocktail was also administered to CBECFCs during their recovery from

stress-induced senescence. As expected, quercetin concentration dominated the effectiveness of the treatment (Figure 25). The decrease in senescence and inflammation was still modest in comparison to the senotherapeutic effects seen from the same concentrations of tacrolimus. Therefore, tacrolimus was used for future experiments involving TEBVs.

TEBVs were fabricated and matured in normal growth media for one week. 100 μM H_2O_2 was then added to the perfusion media for five days. Then the vessel was either allowed to recover in control media, continued in 100 μM H_2O_2 and 10 nM tacrolimus, or allowed to recover in 10 nM tacrolimus without H_2O_2. As seen in prior experiments, endothelium-dependent vasodilation was compromised by 5-day H_2O_2 treatment. When TEBVs recovered in control media for 48 hours, there was no recovery of endothelium-dependent vasodilation. Co-treatment with 100 μM H_2O_2 and 10 nM tacrolimus resulted in a small, but ultimately insignificant recovery of endothelium-dependent vasodilation and corresponding decrease in endothelium-independent vasodilation. When TEBVs recovered in 10 nM tacrolimus without H_2O_2 present endothelium-dependent vasodilation was fully restored (Figure 27). This data is supported by immunofluorescent testing that confirmed that p21 expression was still high in TEBVs recovering in control media. Vessels co-exposed to 100 μM H_2O_2 and 10 nM tacrolimus had a partial reduction in p21 expression, while vessels recovering in 10 nM tacrolimus without H_2O_2 had little p21 expression. TEBVs recovering with 10 nM

tacrolimus present had p21 levels similar to those seen in vessels never exposed to H_2O_2 (Figure 11). This confirms both that the TEBVs are drug-responsive, and that 10 nM tacrolimus is capable of effecting measurable changes in vessel health after the induction of stress-induced senescence.

Senomorphics are proposed as a novel therapeutic approach for the treatment and prevention of atherosclerosis. In order to investigate the capacity of this model to study tacrolimus and similar drugs that specifically target senescence and the SASP, tacrolimus was introduced to the atherogenic conditions explored in Chapter 3. As in Chapter 3, TEBVS were matured for 7 days, then exposed to 100 μM H_2O_2 for 5 days. 50 μg/mL eLDL and 1 x 10^6 monocytes/mL were added on Day 8 after fabrication. This time, 10 nM tacrolimus was added for the duration of H_2O_2 exposure. This resulted in preservation of endothelium-dependent vasodilation in vessels treated with the atherogenic H_2O_2, eLDL, and monocyte mixture (Figure 30). This preservation of endothelium-dependent vasodilation was accompanied by a reduction in VCAM and p21 expression. This resulted in decreased lipid uptake within the vessel, although a number of monocytes still adhered to the vessel wall. Given that a small amount of eLDL is taken up by hNDFs even in healthy conditions (Figure 18), and that monocytes have been found to adhere in small amounts in the absence of any inflammatory stimuli (Figure 19).

TEBVs exposed to atherogenic stimuli had significant improvements in function and reduced lipid uptake and monocyte adhesion when tacrolimus was used to mitigate the effects of stress-induced senescence on the endothelium. This confirms that senotherapeutics can effectively be used to protect against atherogenesis in this model. Given the large number of new senolytics and senomorphics currently in development, a model of vascular senescence which responds effectively to this class of drugs can be a valuable tool in determining which drugs are the best candidates to move forward in clinical trials. It also confirms that drugs which target senescence or it's associated secretory pathways are a viable target for treating or preventing atherosclerosis. Improvements in targeting senescence may address some of the inadequacies of current therapeutics which focus only on blood pressure or on directly inhibiting inflammation.

4.5. Chapter-Specific Acknowledgments

We thank Jason Breithaupt, Kevin Shores, Ellery Jones, and especially Hailee Patel for their assistance in preparation and enzyme-modification of low-density lipoprotein.

5. Dissertation Summary and Future Work

5.1. Dissertation Summary

The development of novel therapeutics is an increasingly time and resource intensive venture. Promising drug candidates can perform excellently on cells grown in a monolayer *in vitro*, and even *in vivo* in preclinical animal trials. Yet, half of these drugs fail in clinical trials due to lack of efficacy or previously unidentified toxicity[86]. Animal models have served as a cornerstone of preclinical drug trials, but gaps between the pathology of many diseases between animal models and humans are identified at an increasing rate. This can be particularly true in diseases with issues of inflammation, diet, and immune system function such as rheumatoid arthritis and atherosclerosis[31,128]. The development of human microphysiological systems (MPS) represents an invaluable step towards increasing the utility of preclinical *in vitro* tests of drug efficacy and toxicity. Human MPS retain fidelity to native biology while maintaining the high tunability and ease of analysis valued in two-dimensional *in vitro* systems. Cellular behavior, for example shear-mediated endothelial cell gene expression, is more faithful to human biology in MPS than in static monoculture, ensuring that the drug response *in vitro* will be retained *in vivo*. Tissue toxicity, drug metabolism, and loss of function due to off-target effects can all be evaluated with a series of human MPS to identify the most promising drug candidates to bring forward to clinical trials.

The development of tissue engineered blood vessel (TEBV) microphysiological systems that are useful for evaluating drug response in both healthy and diseased states is a valuable component of any effort to develop a "human-on-a-chip" platform[132,147]. Nearly all drug or protein therapies administered will travel through the vasculature in some form before being fully metabolized, degraded, or excreted by the body. In addition there are a number of vascular diseases which are themselves areas in which novel therapeutics can be of service.

In this work, we focus specifically on atherosclerosis and the development of a tissue engineered blood vessel (TEBV) model for atherosclerosis. Atherosclerosis, a narrowing of the arteries due to accumulation of fatty plaques within medial layers of blood vessels, is the chief cause of mortality and morbidity in the developed world[116]. Numerous therapies for atherosclerosis currently exist, many targeting hyperlipidemia or high blood pressure, but these therapies offer only transient benefits and must be taken continuously to maintain health rather than fully addressing the underlying pathology[67]. In addition to circulating inflammatory stimuli, blood lipid levels, and aberrant shear signaling within the vasculature, cellular senescence is being recognized as an important factor in the development of atherosclerosis. Senescence within the endothelium in particular is associated with poor oxidative stress response, increased presentation of monocyte adhesion molecules, greater permeability to circulating lipids, and even clinically observable reductions endothelium-dependent vasoreactivity[34,45].

In Aim 1, we developed a tissue-engineered blood vessel model for vascular aging by exposing a TEBV to 100 μM H_2O_2 for 5 to 7 days. TEBVs were fabricated using hNDFs and CBECFCs. Preliminary tests performed on CBECFCs in 2-D monoculture found revealed that a concentration 100 μM H_2O_2 with an exposure time of 7 days was necessary to induce senescence within the CBECFCs. hNDFs were found to be senescent under these conditions, but did not exhibit decreased expression of calponin or α-SMA. This suggested that endothelium-independent vasodilation would be maintained despite exposure to H_2O_2 in the TEBVs.

TEBVs were fabricated and allowed to mature in normal growth media for 7 days to establish baseline vasoreactivity indicating a healthy and functional endothelium was present and that no errors in vessel fabrication had been made. The vessel was then treated with 100 μM H_2O_2 for 5 or 7 days. Endothelium-independent vasoconstriction was unaffected by H_2O_2 exposure. However, endothelium-dependent vasodilation was significantly reduced by H_2O_2 exposure. In contrast, endothelium-independent vasodilation was increased, since the vessel's dilatory capacity was not maximized by endothelium-dependent means. Immunofluorescence confirmed that p21 expression was increased in the TEBVs, indicating the cells within the vessel were senescent.

H_2O_2 exposure also increased inflammation in the CBECFCs, both in 2-D and in the TEBVs. The number of VCAM-1 positive cells was increased significantly in both 2D

CBECFCs and within the TEBVs. E-selectin expression was also increased in with H_2O_2 expression, although it was only measured in 2D cells due to high background staining. Interestingly, ICAM-1 expression was not increased from H_2O_2 treatment. This was followed up by qRT-PCR analysis of expression of iNOS, eNOS, SIRT1, and several inflammatory proteins. iNOS expression was increased significantly, a common response in cases of vascular injury[103]. eNOS expression was significantly lower in TEBVs treated with H_2O_2, ultimately causing the observed reduction in endothelium-dependent vasodilation in response to acetylcholine.

In Aim 2, we build upon this model for vascular senescence to create a senescence-associated model for atherogenesis. *In vivo*, atherogenesis occurs when lipids and monocytes accumulate within the intima of blood vessels. There are several varieties of circulating lipids. Of particular importance to the development of atherosclerosis is enzyme-modified low-density lipoprotein (eLDL). eLDL induces greater inflammation within the endothelium and uptake of eLDL is greater than uptake of unmodified LDL or other lipoproteins within vascular smooth muscle cells[20]. The medial layer of the TEBVs made in this study is comprised of hNDFS rather than vSMCs. Unlike oxidized LDL, which is also capable of turning vSMCs or monocytes into foam cells, eLDL is retained by hNDFs[121]. oxLDL also causes a much smaller degree of endothelial cell inflammation, making it a less potent inflammatory reagent to induce atherogenesis in the TEBV model[90]. After confirming that exposing CBECFCs to both 100

μM H_2O_2 and concentrations of eLDL up to 50 μg/mL for up to 72 hours did not reduce cell viability, the effects of this atherogenic mixture on the endothelium and vasoreactivity could be explored.

In 2-D, CBECFCs were treated with 100 μM H_2O_2 for a total of 7 days, with 50 μg/mL eLDL also included for the final 24 hours of H_2O_2 exposure. Treated CBECFCs did not have increased expression of VCAM-1 or E-selectin, suggesting that the expression of these adhesion molecules was already maximized by 100 μM H_2O_2 exposure alone. ICAM-1 expression was significantly increased by co-treatment with eLDL, although there was no interaction effect with H_2O_2 concentration. In TEBVs, 100 μM H_2O_2 treatment is combined with addition of enzyme-modified low-density lipoproteins. As before, TEBVs are fabricated and matured for 7 days to ensure healthy vessel function. Then, 100 μM H_2O_2 is added for days 7-12 after initial fabrication, with 50 μg/mL eLDL and 1 x 10^6 monocytes/mL being added alongside it for Days 8-12. Lipid uptake and monocyte adhesion were increased in TEBVs treated with 100 μM H_2O_2 compared to controls in normal growth media. In previous studies, it was necessary to include TNF-α to maximize monocyte adhesion. In this system, it is possible to achieve the same degree of monocyte adhesion using only eLDL in a senescence-inducing environment. This demonstrates that the development of a vascular senescence model can be used as a tool for modeling vascular diseases for which cellular senescence is an important risk factor.

In recent years, drugs which specifically target senescence and its associated secretory pathways have gained traction in treating a number of diseases including arthritis and diabetes[141]. Some have also been incorporated into drug-eluting stents to improve outcomes after bypass surgeries[64]. These drugs, senolytics and senomorphics transiently block the anti-apoptotic pathways that prolong the life of senescent cells or target proteins within the senescence-associated secretory pathway (SASP). We explored the effects of these drugs on the vascular senescence and atherogenesis model in Aim 3. Tacrolimus, dasatinib, and quercetin were all tested on CBECFCs in 2-D after their exposure to 100 μM H_2O_2. Of the three drugs tested, tacrolimus had the most potent effect on both p21 and VCAM-1 expression in the endothelial cells. Quercetin was effective at reducing the number of p21 positive cells, but had a smaller effect on VCAM-1 expression compared to the tacrolimus. Dasatinib does not typically affect endothelial cells significantly and is best administered as a cocktail with quercetin. Future work could explore the effectiveness of this combination treatment in the TEBV system to evaluate the effects of dasatinib on the encapsulated hNDFs.

Tacrolimus was introduced to the TEBVs for 48 hours after 5 days of exposure to 100 μM H_2O_2. It significantly increased recovery of endothelium-dependent vasodilation in response to acetylcholine. When TEBVs were left to recover from H_2O_2 without tacrolimus for 48 hours, endothelium-dependent vasodilation did not return at all. When tacrolimus was included alongside H_2O_2 for 48 hours, extending the total H_2O_2

exposure time to 7 days, there was a small, but ultimately insignificant recovery of endothelium-dependent vasodilation.

Introduction of tacrolimus for the duration of H_2O_2 exposure reduced lipid uptake within the vessel intima. It also corresponded with a slight decrease in monocyte adhesion due to the reduced expression of monocyte adhesion molecules on the endothelium with tacrolimus treatment. Endothelial cell senescence was also decreased in TEBVs treated with tacrolimus while exposed to H_2O_2 with and without eLDL and monocytes included in perfusion media. The work in this aim demonstrates that this method of generating vascular senescence can be used to model a senescence-associated disease and responds to relevant therapeutics.

5.2. Strengths and Weaknesses of the Work

This protocol for fabricating and culturing TEBVs results in a vascular senescence model that is capable of effectively modeling early-stage atherosclerosis and responding to relevant therapeutics. These TEBVs can be tested with clinically relevant measures of vasoreactivity, as well as easily analyzed via immunofluorescence, analysis of perfusion media samples, or qRT-PCR[45]. However, there are steps that could be taken to further improve the fidelity of the system to native arterioles.

Prior studies have fabricated TEBVs from not only hNDFs, but vascular smooth muscle cells, mesenchymal stem cells, and even iPSC-derived vascular smooth muscle cells. Tests of vasoreactivity after one week of maturation found that vSMCs, MSCs and

iPSCs resulted in vessels which responded less strongly to the same concentration of phenylephrine or acetylcholine than vessels made with hNDFs[103,148]. For these studies, hNDFs were chosen because they have the most robust vasoreactivity, allowing for the greatest dynamic range over which stimuli could reduce or restore vasoreactivity. While this results in optimal vasoreactivity data, hNDFs do not comprise this percentage of the intimal layer in healthy vessels. The choice of hNDFs as the medial cell layer does limit the opportunity to model certain diseases. When modeling atherosclerosis, only eLDL can be used as a circulating lipid and produce a significant effect. Oxidized LDL which is also implicated in atherogenesis *in vivo* is not readily taken up by hNDFs, but is retained by vSMCs.

The current TEBV system also contains two sets of tubing, one perfusing the lumen of the vessel, the other maintaining a volume of cell culture media around the outside of the vessel to ensure even distribution of nutrients and hydration of the vessel. Given that these lines of tubing share a common reservoir, when monocytes and eLDL are added to the perfusion circuit, the vessel is exposed to them from both the vessel lumen and the media surrounding the outer wall of the vessel. Depending on the degree to which hNDFs express monocyte adhesion molecules of their own, baseline monocyte adhesion may be higher in this system than in alternative systems where the fluid for the lumen and the exterior of the vessel can be completely separated.

In Aim 3, the drug-responsiveness of the system was evaluated by exploring exposing the system to different drugs during and after H_2O_2 exposure. Pilot tests of these drugs were conducted on CBECFCs alone in 2-D. Since TEBVs contain multiple cell types and hNDFs retaining eLDL is also a significant factor in foam cell formation, to paint a full picture of the most effective drug choice, evaluation of these drugs in both CBECFCs and hNDFs to evaluate a drug which works optimally in both choices. Increasing the duration of co-treatment with the senolytics in 2-D to the full duration of H_2O_2 exposure would also have painted the most accurate picture degree to which different senolytics would reduce monocyte adhesion and/or lipid uptake in the TEBVs.

Further studies examining additional drugs will continue to validate the utility of TEBVs as a clinically relevant tool for evaluating the efficacy of novel therapeutics in development. For example, dasatinib has poor efficacy in endothelial cells[62]. Thus, introduction of dasatinib is expected to do little to protect endothelium-dependent vasodilation if applied to the TEBVs. Conversely, the use of tacrolimus has been well characterized as effective in drug-eluting stents[64]. The results in the TEBV system, while newly documented, are not surprising. Further evaluating the effects of drugs proven both effective and ineffective will more completely validate the system and confirm its utility as a predictor of future drug performance.

5.3. Recommended Studies to Complete the Work

In Specific Aim 2, an atherogenesis model was developed by treating TEBVs with 100 μM H_2O_2 and enzyme-modified low-density lipoprotein (eLDL) while introducing monocytes to the perfusion media. Vasoreactivity data could not be collected for vessels treated with 100 μM H_2O_2 and monocytes without eLDL. While the vasoreactivity data for these vessels is not expected to be significantly different from the vasoreactivity of vessels that are treated with 100 μM H_2O_2, monocytes, and eLDL, obtaining and including these data is ideal for completing the work.

Additionally, in the data presented here, the degree of senescence-induced monocyte adhesion and foam cell formation was compared to negative controls obtained in an alternate TEBV system developed by Xu Zhang[90]. This system contains 4 smaller TEBVs running in parallel in a single chamber, with the overall system flow rate adjusted to produce identical shear stresses along the endothelium. For a more accurate comparison of monocyte accumulation and foam cell formation in the TEBVs, additional vessels should be fabricated in the system described here and treated with monocytes and/or eLDL in the absence of H_2O_2.

In Specific Aim 3, the capacity of senolytic and geroprotective agents to enhance recovery from oxidative stress and protect against endothelial dysfunction was explored. The preliminary tests conducted on CBECFCs growing in 2-D monoculture only found tacrolimus to significantly reduce p21 expression (Figure 22). Tacrolimus

only produced a protective effect in the TEBVs when introduced after removal of H_2O_2 or for the duration of H_2O_2 treatment, not when it was only introduced for the final 48 hours of H_2O_2 exposure. It is similarly possible that dasatinib, quercetin, or the dasatinib and quercetin cocktail will produce a more consistent and significant effect when administered for the duration of H_2O_2 exposure. It is also possible that the effects of dasatinib and querecetin may be more pronounced when administered to the TEBVs than to the CBECFCs. Further exploration of potential treatment conditions for these drugs in the TEBVs should be explored to better evaluate the ability of this system to respond to senolytics and other senescence-targeting drugs.

5.4. Future Directions for Senescent TEBVs

The work presented here builds upon a single TEBV system developed by prior members of the Truskey lab. This single TEBV system has previously been used to study the atheroprotective effects of statins, as well as model the rare genetic disease progeria[103,148]. While this model is excellent for modeling purely pharmacological phenomena, like preventing TNF-α-induced endothelial dysfunction through treatment with lovostatin[103], the size and volume of the system limits the throughput of the system and the ability to develop things like the atherogenesis model due to the quantity of cells and lipids required to treat the entire volume of the chamber and the perfusion circuit. To mitigate this, the volume of the perfusion circuit was reduced by shortening the

tubing used, and using the smallest diameter tubing compatible with the existing chambers. This reduced the overall volume from 30 mL to 13 mL

An additional difficulty of the system is the low-throughput. Each vessel must be maintained individually, and can only be used for either immunofluorescence or qRT-PCR at the conclusion of the experiment due to differences in the method of fixation in preparation for analysis and the amount of tissue required for analysis. One step to address this was the development of a higher-throughput tissue-engineered blood vessel (TEBV) chip which runs four slightly smaller vessels in parallel within a single chip[90]. The system had the added benefit of fabricating the vessels directly within the chamber, eliminating the need to position each vessel on the hollow perfusion adapters, which can damage the vessel when performed incorrectly. This enables us to collect vessels that can be used for qRT-PCR and a number of immunofluorescent analyses simultaneously, rather conducting additional independent experiments to obtain the required number of samples for the same conditions.

However, this system has room for improvement as well. To minimize the volume of the chamber, several small parts had to be made to connect to the smaller vessels within their chamber. This has made it difficult to ensure the system is free of leaks and generating appropriate shear stresses within the vessel lumen. Custom connectors must be used to connect the chamber to commercially available tubing which must be designated for a specific chamber, personalized to ensure they fit the chamber

ports well, and cannot be easily replaced in the event of a failure. A chamber utilizing the *in situ* multi-vessel fabrication method used by the newer system, but retaining the larger, more reliable fluid connectors of the original system would necessitate a larger fluid volume than the smallest chamber alone (only a 6 mL volume in total), but would improve the reliability of the system and maintain the throughput of the 2.0 system.

The development of this method of treating TEBVs with H_2O_2 can also serve as a platform to investigate other phenomena related to vascular aging and relevant pharmaceutical intervention. This could also be used in series with human skeletal muscle microphysiological systems to investigate multi-system effects of oxidative stress and inflammation. Many senolytics can have problematic off-target effects in other human tissues[56]. Development of a series of organs-on-a-chip to evaluate the safety and efficacy of senolytics presently in development would be extremely valuable in identifying the best candidates to push through to clinical trials.

In this work, we focused specifically on stress-induced senescence. This is considered to be the primary method of endothelial cell senescence *in vivo*[42]. However, with this model it is possible to directly compare the effects of replicative senescence and stress-induced senescence on the vasculature. The effects of replicative senescence on CBECFC shear responsiveness, permeability, and glycocalyx formation have already been well-documented[43,85,98]. Preliminary studies showed that replicative senescence reduced endothelium-dependent vasoreactivity in TEBVs, but the effects of replicative

senescence on endothelial cell activation or atherogenic potential are currently unexplored. It would also be worth investigating the potential of senolytic and senomorphic drugs to mitigate the effects of this alternate type of senescence.

5.5. Implications for Treatment of Atherosclerosis and Cardiovascular Tissue Engineering

Cellular senescence is increasingly being recognized as one of the key factors in the development of atherosclerosis and other diseases[5]. While lifestyle interventions can have a significant effect, pharmaceutical intervention can greatly assist in increasing the healthspan of those predisposed to atherosclerosis[34]. This system represents an exciting new method of testing the effects of anti-atherogenic treatments, particularly those targeting senescence in a clinically relevant *in vitro* model. The TEBVs can undergo clinically relevant, non-destructive measures of vasoreactivity in response to phenylephrine, acetylcholine, and sodium nitroprusside, allowing characterization of vasoreactivity by endothelium-dependent and endothelium-independent means. We have also demonstrated responsiveness to the senomorphic tacrolimus.

By developing a system which provides a control over the degree of senescence within the vasculature, the role of senescence in the progression of atherosclerosis and its value as a therapeutic target can be fully explored in a biomimetic system with a high degree of tunability. This work demonstrates the utility of a tissue engineered blood vessel model for studying vascular senescence and senotherapeutics. Furthermore, it confirms that targeting cellular senescence and the associated inflammatory pathways

has an atheroprotective effect and the utility of senotherapeutics in treating atherosclerosis.

6. Conclusions

In this work, we developed a tissue-engineered blood vessel (TEBV) model for vascular aging and used it to model age-related vascular disease, as well as the efficacy of geroprotective drugs in preventing atherosclerotic lesions. Atherosclerosis, characterized by full or partial occlusion of the arteries by fat and monocyte-laden plaques, places a significant burden on the health system around the world[136]. It is the leading cause of morbidity and mortality in the world[6]. As such, the development of drugs to manage the symptoms and causes of atherosclerosis are a significant area of clinical research.

Human microphysiological systems (MPS) are being developed to increase the power of *in vitro* studies to predict the performance of preclinical drug candidates in human trials. Here, we developed a TEBV MPS with the ultimate goal of evaluating drugs with therapeutic relevance for atherosclerosis or evaluating the effect of other drugs on agitating the atherosclerotic phenotype.

Atherosclerosis is primarily an aging disease absent an underlying pathology. To that end, we applied reactive oxygen species (ROS) to the TEBV model to model an accelerated aging process. With this approach, we were able to replicate clinically-observed losses of endothelium-dependent vasoreactivity while maintaining full function of the surrounding medial cells[45]. This senescence also resulted in increased adhesion of monocytes within the TEBV.

After inducing a disease state within the TEBV system, I examined the ability of drug treatments to reduce the disease phenotype and restore proper vessel function. The senomorphic tacrolimus, which reduced the burden of senescent cells within the vessel and reduced inflammation within the endothelium, was introduced to the TEBV. It was found to protect against the loss of endothelium-dependent vasoreactivity, as well as reduce the number of foam cells and adherent monocytes within the vessel wall.

This study demonstrates that inducing senescence in a TEBV model and introducing a mixture of lipids and monocytes to the TEBV perfusion media was sufficient to develop a model for early-stage atherosclerosis in only two weeks. Drugs targeting senescence could then be used to mitigate the atherosclerotic phenotype within the vessel. Continued characterization of new and existing therapeutics within this system will elucidate the full ability of the TEBV system to predict drug performance. Ultimately, the system may prove useful in reducing our reliance on animal models in preclinical trials and streamlining the drug development pipeline so more resources can be devoted to the most promising candidates in development.

Appendix A: Cell Culture Media Formulas

A.1: Endothelial Cell Media (Lonza)

*Used for all endothelial cell experiments 2014-2016

Materials

- EBM-2 base media
- EGM2 Singlequots Kit
- 5 mL Antibiotic/Antimycotic (can substitute penicillin/streptomycin)
- 50 mL heat inactivated (HI) FBS
- 500 mL and 150 mL vacuum filtration units

Procedure

1. Place EGM2 Singlequots Kit contents, Pen/Strep, and HI FBS into the warm water bath until thawed
2. Move Singlequots kit and EBM-2 media into the hood
3. Pour all the Singlequots contents EXCEPT the 10 mL FBS bottle into the EBM-2
4. Add 5 mL Anti/Anti to EBM-2
5. Invert media bottle until thoroughly mixed. If making serum-free media stop here.
6. Transfer 50 mL FBS-free media to a 50 mL conical and label "Serum-Free EPC media"
7. Add 50 mL HI FBS to EBM-2 (don't use the aliquot from the EGM2 kit yet)
8. Pour contents into 500 mL vacuum filtration unit
9. Label filtered contents with media type (EPC Completed Media). Attach EGM2 singlequots sticker to filtered bottle
10. Transfer 90 mL freshly filtered media to top of 150 mL vacuum filtration unit
11. Add 10 mL HI FBS from EGM2 kit
12. Filter media. Label solution "EPC Thaw Media"

A.2: Endothelial Cell Media (Cell Applications)

*Used for all endothelial cell experiments 2016 onwards

Materials

- Endothelial Cell Complete Growth Medium (Cell Applications, 211-500)
- 5 mL Antibiotic/Antimycotic (can substitute penicillin streptomycin)

Procedure

1. Add 5 mL Antibiotic/antimycotic to 500 mL endothelial cell complete growth medium.

A.3: Human Neonatal Dermal Fibroblast (hNDF) Media

Materials

- HG DMEM (Gibco Cat no. 11960-044) – 500 mL
- B-mercaptoethanol (500 uL)
- Antimycotic/Antibacterial (5 ml)
- MEM NEAA (5 mL)
- GlutaMAX (5 mL)
- Sodium Pyruvate (5 mL)
- HI-FBS (50 mL)

Procedure

1. Thaw HI-FBS and Anti/Anti in the water bath. *If using for cell culture immediately, warm HG DMEM in water bath as well.
2. Add all components except for HI-FBS to the DMEM. Mix by inverting.
3. Remove 50 mL of media/supplement mixture from DMEM.
4. Add 50 mL HI-FBS to media stock. Mix by inverting.
5. Run through 500 mL filter bottle.
6. Write makers name, current date, and "TEBV Media" on the bottle with a list of additives. Write an expiration date of one month from the date of preparation.

A.4: Tissue Engineered Blood Vessel Media

1 Week Base Media:

- 500 mL LG DMEM Media (1 g/L glucose + Sodium Pyruvate + L-Glutamine; GIBCO Cat No. 1185-084)
- 18.5 mL Heat Inactivated Fetal Bovine Serum
- 5 mL MEM NEAA (GIBCO 11140-076)
- 5 mL Anti/Anti (Pen/Strep/Fungizone)

For Multi-Week TEBV Media mix:

- ~500 mL TEBV media
- 1120 mg 6-aminocaproic acid (Sigma)

Procedure

1. Mix desired components in the top portion of a vacuum filtration unit. Stir well with sterile pipette to mix in any powdered components.
2. Vacuum filter solution. Label bottle with contents and media type

Appendix B: Human Umbilical Cord Blood Endothelial Cell Isolation

Materials needed:

1. 50 ml or more of whole blood (anti-coagulated, fresh not frozen)
2. 50 μg/ml of Rat Tail Collagen type I in 0.02N acetic acid (RTC I) (should be sterile and filtered)
3. 6-well plate
4. Histopaque 1077 (taken out of refrigerator and equilibrated to room temperature)
5. Hank's Buffered Salt Solution (HBSS) w/o $CaCl_2$, $MgCl_2$, & $MgSO_4$
6. Six 50-ml Falcon Tubes
7. Wash media (EBM-2 media—Lonza with 10% FBS and no bullet kit)
8. DPBS -/-.
9. EBM-2 complete media containing 10% FBS and bullet kit (Lonza)

Procedure:

Note: Maintain blood at room temperature after receiving. Procedure is for isolating EPCs from 50 mL of whole blood.

1. Coat 6-well plate with 50 ug/ml of Rat tail collagen type I (BD Biosciences) in 0.02 N acetic acid (1-0.5 days before plating)
2. Remove Histopaque (Sigma) from refrigerator and equilibrate to room temperature
3. 50 ml of anti-coagulated blood is diluted 1:1 with HBSS w/o calcium chloride, magnesium chloride, and magnesium sulfate
4. Blood-HBSS mixture is layered on top of equal volume of Histopaque slowly with 25 mL pipette to create well defined layers
5. Centrifuge tubes for 30 minutes at 740g, with low brake (centrifuge setting 1)
6. Aspirate off platelet rich plasma layer
7. Use 10 mL pipette and remove mononuclear cell layer and place into a fresh 50 mL conical tube

8. For every 10 ml of MNC mixture, add approx 15 ml of EBM-2 media + 10% serum (w/o bullet kit)
    a. Starting with 50 ml blood, should have two tubes with each with 20 ml of MNC mixture and 30 ml of wash media
9. Centrifuge tubes for 10 minutes at 515g. high brake (setting 3)
10. Resuspend each pellet in 20 ml of EBM-2 media and combine into single tube (total volume 40 ml)
11. Centrifuge tubes for 10 minutes at 515g. high brake (setting 3)
12. Resuspend cell pellet in 20 ml of EBM-2, remove 10 microliters and perform cell count and record.
13. Centrifuge tube for 10 minutes at 515g.
14. While spinning, wash collagen-I coated pates 3X in DPBS
15. Resuspend pellet in 12 ml of EBM-2 Complete Media (contains all growth factors, antibiotics, +10% additional serum)
16. Seed MNCs into each well of a 6-well plate (4 ml cell solution per well) pipetting slowly and gently.

24 hours later

1. Slowly remove media from each well with a 5 ml pipette. Slowly rinse with 2 ml of fresh media. Slowly add 4 mL media.

In the first 7 days

1. Change media every day in the first 7 days. Slowly remove media from each well with a 5 ml pipette. Slowly add 4 ml of fresh media.

    Note: removal and addition of media in the first 7 days should be done as slow as possible (rate of about 1 ml per 4-5 seconds)

After first 7 days

1. Change media every other day. Remove media from each well by vacuum. Slowly add 2 ml of fresh media. Carefully check daily if the colonies show up which generally happens within 10 ~14 days.

Upon seeing colonies

1. Check if they are EC-like colonies. Carefully remove unwanted colonies using cell scraper and wash the wells with warm media twice. 1 ~ 2 colonies recommended for each 6-well.
2. Use 300 ul of 0.025% trypsin per colony at 5 minutes for lifting it. If the colony is not detaching well, add an extra 200 uL trypsin and wait an additional 5 minutes. Add 2 ml of culture medium to neutralize it and gently spread cells in the same well. (NO CENTRIFUGATION, P1)
3. Change medium the next day.

Expanding the EPCs

1. When cells in the 6-well are near confluency, use 1 mL of 0.025% trypsin per well at 5 minutes for lifting cells. Add 5 ml of culture medium to neutralize it. Expand them in 3 6-wells with 2 mLs media/trypsin in each well. (NO CENTRIFUGATION, P2).
2. Change medium the next day. Add 2 ml of medium in each well.
3. When EPCs reach confluency, trypsinize cells as Step 7 and pool all EPCs from your original well (3 wells in a 6 well plate) (CENTRIFUGATION & COUNTING IS POSSIBLE, P3)
4. Seed cells at a minimum density of ~6,700 cells/cm^2 or 500,000 cells/T-75 into appropriate number of flasks/well plates.
5. Freeze cells down when confluent at 1 x 10^6 cells/mL in Cell Applications Freezing media. (P4)

*Note, colony-bearing well cells should be frozen down and characterized individually rather than being pooled to ensure that any wells containing mixed populations do not contaminate more pure wells.

Appendix C: Flow Cytometry of CBECFC Isolations

Materials

1. DPBS with Mg^{2+} and Ca^{2+} (PBS +/+) *optional
2. DPBS without Mg^{2+} and Ca^{2+} (PBS -/-)
3. 0.025% trypsin/EDTA
4. EPC media
5. 20 mL solution of 10% Goat Serum in DPBS
6. 0.5% PFA in PBS or 10% formalin
7. Clear flow tubes with caps
8. Flow cytometry antibodies described in Table 1

Table 1: Antibodies used for flow cytometry characterization of CBECFCs after isolation and expansion.

Tube No.	Antibody	Conjugate	Vendor	Cat #	Goal Marker Result
1	CD31	FITC	BioLegend	303103	POS
2	CD34	FITC	BioLegend	343603	POS
3	VE Cad.	PE	BioLegend	348505	POS
4	CD14	FITC	BioLegend	325603	NEG
5	CD45	FITC	BioLegend	304005	NEG
6	CD115	PE	BioLegend	347303	NEG
7	CD105	FITC	BioLegend	323204	POS
8	Mouse IgG1	FITC	BioLegend	406605	N/A
9	Mouse IgG1	PE	BioLegend	406607	N/A
10	None	N/A	N/A	N/A	N/A

Methods

*For each well of each donor of ECFCs that produces colonies appearing morphologically as ECs and having uniform appearance.

1. Rinse each T-75 flask with 5 mL DPBS (-/-) 2X
2. Add 2 mL 0.025% trypsin to flask for 5 minutes to detach cells

3. Neutralize trypsin with 8 mL EPC Media per flask. Pipet up and down to mix into single cell suspension. Combine cell suspensions from all flasks into one mixture.
4. Remove 15 uL from suspension for cell counting
5. Separate 5,000,000 cells into a conical. Centrifuge at 1500 rpm for 5 minutes.
6. Resuspend pellet with 2 mL DPBS (+/+)
7. Centrifuge pellet at 1500 rpm for 5 minutes.
8. Resuspend pellet in 2 mL DPBS +/+
9. Centrifuge at 1500 rpm for 5 minutes.
10. Resuspend pellet in 1000 μL 10% Goat Serum solution
11. Divide into 10 95 uL aliquots (~$5x10^5$ cells / sample) in 1.6 mL microcentrifuge tubes
12. Add 5 uL preconjugated antibody to each aliquot.
13. Incubate covered in foil on ice (can put on shaker if desired) for 30 minutes.
14. Centrifuge at 1500 rpm for 5 minutes to remove antibody
15. Add 1 mL of 10% GS solution to each tube
16. Centrifuge at 1500 rpm for 5 minutes.
17. Fix using 0.5% PFA or 10% formalin for 20 min at RT on cell rotator. (Add fixative in the fume hood).
18. Resuspend cells in 500 uL DPBS in numbered flow tubes (clear polystyrene tubes, non-sterile, without cracks in the walls!).
19. Store at 4 ºC until analysis. Immediately before analysis transfer suspensions to numbered flow tubes. Keep samples protected from light after antibody conjugation
20. Collect 9,000 events per sample at flow cytometry core facility.

Appendix D: Culture and Passage of 2-D Monocultures

D.1: Passage and Seeding of CBECFCs

Materials

- EPC media (Lonza or Cell Applications)
- Sterile PBS -/- (Gibco 1X DPBS no calcium/magnesium)
- 0.025% Trypsin (made by diluting 0.05% trypsin 1:1 with DPBS -/-)
- T-75 flask(s)
- 15 mL conical *if counting
- 5 mL pipettes
- 10 mL pipettes
- Hemacytometer *if counting
- P20 micropipette and sterile pipette tips *if counting

Procedure

1. Place EPC media in the water bath for 5-10 minutes before use. Leave trypsin out for 5-10 minutes until it has reached room temperature before use
2. Spray the hood down with 70% ethanol and wipe with Kimwipe
3. Spray all materials except hemacytometer & pipettes with 70% ethanol and place in hood
4. Remove cells from incubator. Spray outside before placing inside hood.
5. Aspirate the media
6. Wash cells twice with PBS -/- (~5 mL/rinse), aspirating between rinses
7. Add 2 mL 0.025% trypsin to flask and wait five minutes. Ensure trypsin coats the entire surface with cells growing.
    a. Can place flask into incubator if desired.
    b. Check on the microscope after 5 minutes. Rap gently to detach cells that may be stuck.
8. Add 8 mL media to flask. Use the media to wash the TC treated side of the flask to dislodge any remaining cells. Mix well to ensure even distribution of cells

To Passage 1:10

9. Add 1 mL suspension to a fresh T-75
10. Add 9 mL warm media to flask to bring total volume to 10 mL

11. Label flask with your name, cell type, date, passage number, and isolation information

To Count and Passage

9. Transfer 10 mL cell suspension into a 15 mL conical *ensure cell suspension is **well-mixed** when you transfer
10. Take a 15 uL sample from the cell suspension and pipette into one side of a hemacytometer
11. Place 15 mL conical containing cell suspension into the centrifuge at 1000-1400 rpm for 5 minutes (setting #1 on the centrifuge)
12. While cell suspension is on the centrifuge, count the cells in the hemacytometer
13. Use the following formula to calculate the total number of cells in your suspension.
    a. $\frac{\#\ cells\ counted}{\#\ quadrants\ looked\ at} * 10{,}000 * volume\ suspension = tot\ \#\ cells$
14. After centrifugation, aspirate media from the 15 mL conical *careful not to suck up the pellet!
15. Re-suspend cells as needed, mixing thoroughly.
16. Seed into a new flask or well-plate as appropriate for experimentation

D.2: Passage and Seeding of hNDFs

Materials

- hNDF media
- Sterile PBS -/- (Gibco 1X DPBS no calcium/magnesium)
- 0.05% Trypsin (aliquots in freezer and/or fridge)
- T-175s (Halve all volumes if using a T-75)
- 50 mL conical
- 10 mL pipettes
- 25 mL pipettes
- Hemacytometer *if counting
- P20 micropipette and sterile pipette tips *if counting

Procedure

12. Place hNDF media in the water bath for 5-10 minutes before use. Leave trypsin out for 5-10 minutes until it has reached room temperature before use
13. Spray the hood down with 70% ethanol and wipe with Kimwipe
14. Spray all materials except hemacytometer with 70% ethanol and place in hood
15. Remove cells from incubator. Spray outside before placing inside hood.
16. Aspirate the media
17. Wash cells twice with PBS -/- (~10 mL/rinse), aspirating between rinses
18. Add 10 mL 0.05% trypsin to flask and wait five minutes. Ensure trypsin coats the entire surface with cells growing.
    a. Can place flask into incubator if desired.
    b. Check on the microscope after 5 minutes. Rap gently to detach cells that may be stuck.
19. Add 10 mL media to flask. Use the media to wash the TC treated side of the flask to dislodge any remaining cells. Mix well to ensure even distribution of cells

To Passage 1:10

20. Transfer 20 mL cell suspension to a 50 mL conical
21. Centrifuge for 5 minutes at 1000 rpm.
22. Aspirate liquid material. Resuspend cells in 10 mL warm media.
23. Transfer 1 mL new cell suspension to a new T-175. Cover with an additional 24 mL cell-free media.
24. Label flask with your name, cell type, date, passage number, and isolation information

To Count and Passage

17. Transfer 20 mL cell suspension into a 50 mL conical *ensure cell suspension is *well-mixed* when you transfer
18. Take a 15 uL sample from the cell suspension and pipette into one side of a hemacytometer
19. Place 50 mL conical containing cell suspension into the centrifuge at 1000 rpm for 5 minutes (setting #1 on the centrifuge)
20. While cell suspension is on the centrifuge, count the cells in the hemacytometer.
    a. $\frac{\#\ cells\ counted}{\#\ quadrants\ looked\ at} * 10{,}000 * volume\ suspension = tot\ \#\ cells$
21. After centrifugation, aspirate media from the 15 mL conical *careful not to suck up the pellet!
22. Re-suspend cells as needed, mixing thoroughly.

23. Seed into a new flask or well-plate as appropriate for your experiments

Appendix E: Fluorometric Hydrogen Peroxide Concentration Assay

Product No: MAK165 (Sigma-Aldrich); stored at -20°C

Fluorescence Specs:
Excitation Wavelength = 540 nm
Emission Wavelength = 590 nm

Stock Solution Preparation
Peroxidase Substrate Stock Solution
1. Reconstitute Peroxidase substrate in 250 µL DMSO (provided in kit). Mix well.
2. Aliquot into 25 µL and store at -20°C **protect from light**

Horseradish Peroxidase/Red Peroxidase
1. Reconstitute contents in 1 mL Assay Buffer. Mix well.
2. Aliquot into 100 µL and store at -20°C **protect from light**

Protocol

Hydrogen Peroxide Standard Preparation
1. Add 12.5 µL 3% H_2O_2 to 487.5 µL Assay Buffer to make 20 mM stock solution H_2O_2
2. Dilute 1 µL 20 mM stock in 1.999 mL Assay Buffer to make 10 µM working solution. Dilute 90 µL 10 µM stock in 210 µL Assay Buffer.
3. Prepare standard curve from working solutions serially diluting 1:10.

Table 2: Preparation of Standards for Fluorometric Hydrogen Peroxide Assay

The solutions here are made by diluting from the solution made in the row directly above it. Standards 1, 3, 5, and 7 are serial dilutions made in parallel with standards 2, 4, 6, and 8.

Std No.	Solution Concentration	Volume Stock	Volume Assay Buffer	Std No.	Solution Concentration	Volume Stock	Volume Buffer
1	10 μM	120 μL	0 μL	2	3 μM	120 μL	0 μL
3	1 μM	12 μL	108 μL	4	0.3 μM	12 μL	108 μL
5	0.1 μM	12 μL	108 μL	6	0.03 μM	12 μL	108 μL
7	0.01 μM	12 μL	108 μL	8	0 μM	0	50 μL

4. Add 50 μL/well prepared standards to appropriate wells in 96 well plate (2 wells/concentration)

Sample Preparation

1. Harvest 500 μL samples from TEBV reservoir or well plates while changing media.
2. Dilute samples and/or fresh media controls along the following dilution curve (prepare in well):

Table 3: Guidelines for dilution of samples to working range of the fluorometric hydrogen peroxide assay

Concentration	Volume Stock	Volume Assay Buffer
100	50	0
50	25	25
10	5	45
5	2.5	47.5
2	1	49
1	0.5	49.5

3. Prepare media "blanks" (0 μM control media sample to correct for media-only effects on sample fluorescence) using the same dilution curve as above using 0 μM H2O2 media.

Assay Reaction

1. Prepare Master Mix: (recipe is for ~31 wells)
    - Red Peroxidase Substrate Stock: 25 μL
    - 20 units/mL Peroxidase Stock: 100 μL
    - Assay Buffer: 2.375 mL

        *Note: Master Mix is not good after 2 hours

2. Add 50 μL Master Mix to all

3. Mix plate by shaking gently and incubate at room temperature, protected from light, for 15 minutes
4. Measure fluorescence with plate reader

Analyzing Results

1. Average values for the two 0 μM (blank) H_2O_2 standard wells. This is the background signal for the standard curve. Subtract this value from all points in the standard curve.
2. Average values for the media blanks and subtract each blank from the appropriate media dilution condition.
3. Calculate sample H_2O_2 concentrations using a regression equation calculated from the linear portion of the standard curve held to a y-intercept of 0.
4. Compare the values of the fresh media samples to the values of the conditioned media samples along their respective dilution curves.

Appendix F: Hydrogen Peroxide Treatment of Cells in 2-D Monoculture

1. Thaw Cells

1. Fill a T-75 flask with 10 mL warm 10% complete EPC media.
2. Remove EPCs from liquid nitrogen storage. Warm by hand or in water bath until just thawed. Pour contents into T-75 flask.
3. Label flask with isolation & passage information and place in incubator.
4. Change media on cells after 24 hrs and return to incubator.
5. Allow the cells to grow in incubator until confluent or almost confluent before beginning experiment

2. Seed for Experiment

1. Harvest EPCs from T-75 flask
    a. Rinse 2X with sterile PBS -/-
    b. Cover cells with 2 mL 0.025% trypsin for 5 minutes at 37C
    c. Add 8 mL media to flask, rinsing well, and mixing the cell suspension thoroughly.

d. Transfer to a 15 mL conical.

2. Take a 15 uL sample of the cells and count on a hemacytometer.
    a. Centrifuge the cell suspension at 1000 rpm for 5 minutes (setting #1 on the centrifuge) while counting cells
    b. Equation: $\frac{\#\ cells\ counted}{\#\ quadrants\ looked\ at} * 10{,}000 * volume\ suspension = tot\ \#\ cells$
    c. Resuspend cells at 1.0 x 10^6 cells/mL
3. Plate cells at the following density:
    a. 10,000 cells/well in 24 well plate (20,000 cells/well in a 12 well plate) for control or 50 uM conditions
    b. 15,000 cells/well in 24 well plate (30,000 cells/well) for 100 uM conditions
4. Allow the cells time to adhere to the flask overnight[98,149,150].

Table 4: Serial dilutions for preparation of 100 and 50 μM H_2O_2 solutions.

Each solution is prepared by diluting from the solution made in the previous line. *50 μM H_2O_2 is made by diluting from the 1 mM stock rather than the 100 μM solution.

Stock Volume	Media Volume	Final Ccn
10 uL	87.7 uL	1 M
10 uL	90 uL	100 mM
40 uL	1.96 mL	1 mM
1 mL	19 mL	100 uM
0.5 ml	19.5 mL	50 μM*

During this time, prepare a diluted H2O2 solution. Replace media in flasks with appropriate concentration for condition. Change media every 48 hours

    a. Warm complete, peroxide free media and allow H2O2 to reach room temperature
    b. Dilute H2O2; Stock concentration: 9.77 M
    c. Aspirate old media from T-75 flask. If media contains H2O2, it must be removed with a pipette and transferred to a secondary container until it can be placed in the H2O2 waste container in the fume hood.
    d. Rinse with ~10 mL sterile PBS -/-
    e. Add 20 mL fresh media with 0 or 100 uM H2O2 concentration to flask
6. On Day 6 after plating the cells, change the media. Include 100 U/mL TNFa to one replicate of each concentration.
7. Fix all conditions on Day 7.

Appendix G: Immunofluorescence of 2-D Cells

Materials:

- 10% Neutral Buffered Formalin
- 0.1% Triton Solution diluted in PBS +/+ (nonsterile)
- PBS +/+ (Gibco)
- Goat Serum (diluted to 10% in PBS +/+)
- Primary Antibodies
- Secondary Antibodies
- Hoechst 33342 dye

Protocol for Cells in a 24-well plate:

1. Aspirate media from wells at the conclusion of the experiment.
2. Fix cells in formalin (enough to cover bottom of well) for 10 minutes (must fix in the fume hood)
    a. If stopping rinse cells 3X with PBS +/+ and store at 4C
3. Add 500 uL 0.1% Triton-X for 5 minutes to permeabilize cells
4. Rinse wells 3 times with 500 uL PBS +/+
5. Block with 500 uL 10% goat serum at room temperature for 45 minutes.
6. Aspirate goat serum
7. Add primary antibodies each at 1:250 dilution if Abcam antibodies or 1:200 if SCBT antibodies in 1% goat serum. Incubate overnight (> 12 hours) at room temperature on a rocker (250 uL solution/well)
8. Rinse wells 3 times with 500 uL PBS +/+ (5 minutes for each rinse)
9. Turn off overhead lighting. *Note:* After this step, plates must be handled in darkness and/or covered with aluminum foil unless imaging
10. Add secondary antibodies each at 1:500 dilution in 1% goat serum plus 1 uL/mL Hoechst 33342 dye. Incubate **covered with foil** for 1 hr at room temperature (250 uL solution/well)
11. Rinse wells 3 times with 500 uL PBS +/+ (10 minutes for each rinse). Image immediately, or store with 500 uL PBS +/+ covering wells refrigerated and wrapped in aluminum foil until imaging

Appendix H: Live Dead Stain of 2-D Cells

*Stock reagents should be stored in a 50 mL dark conical at -20°C when not in use
**Everything should be conducted protected from light/all plates should be covered

1. Allow the LIVE/DEAD® stock solutions to warm to room temperature
2. Add 20 uL of 2mM EthD-1 (Component B) stock solution to 10 mL D-PBS -/-
3. Add 5 uL of 4 mM calcein-AM (Component A) to the EthD-1/PBS solution.
4. Add 10 uL Hoechst 33342 to solution.
5. Vortex to mix thoroughly. Working solution must be used within 24 hours.
6. Add 1 mL to each well/
7. Incubate for 40 minutes at room temperature on a rocker. Wrap plate with foil to protect from light.
8. Rinse and replace with fresh D-PBS (-/-) if fixing or phenol-free media if cells are being imaged immediately
9. Image right away at 37°C and return to normal growth media for continued experimentation.

-OR-

10. Fix cells with Paraformaldehyde for 10 minutes
11. Rinse with PBS 3X and store at 4°C until ready to image.

Appendix I: Fabrication of Tissue Engineered Blood Vessels

Materials

1. Rat tail collagen I (BD Biosciences, 354236)
2. Acetic acid (0.6%)
3. Dulbecco's Modified Eagle's Medium, Low Glucose, 10X, (Sigma, D2429)
4. 5M NaOH
5. Neonatal human dermal fibroblasts (hNDFs), P6-11 (Lonza, CC-2509)
6. Umbilical Cord blood derived endothelial colony forming cells (CBECFCs), P4-P7
7. hNDF growth media warmed
8. TEBV perfusion media, warmed
9. Endothelial cell (EC) growth media, warmed
10. 0.025% trypsin, warmed
11. 0.05% trypsin, warmed
12. DPBS -/- (Gibco, 14190144)
13. 50 mL falcon tubes
14. 3-mL sterile disposable syringes, Luer Lok tip, (BD Biosciences, 309657)
15. 1-mL sterile disposable syringes, slip tip, (BD Biosciences, 309659)
16. PVDF One-way Stopcock with male Luer Lok (Masterflex, HV-31200-91)
17. Stainless steel mandrels, 0.032" (0.81mm) diameter (McMaser Carr,
18. 10-12 1-ply Kimwipes
19. Nylon mesh, 0.8 μm pore size (Whatman, 7408004)
20. Parafilm
21. Two stainless steel tweezers, autoclaved (Sigma,
22. 6 Stainless steel screws, 8-32, flathead, 1.25" length (McMaster Carr, 91500A201)
23. 6 Stainless steel thumb nuts, 8-32, ½" head size (McMaster Carr, 91833A121)
24. Stainless steel tray (McMaster Carr, 4189T7)
25. Phillips head screwdriver

Preparation of Stock Solutions

1. Prepare 0.6% v/v acetic acid solution from glacial acetic acid stock
    1.1. In a fume hood, add 497.0 mL deionized (DI) water to a clean glass 1L beaker.
    1.2. Add 3.0 mL glacial acetic acid.
    1.3. Stir using a magnetic stir bar at medium speed until well mixed.
    1.4. Carefully move beaker to a sterile biosafety cabinet and filter using a 500 mL 0.1 μm filter unit. Assign an expiration date of 1 year after preparation.
2. Prepare 5M NaOH solution from solid pellets (CAS 1370-73-2)
    2.1. Weight out 4.0 g NaOH pellets in a fume hood

2.2. Transfer NaOH pellets to a clean 100 mL beaker containing a magnetic stir bar
2.3. Slowly add 20.0 mL DI water to beaker
2.4. Stir with stir bar at medium speed until fully dissolved and allow mixture to cool to room temperature.
2.5. Transfer beaker and contents to a sterile biosafety cabinet. Using a 30 mL syringe, filter the solution with 0.22 μm PVDF filter and store in a sterile falcon tube. Assign an expiration date of 1 year after preparation.

Chamber Assembly & Sterilization of Materials

1. Preparation of Kimwipes for Plastic Compression
    1.1. Place 10 single ply kimwipes on top of each other
    1.2. Lay nylon mesh circle in the center and place into sterilization pouch and autoclave.
2. Also sterilize by autoclaving for 20 minutes at 120C:
    2.1. Two pairs of stainless steel tweezers
    2.2. Stainless steel scissors
    2.3. Two-way stopcock and 0.81 mm mandrel (one each per vessel)
    2.4. Stainless steel screws and screw nuts (6 each per chamber to be used)
3. Wrap TEBV grip threading in 2-3 layers of Teflon tape and screw into chamber base until finger-tight.
4. Attach short pieces of tygon tubing equipped with female:barbed luer lock port on one end to the barbed outlets of chamber base.
5. Add luer lock caps to the open ends of grips and tubing.
6. Wrap assembled chamber base and chamber top in fabric and place in appropriate sterilization pouch with Gas-Chex indicator visible through bag. **Record BME Department, office phone number, initials, and date on bag as well**
7. Take chamber and tube sets for gas sterilization at core facility in Duke Hospital.
8. **NOTE*:* If preparing more than 2 TEBVs at one time, passage ~1,300,000 EPCs into T-25 flasks (one per pair of TEBVs that will be made) at this time as well.

Preparation of Fibroblast-seeded 3-mL Collagen Constructs

1. Prepare the syringe mold by attaching the syringe to the luer lock of the stopcock and closing the stopcock.
2. Passage hNDFs according to normal protocol. Resuspend at a concentration of 5×10^6 cells/mL. Work as quickly as possible.
3. Combine Collagen I, 0.6% acetic acid, and 10X DMEM in the order and volumes specified in the TEBVReagentCalculations.xlsx file in a 50 mL conical tube. Mix after adding DMEM by gently swirling conical until color is dispersed.

Note: collagen I stock solution is highly viscous – pipette very slowly to limit adhesion to pipette tip walls
Note 2: use a fresh pipette tip for each draw of collagen from the bottle
4. Raise pH to 8.5 by adding 85% of the recommended volume of 5M NaOH. Gently mix solution as before. Titrate in 0.5 uL increments until color changes from yellow/orange to magenta/
Note: This step is critical for gelation – collagen will not gel if solution is orange or red.
5. Add hNDF fibroblast suspension to collagen solution. Mix gently by swirling.
6. Pour the collagen/hNDF solution into the syringe mold and use sterile tweezers to place the mandrel in the center (base should be resting in center of luer stopcock). Stretch parafilm over the top of the syringe keep the mandrel in the center of the syringe (can adjust position as needed with sterile tweezers).
7. Allow to gel at room temperature for 30 minutes.
Note: when making multiple TEBVs simultaneously, stagger the timing of NaOH addition so that you can gel each vessel for 30 minutes and monitor it while it compresses.
8. Remove sterilized kimwipes/filter set from sterilization pouch.
9. After the collagen solution has gelled, gently push the collagen tube out of the open end of the syringe, keeping the gel on the mandrel. Use sterilized tweezers to hold the mandrel and gently lay the gel in the center of the nylon mesh.
10. Fold the Kimwipes around the gelled solution and pinch at the top. Suspend solution for 6-8 minutes.
11. Remove vessel from Kimwipes and place immediately in well of a 6-well plate filled with ~5mL warm TEBV media.
Note: If preparing multiple vessels simultaneously, compress and store all vessels in TEBV media before preparing chambers and mounting vessels
12. Prepare chamber for vessel:
    a. Remove chamber from sterilization pouch being careful not to touch internal surfaces with gloves or place on surface of hood.
    b. *BEFORE YOU PUT THE VESSEL IN THE CHAMBER* screw the screws into the base of the chamber until flush with the acrylic.
    c. Use sterile tweezers to place TEBV on grips being careful to insert grips into lumen of prepared vessel. Pull vessel on either side to confirm fit.
    d. Gently pipette ~5 mL warm TEBV media into the container, being careful not to pipet directly onto the vessel and disturb its position.
    e. Secure vessel by lightly pressing ligation clips onto each end of the vessel. If possible, attach ligation clips over thicker portion of grips to minimze risk of unintentionally crushing thinner portion and blocking grip lumen.
    f. Place chamber top down carefully. Tighten screw nuts onto exposed ends of screws until finger tight.

g. Keep in incubator until ready to endothelialize. Do not leave for more than 4 hours without perfusion or the insides of the lumen may begin to fuse.

Endothelializing and Perfusing TEBVs

1. Harvest EPCs and re-suspend at a concentration of $1x10^6$ cells/mL in *TEBV* media rather than EPC media.

Note: If making multiple vessels at once, ECs should be harvested immediately before injecting into each vessel otherwise they will begin to adhere to the conical they are being stored in and vessels will have poor functionality.

2. Set aside 500 uL of the cell suspension.

3. Remove caps from the TEBV grips. If caps do not come off easily, use a pair of pliers to hold the grips steady so that turning the cap does not twist the TEBV (which may block the lumen).

4. Use a large gauge needle attached to a 1 mL slip tip syringe to collect 500 uL solution of ECs.

5. Press empty 1-mL syringe on one outlet of the chamber. Remove needle from other syringe (and push out any excess air), then press into the other chamber outlet.

6. Slowly push the EC solution into the vessel lumen while drawing back on the other syringe to draw solution into vessel. Push media back and forth 2-3 times.

7. Replace caps on chamber grips and mount chamber on rotation device and place in incubator. Allow to rotate for 30 minutes.

8. Prime perfusion system for attachment to chamber:

a. Pipette 25 mL warm TEBV media into reservoir of sterile perfusion system.

b. Run tube set (without connecting to chamber) on pump to prime flow circuit before mounting on chamber.

9. Remove caps from TEBV chamber and attach each port to the corresponding flow port on the perfusion system. Minimize introduction of air into tubing. If necessary, clip tubing while attaching components. Make sure to keep ends of tubing/caps sterile.

Appendix J: Immunofluorescence in TEBVs

Materials:

- DPBS
- 10% neutral buffered formalin
- Goat serum
- 0.1% Triton-X
- Primary antibody
- Secondary Antibody
- Hoechst 33342 dye

Protocol:

1. Using two 1-mL syringes, perfuse TEBV lumen with 10% neutral buffered formalin. Incubate for 10 minutes at room temperature. Fill chamber with 10% formalin to bathe TEBV as well.
2. Cut appropriate portion of TEBV off grips and place in 6-well plate. Incubate in 10% neutral buffered formalin for an additional 30 minutes. After this try to minimize handling of the TEBV.
3. Rinse TEBV 3x with +,+ DPBS.
4. Cut TEBV *en face* with scissors. Cut into smaller sections if desired. Smaller sections may be stained in a 24 or 48-well plate to save antibody solution.
5. Permeabilize with 0.1% Triton-X for 5 minutes.
6. Rinse 3X with DPBS
7. Block with 10% goat serum. Incubate at room temperature for 8 hours, or at 37 ºC for 4 hours.
8. Aspirate goat serum.
9. Add primary antibody at 1:100 ratio in 10% goat serum. Incubate overnight at 4ºC.
10. Rinse well 3 times with DPBS to remove unbound primary antibody.
11. *In darkness.* Add secondary antibody at 1:500 ratio in 10% goat serum and Hoechst dye at 1 uL/mL. Cover well plate in aluminum foil. Incubate for 1 hour at room temperature.
12. Rinse well 3 times with DPBS to remove unbound secondary antibody.
13. Transfer TEBV pieces to labeled microscope slides with fluoromount and cover with coverslip. *Ensure there are no air bubbles trapped in the slide/slip space, this will interfere with microscopy later.

Appendix K: Protocol for Processing and Quantifying Images in ImageJ

For All steps: use the feature
Process -> Batch -> Macro

K.1: DAPI Nuclear Processing

1. Open batch processor and select appropriate input and output folders
2. First adjust the background and contrast of the DAPI images
    a. Make sure to specify "DAPI" in the file name contains field
    b. Code:

```
run("Subtract Background...", "rolling=50");
run("Enhance Contrast", "saturated=0.35");
```

3. Run nuclear counter macro on the processed images
    a. Reopen the batch processor
    b. Reselect appropriate input and output folders
    c. Make sure to specify
    d. Run code:

```
setAutoThreshold("Huang dark");
setOption("BlackBackground", true);
run("Convert to Mask");
run("Fill Holes");
run("Remove Outliers...", "radius=10 threshold=50 which=Bright");
run("Despeckle");
run("Despeckle");
run("Watershed");
run("Analyze Particles...", "size=450-Infinity summarize");
```

4. Copy the contents of the summary box into an excel file and save the count values into appropriate rows/columns for analysis

K.2: P21 Nuclear Counting

1. Open batch processor and select raw folder again
2. Adjust background and contrast of the images using averaged values for max and min pigment values
    a. Open 3-5 random treated P21 images

b. Manually subtract background (process-> subtract background -> 50 pixel radius)
c. Adjust brightness contrast (Image -> adjust brightness/contrast -> Auto
d. Record the max and min pixel values on the display below histogram box
e. Repeat for all random images and average together the pixel values
f. Run batch code *specify P21 in file name contains* replacing the setMinandMax numbers with your averaged pixel min and max values:

```
run("Subtract Background...", "rolling=50");
run("Enhance Contrast", "saturated=0.35");
setMinAndMax(30, 555);
```

3. Determine threshold to use for nucleus counting
a. Open 3-5 processed images
b. Open the threshold adjuster (Image -> adjust -> threshold)
c. Determine the max/min accepted pixel intensities using the Otsu threshold and average the values from your representative images
d. Open batch processor and reselect input and output folders.
e. Run Code modifying the threshold numbers with your calculated values specifying P21 in file name contains field:

```
setThreshold(207, 3513);
setOption("BlackBackground", true);
run("Convert to Mask");
run("Fill Holes");
run("Remove Outliers...", "radius=10 threshold=50 which=Bright");
run("Despeckle");
run("Despeckle");
run("Watershed");
run("Analyze Particles...", "size=225-Infinity summarize");
```

f. Copy summary data from text box into excel file and sort into appropriate rows/columns for analysis

K.3: Membrane Protein Processing (e.g. ICAM/VCAM/SMA/Calponin, etc.)

1. Open a couple representative images and perform steps 1 and 2 of the P21 nuclear counting protocol specifying the appropriate protein.
2. Process the batch using the appropriate signifier for the protein of interest
3. Manually count positive cells from your **composite images**

K.4: Batch Composite Making

1. Open a set of images for a condition (e.g. all DAPI, P21, and ICAM images from one well on a plate)
2. Stack images for each stain type (Image -> Stacks -> Images to Stack) specifying the protein/stain type in the file name contains field
3. Merge the images into a composite
    a. Open Image -> Color -> Merge Channels
    b. Select the right channel for each stain type (DAPI/Hoechst = blue, P21/contractile proteins = red, membrane proteins = green)
    c. Save each image in the resulting stack as a .jpeg with the appropriate file name

Appendix L: Isolation of RNA from flash frozen TEBV samples

Appendix M: SYBR Green qRT PCR Protocol

Measuring RNA Concentration using Nanodrop (NOTE: Avoid rethaw cycles as RNA degrades quickly. Keep RNA samples on ice.)

1. Place RNA samples (and REF sample) in cooler and grab nuclease-free water, P2 pipette, and 10µl filter tips.
2. Log into computer (username: microarray, password: extraction) and select ND-1000 V3.7.1 >> Nucleic Acids.
3. Wipe down stage with Kimwipe. Add 1µl of nuclease-free water onto the stage and click "ok" in the initialization window that pops up.
4. Change DNA-50 (green) to RNA-40 (pink) using the pull-down menu in the upper-right corner.
5. Click "Blank" in the upper-left corner.
6. Wipe down stage with Kimwipe. Add 1µl of sample onto the stage and click "Measure" in the upper-left corner.
7. Record the RNA concentration (ng/µl), $A_{260/280}$, and $A_{260/230}$ of the sample. The $A_{260/280}$ purity level should be ~2; the $A_{260/230}$ purity level should be ~2.
8. Repeat steps 6-7 for each RNA sample.
9. After measuring the last sample, wipe clean the stage.
10. Exit out of the program and log off

B. Making cDNA

(NOTE: Complete RT on the same day that the RNA concentration measurements are made to avoid freezing and rethawing RNA samples.)

1. Calculate the appropriate volume (µl) of RNA sample needed for 250 ng of RNA. This is done by dividing 250 ng by RNA concentration in µg/µl. (Note: you may need to optimize the RNA amount for your own

assays, but it is advised not to go lower than 100 ng of RNA to make cDNA)

2. Calculate the volume (µl) of nuclease-free water such that the total amount of nuclease-free water + RNA sample is 18µl.

3. Wipe down bench, pipettes, and gloves with RNAse Zap. Grab the 96-well freezer boxes in the -20°C freezer pull-out shelf and wipe down the lid with RNAse Zap.

4. Add 5x iScript Reaction Mix (blue tube) and iScript Reverse Transcriptase (yellow tube) to ice bucket.

5. Take a 0.2ml colored reaction tube for each sample and place in the 96-well freezer box.

6. Add the calculated amount of nuclease-free water to the reaction tubes.

7. Add the calculated amount of RNA to the reaction tubes.

8. Add 5µl of the 5x iScript Reaction Mix (blue tube) to each reaction tube.

9. Add 1.25µl of the iScript Reverse Transcriptase (yellow tube) to each tube (NOTE: This is the polymerase that initiates the reaction, so add this component last.).

10. Mix by gently pipetting up and down (NOTE: Do not vortex.).

B.1. RT Process using MWG-Biotech thermocycler at the RNA station.

1. Turn the thermocycler on (behind the machine above the plug) (NOTE: Be careful when moving the thermocycler to avoid unplugging the machine.).

2. Select 2. Select Protocol >> 25-42.cyc.

3. Continue selecting Run/Enter until the thermocycler begins.

4. Sample will take about 45 minutes to run. Once the RT process is complete, you may choose to complete the PCR step or wait to complete

the PCR a different day (PCR takes 2.5hr to complete) and store the cDNA in the -20°C freezer in a sample box.

5. If you choose to complete the PCR on a different day, turn the thermocycler off.

C. PCR

(NOTE: Keep everything on ice or in freezer boxes during this process as this step is heat-sensitive; also, turn off the lights as this step is light-sensitive.)

C.1. Preparing cDNA Samples

1. Wipe down bench, pipettes, and gloves with RNAse Zap.

2. Grab cDNA samples and dilute with 20 μl of RNA-ase/DNA-ase free water; mix gently by pipetting up and down (NOTE: Be sure to mark that the samples have been diluted to avoid confusion with undiluted cDNA samples.).

3. Take two freezer boxes from the -20°C freezer. Wipe down the lids with RNAse Zap and place a 96-well PCR plate in the freezer box. (NOTE: Make sure that you do not touch the bottom of the 96-well PCR plate. Hold the plate by its sides to avoid initiating the reaction when samples have been aliquoted into the wells.)

4. Let y be the number of genes of interest. For x cDNA samples, obtain x*y 0.2-mL clear reaction tubes and place in the second freezer box.

5. Place iQ SYBR Green Supermix (orange tube) and primers (both forward and reverse primers) in ice bucket.

C.2. Preparing the reaction mixtures for each gene of interest

1. Label a 2.0ml colored microtube with the name of the gene for each gene of interest.

2. Combine the following reagents in each 2.0ml tube:

a. 6.6*[(3.5*x*1)+3] µl nuclease-free water

b. 1.2*[(3.5*x*1)+3] µl 3′ primer for gene of interest

c. 1.2*[(3.5*x*1)+3] µl 5′ primer for gene of interest

d. 10*[(3.5*x*1)+3] µl iQ SYBER Green Supermix

3. Mix solutions by pipetting up and down.

4. Repeat steps 6-7 for each 2.0ml tube labeled with the gene of interest.

C.3. Finalizing the reaction mixtures

1. Add 66.5µl of the solution prepared in step 7 to each of the 0.2-mL microtubes from step 4.

2. Add 3.5µl of the cDNA sample from the RT step to each 0.2-mL clear reaction tube.

3. Mix the solution by pipetting up and down.

4. Add 20µl of the mixed solution to each of 3 wells of the 96-well plate (NOTE: Add the mixed solution to the side of the well and let it drip down to the bottom. Make sure to avoid making air bubbles.).

5. Repeat for the other microcentrifuge tubes in an order according to the determined plate set-up.

6. Cover the 96-well PCR plate with optical tape and secure the cover.

7. Centrifuge the PCR plate at 1400 rpm for 3 minutes (NOTE: When transferring the PCR plate to the centrifuge, hold by the sides and avoid touching the bottom of the plate.).

C.4. Setting up the Thermocycler

1. Turn on the machine (switch in the back)

2. Open the Bio-Rad CFX Manager program

a. Under Select Run Type click on user-defined

b. Choose your Run Type:

i. Since you have already made cDNA, you will use the "3-step" options.

1. For qPCR with a melt curve, choose CFX_3StepAmp+Melt.prcl

a. The default annealing temperature is a bit low (55 ºC) – edit the annealing temperature to your optimized value (59.5 generally).

b. Edit solution volume to 20 μL.

2. To perform an annealing temperature assay, choose CFX_2StepGradientAmp+Melt.prcl

c. Click "next" to edit the plate.

i. Choose Express Load > QuickPlate_96wells_SYBROnly.pltd to load up a full plate – there is no need to de-select blank wells.

ii. You can manually set up your plate to your configuration and label samples and replicates if desired.

d. Click "next" to move to the run screen

i. Click "open lid" to open the lid and place your sample. Make sure "A1" is in the top left corner. (Note: only open and close the lid using the software OR by clicking the button on the front of the machine. DO NOT manually try to open and close the lid like older machines – this one is not designed that way and it will break the mechanism!)

ii. Click "close lid" to close the lid.

iii. Click “start run” to start the run. Save the run file in the “run files” folder. The run will take about 1.5 hours to complete.

Appendix N: Primer Sequences

Gene	Forward Sequence	Reverse Sequence
eNOS (NOS3)	5′-CATCTTCAGCCCCAAACGGA-3′	5′-ACGGGATTGTA GCCTGGAAC-3′
iNOS (NOS2)	5′-CCCCCAGCCTCAAGTCTTATTTC-3′	5′-CAGCAGCAAGTTC CATCTTTCAC-3′
SIRT1	5′-TGCTGGCCTAATAGAGTGGCA-3′	5′-CTCAGCGCCATGGAAAATGT-3′
NOX4	5′- GCAGGATCCGTCATA AGTCATCCCTCAGA-3′	5′-CTGTTAACGTCGA CTCAGCTGAAAGACTCTTTAT-3′
vWF	5′-GCAGTGGAGAACAGTGGTG-3′	5′-GTGGCAGCGGGCAAAC-3′
P4HB	5′-GGACGTGGAGTCGGACTCTG-3′	5′-GGCTGTCTGCTCGGTGAACT-3′
FSP-1	5′-GATGAGCAACTTGGACAGCAA-3′	5′-CTGGGCTGCTTATCTGGGAAG-3′
NF-κB p65 (RELA)	5′-AGCTCAAGATCTGCCGAGTG-3′	5′-ACATCAGCTTGCGAAAAGGA-3′

Appendix O: Antibodies Used

Table 5: Primary Antibodies Used for Immunofluorescence

Antigen	Conjugate	Source	Clonality	Isotype	Vendor	Catalog Number
vWF	–	mouse	monoclonal	IgG1	Abcam	ab194405
Calponin	–	rabbbit	monoclonal	IgG1	Abcam	ab56794
p21	–	rabbit	monoclonal	IgG1	Abcam	ab109520
VCAM1	–	rabbit	monoclonal	IgG1	Abcam	ab134047
E-Selectin	–	mouse	monoclonal	$IgG_{2a\kappa}$	SCBT	sc-137054
α-SMA	–	rabbit	monoclonal	IgG1	Abcam	ab124964
ICAM-1	–	mouse	monoclonal	$IgG1_{\kappa}$	SCBT	sc-107
mouse IgG	Alexa Fluor 594	goat	polyclonal	IgG	Life Technologies	A11037
rabbit IgG	Alexa Fluor 488	goat	polyclonal	IgG	Life Technologies	A11029
rabbit IgG	Alexa Fluor 633	goat	polyclonal	IgG	Life Technologies	A21070

Appendix P: Oil Red O Staining Protocol

Materials

- Oil Red O (Sigma, O0625-25G)
- Hematoxylin, Gill No. 2 (Sigma, GHS216)
- Isopropyl alcohol
- 10% Formalin
- DPBS +/+ (Gibco, 14040-133)
- Triethyl phosphate (Sigma, 538728-1L)
- DI water

Procedure

Preparing Oil Red O Stock Solution

1. Using Isopropanol1.Dissolve 0.35g Oil Red O in 100 ml isopropanol. Stir well for a few hours or overnight using stir bar and plate.

2. Sterile filter the solution3.Store at room temperature. The solution is stable for a year

Preparing Oil Red O Stock Solution Using Triethyl Phosphate

1. Create a 60% triethyl phosphate solution by mixing 60 ml of triethyl phosphate with 40 ml of DI water.

2. Dissolve 500mg of Oil Red O in the 60% triethyl phosphate solution. Use stir plate and let stir for at least 1 hour.

3. Filter the stock solution to remove Oil Red O aggregates.

Fixing Cells

*Procedure assumes 12-well plate. Modify the volumes accordingly for other well sizes.

1. Aspirate out the old media from the cells.

2. Wash cells to be fixed twice with1mlPBS++.

3. Aspirate PBS++.

4. Go to fume hood.

5. Fix the cells by adding 1 ml of 10% formalin. DO NOT add the formula directly onto the cells. Add onto to the wall and mix by gently rotating.

6. Incubate for one hour at room temperature. If staining on the same day as fixing:

    a. Prepare 60% isopropanol

    b. Prepare Oil Red O Working solution during this time (see next section)

7. Remove the formalin using a micropipette and eject the formalin into a designated container in the hood.

8. Rinse the cells twice with1 mL DI water

    a. If staining another day add 1 mL PBS to cells before storing at 4˚C until ready to stain.

Oil Red O Working Solution

1. Obtain a 50 or 15ml conical tube depending on how much Oil Red O you need

2. Add Oil Red O Stock to DI water in a 3:2 ratio. Ex: 6 Oil Red O Stock to 4 ml DI Water.

3. Let the solution stand for 10 minutes.

4. Sterile filter this solution using a syringe filter.

5. Store at room temperature (note: the solution will only be useful for about 2 hours)

Oil Red O Staining

1. Before starting, obtain a 50 mL conical tube that will serve as a waste for Oil Red O and hematoxylin. You can use an aspirator after removing the initial Oil Red O and hematoxylin.

2. If you are using the isopropanol solution:

   a. Incubate the cells in 1 ml 60% isopropanol for 5 minutes at room temperature. Ex: Add 6 ml isopropanol to 4 ml DI water for dilution
   b. Remove the isopropanol and cover the cells evenly with 1 mL of Oil Red O working solution to stain lipids. Incubate for about 15-20 minutes on a rocker at room temperature.

3. If you are using the triethyl phosphate solution:

   a. After removing the formalin or PBS, add 1 mL of Oil Red O solution.
   b. Incubate on a rocker for 30 minutes

4. Remove the Oil Red O solution using a micropipette and dispose of it in the waste conical tube

5. Rinse the cells with water 2-5 times (until there is no visible stain)

6. Add 1 mL hematoxylin to the cells and incubate on rocker for 1 minute to stain nuclei.

7. Remove the hematoxylin using a micropipette and dispose of it in the waste conical tube.

8. Wash the cells 2-5 times with water (until there is no visible stain)

9. Cover the cells with water or PBS++ and view under a light microscope

    a. Lipid droplets will appear red and nuclei will appear blue

10. You should expect to see a higher density of red in cells treated with eLDL

11. Dispose of the Oil Red O and hematoxylin waste in the red non-halogenated waste can.

References

1. Atchison, L., Zhang, H., Cao, K. & Truskey, G. A. A Tissue Engineered Blood Vessel Model of Hutchinson-Gilford Progeria Syndrome Using Human iPSC-derived Smooth Muscle Cells. *Sci. Rep.* 7, 1–12 (2017).

2. Marx, U. Biology-inspired microphysiological systems to advance medicines for patient benefit and animal welfare. *ALTEX* 37, 364–394 (2020).

3. WHO Media Centre. Cardiovascular Disease (CVDs). (2013).

4. Singh, U. & Jialal, I. Oxidative stress and atherosclerosis. *Pathophysiology* vol. 13 129–142 (2006).

5. Minamino, T. *et al.* Endothelial Cell Senescence in Human Atherosclerosis. *Circulation* 105, 1541–1544 (2002).

6. Salunke, N. V. & Topoleski, L. D. T. Biomechanics of atherosclerotic plaque. *Critical Reviews in Biomedical Engineering* vol. 25 243–285 (1997).

7. Berliner, J. A. *et al.* Atherosclerosis: Basic Mechanisms : Oxidation, Inflammation, and Genetics. *Circulation* 91, 2488–2496 (1995).

8. Gimbrone, M. A. & García-Cardeña, G. Endothelial Cell Dysfunction and the Pathobiology of Atherosclerosis. *Circ. Res.* 118, 620–636 (2016).

9. Navab, M., Reddy, S. T., Van Lenten, B. J. & Fogelman, A. M. HDL and cardiovascular disease: Atherogenic and atheroprotective mechanisms. *Nature Reviews Cardiology* vol. 8 222–232 (2011).

10. Rosenson, R. S. *et al.* HDL and atherosclerotic cardiovascular disease: Genetic insights into complex biology. *Nature Reviews Cardiology* vol. 15 9–19 (2018).

11. Rosenson, R. S. *et al.* Dysfunctional HDL and atherosclerotic cardiovascular disease. *Nat. Rev. Cardiol.* 1–13 (2015) doi:10.1038/nrcardio.2015.124.

12. Zhang, S. *et al.* Natural products: The role and mechanism in low-density lipoprotein oxidation and atherosclerosis. *Phytotherapy Research* (2020) doi:10.1002/ptr.7002.

13. Wang, Y. I. *et al.* Triglyceride-rich lipoprotein modulates endothelial vascular cell adhesion molecule (VCAM)-1 expression via differential regulation of endoplasmic reticulum stress. *PLoS One* 8, e78322 (2013).

14. Klouche, M. *et al.* Enzymatically modified, nonoxidized LDL induces selective adhesion and transmigration of monocytes and T-lymphocytes through human endothelial cell monolayers. *Arterioscler. Thromb. Vasc. Biol.* 19, 784–93 (1999).

15. Gaut, J. P. & Heinecke, J. W. Mechanisms for oxidizing low-density lipoprotein: Insights from patterns of oxidation products in the artery wall and from mouse models of atherosclerosis. *Trends in Cardiovascular Medicine* vol. 11 103–112 (2001).

16. Lux, C. A., Koschinski, A., Dersch, K., Husmann, M. & Bhakdi, S. Hypersusceptibility of neutrophil granulocytes towards lethal action of free fatty acids contained in enzyme-modified atherogenic low density lipoprotein. *Atherosclerosis* 207, 116–122 (2009).

17. Lilly, B. We Have Contact: Endothelial Cell-Smooth Muscle Cell Interactions. *Physiology (Bethesda).* 29, 234–241 (2014).

18. Lara-Guzmán, O. J. *et al.* Oxidized LDL triggers changes in oxidative stress and inflammatory biomarkers in human macrophages. *Redox Biol.* 15, 1–11 (2018).

19. Goldstein, J. L. & Brown, M. S. *THE LOW-DENSITY LIPOPROTEIN PATHWAY AND ITS RELATION TO ATHEROSCLEROSISl*. www.annualreviews.org (1977).

20. Chellan, B., Reardon, C. A., Getz, G. S. & Bowman, M. A. H. Enzymatically modified low-density lipoprotein promotes foam cell formation in smooth muscle cells via macropinocytosis and enhances receptor-mediated uptake of oxidized low-density lipoprotein. *Arterioscler. Thromb. Vasc. Biol.* 36, 1101–1113 (2016).

21. Aoki, T., Abe, T., Yamada, E., Matsuto, T. & Okada, M. Increased LDL susceptibility to oxidation accelerates future carotid artery atherosclerosis. *Lipids Health Dis.* 11, 4 (2012).

22. Chellan, B., Reardon, C. A., Getz, G. S. & Bowman, M. A. H. Enzymatically modified low-density lipoprotein promotes foam cell formation in smooth muscle cells via macropinocytosis and enhances receptor-mediated uptake of oxidized low-density lipoprotein. *Arterioscler. Thromb. Vasc. Biol.* 36, 1101–1113 (2016).

23. Insull, W. W. The Pathology of Atherosclerosis: Plaque Development and Plaque Responses to Medical Treatment. *Am. J. Med.* 122, S3–S14 (2009).

24. Aviram, M. & Rosenblat, M. Paraoxonases 1, 2, and 3, oxidative stress, and macrophage foam cell formation during atherosclerosis development. *Free Radic. Biol. Med.* 37, 1304–16 (2004).

25. Babaev, V. R. *et al.* Macrophage lipoprotein lipase promotes foam cell formation and atherosclerosis in vivo. *J. Clin. Invest.* 103, 1697–1705 (1999).

26. Doran, A. C., Meller, N. & McNamara, C. A. Role of smooth muscle cells in the initiation and early progression of atherosclerosis. *Arterioscler. Thromb. Vasc. Biol.* 28, 812–9 (2008).

27. Wang, J. *et al.* Vascular Smooth Muscle Cell Senescence Promotes Atherosclerosis and Features of Plaque Vulnerability. *Circulation* 132, 1909–19 (2015).

28. Libby, P. Inflammation and Atherosclerosis. *Circulation* 105, 1135–1143 (2002).

29. Topper, J. N. & Gimbrone, M. a. Blood flow and vascular gene expression: fluid shear stress as a modulator of endothelial phenotype. *Molecular medicine today* vol. 5 40–46 http://ac.els-cdn.com.proxy.lib.duke.edu/S1357431098013720/1-s2.0-S1357431098013720-main.pdf?_tid=2fef90b0-751b-11e5-8ff5-00000aacb361&acdnat=1445119713_9fb95c4ebf7efef7bd6b3c18958d4404 (1999).

30. Conway, D. E. *et al.* Flow-dependent cellular mechanotransduction in atherosclerosis. *J. Cell Sci.* 126, 5101–9 (2013).

31. Getz, G. S. & Reardon, C. A. Animal models of Atherosclerosis. *Arteriosclerosis, Thrombosis, and Vascular Biology* vol. 32 1104–1115 (2012).

32. Nagel, T., Resnick, N., Atkinson, W. J., Dewey, C. F. & Gimbrone, M. A. Shear stress selectively upregulates intercellular adhesion molecule-1 expression in cultured human vascular endothelial cells. *J. Clin. Invest.* 94, 885–91 (1994).

33. Parker, I. K. *et al.* Pro-atherogenic shear stress and HIV proteins synergistically upregulate cathepsin K in endothelial cells. *Ann Biomed Eng* 42, 1185–1194 (2014).

34. Seals, D. R., Kaplon, R. E., Gioscia-Ryan, R. a & LaRocca, T. J. You're Only as Old as Your Arteries: Translational Strategies for Preserving Vascular Endothelial Function with Aging. *Physiology (Bethesda).* 29, 250–264 (2014).

35. Zhang, H. *et al.* Role of TNF-alpha in vascular dysfunction. *Clin. Sci. (Lond).* 116, 219–30 (2009).

36. Wong, P. F. *et al.* Deregulation of hsa-miR-20b expression in TNF-α-induced premature senescence of human pulmonary microvascular endothelial cells. *Microvasc. Res.* 114, 26–33 (2017).

37. Kim, S.-R. *et al.* Visfatin enhances ICAM-1 and VCAM-1 expression through ROS-dependent NF-kappaB activation in endothelial cells. *Biochim. Biophys. Acta* 1783, 886–95 (2008).

38. Scalia, R., Appel, J. Z. & Lefer, A. M. Leukocyte-Endothelium Interaction During the Early Stages of Hypercholesterolemia in the Rabbit : Role of P-Selectin, ICAM-1, and VCAM-1. *Arterioscler. Thromb. Vasc. Biol.* 18, 1093–1100 (1998).

39. Coppé, J.-P., Desprez, P.-Y., Krtolica, A. & Campisi, J. The Senescence-Associated Secretory Phenotype: The Dark Side of Tumor Suppression. *Annu. Rev. Pathol. Mech. Dis.* 5, 99–118 (2010).

40. Pharmacology, E. *The Vascular Endothelium II*. *The American Journal of The Medical Sciences* vol. 258 (1969).

41. Park, H. S. & Kim, S. Y. Endothelial cell senescence: A systematic review and machine learning-based meta-analysis of transcriptomic studies. *Ageing Res. Rev.* 65, 101213 (2020).

42. Tian, X. L. & Li, Y. Endothelial Cell Senescence and Age-Related Vascular Diseases. *Journal of Genetics and Genomics* vol. 41 485–495 (2014).

43. Cheung, T. M. Permeability and Mechanotransduction in Aging Endothelial Cells. (2014).

44. Förstermann, U. & Münzel, T. Endothelial nitric oxide synthase in vascular disease: from marvel to menace. *Circulation* 113, 1708–14 (2006).

45. Egashira, K. *et al.* Effects of age on endothelium-dependent vasodilation of resistance coronary artery by acetylcholine in humans. *Circulation* 88, 77–81 (1993).

46. Mehrhof, F. B., Schmidt-Ullrich, R., Dietz, R. & Scheidereit, C. Regulation of vascular smooth muscle cell proliferation: Role of NF-κB revisited. *Circ. Res.* 96, 958–964 (2005).

47. Rossman, M. J. *et al.* Endothelial Cell Senescence with Aging in Healthy Humans: Prevention by Habitual Exercise and Relation to Vascular Endothelial Function. *Am. J. Physiol. - Hear. Circ. Physiol.* ajpheart.00416.2017 (2017) doi:10.1152/ajpheart.00416.2017.

48. Donato, A. J., Morgan, R. G., Walker, A. E. & Lesniewski, L. A. Cellular and

molecular biology of aging endothelial cells. *J. Mol. Cell. Cardiol.* 89, 122–135 (2015).

49. Salminen, A., Kauppinen, A. & Kaarniranta, K. Emerging role of NF-κB signaling in the induction of senescence-associated secretory phenotype (SASP). *Cell. Signal.* 24, 835–845 (2012).

50. Chien, C. *et al.* Y. Lowe, Control of the senescence-associated secretory phenotype by NF-kappaB promotes senescence and enhances chemosensitivity, Genes Dev. *SI Liochev React. Oxyg. species Free Radic. theory aging Free Radic Biol Med 60 14* 25, 2125–2136 (2013).

51. Wang, H. *et al.* hnRNP A1 antagonizes cellular senescence and senescence-associated secretory phenotype via regulation of SIRT1 mRNA stability. *Aging Cell* 15, 1063–1073 (2016).

52. Strzyz, P. The unusual SASPects. *Nat. Rev. Mol. Cell Biol.* 20, 195 (2019).

53. Deshmane, S. L., Kremlev, S., Amini, S. & Sawaya, B. E. Monocyte chemoattractant protein-1 (MCP-1): An overview. *Journal of Interferon and Cytokine Research* vol. 29 313–325 (2009).

54. Chen, J. *et al.* The Bcl-2/Bcl-X L/Bcl-w inhibitor, navitoclax, enhances the activity of chemotherapeutic agents in vitro and in vivo. *Mol. Cancer Ther.* 10, 2340–2349 (2011).

55. Ruvolo, P. P., Deng, X. & May, W. S. Phosphorylation of Bcl2 and regulation of apoptosis. *Leukemia* vol. 15 515–522 (2001).

56. Hickson, L. T. J. *et al.* Senolytics decrease senescent cells in humans: Preliminary report from a clinical trial of Dasatinib plus Quercetin in individuals with diabetic kidney disease. *EBioMedicine* 47, 446–456 (2019).

57. Fruman, D. A. *et al.* The PI3K Pathway in Human Disease. *Cell* vol. 170 605–635 (2017).

58. Holen, H. L. *et al.* Signaling through ephrin-A ligand leads to activation of Src-family kinases, Akt phosphorylation, and inhibition of antigen receptor-induced apoptosis. *J. Leukoc. Biol.* 84, 1183–1191 (2008).

59. Frémont, L. Biological effects of resveratrol. *Life Sci.* 66, 663–673 (2000).

60. Qin, B., Cao, Y., Yang, H., Xiao, B. & Lu, Z. MicroRNA-221/222 regulate ox-LDL-induced endothelial apoptosis via Ets-1/p21 inhibition. *Mol. Cell. Biochem.* 405, 115–124 (2015).

61. Barbarino, J. M., Staatz, C. E., Venkataramanan, R., Klein, T. E. & Altman, R. B. PharmGKB summary: Cyclosporine and tacrolimus pathways. *Pharmacogenet. Genomics* 23, 563–585 (2013).

62. Myrianthopoulos, V. The emerging field of senotherapeutic drugs. *Future Medicinal Chemistry* vol. 10 2369–2372 (2018).

63. Navarro-Villarán, E. *et al.* Molecular pathways leading to induction of cell death and anti-proliferative properties by tacrolimus and MTOR inhibitors in liver cancer cells. *Cell. Physiol. Biochem.* 54, 457–473 (2020).

64. Giordano, A. *et al.* Differential effect of atorvastatin and tacrolimus on proliferation of vascular smooth muscle and endothelial cells. *Am. J. Physiol. Circ. Physiol.* 302, H135–H142 (2012).

65. Kochi, S. *et al.* Induction of apoptosis in mouse brain capillary endothelial cells by cyclosporin A and tacrolimus. *Life Sci.* 66, 2255–2260 (2000).

66. Childs, B. G. *et al.* Senescent intimal foam cells are deleterious at all stages of atherosclerosis. *Science (80-.).* 354, 472–477 (2016).

67. Borghesan, M., Hoogaars, W. M. H., Varela-Eirin, M., Talma, N. & Demaria, M. A Senescence-Centric View of Aging: Implications for Longevity and Disease. *Trends Cell Biol.* 30, 777–791 (2020).

68. Kohn, J. C., Lampi, M. C. & Reinhart-King, C. A. Age-related vascular stiffening: causes and consequences. *Front. Genet.* 06, 1–17 (2015).

69. Lasheras, J. C. The Biomechanics of Arterial Aneurysms. *Annu. Rev. Fluid Mech.* 39, 293–319 (2007).

70. Wagenseil, J. E. *et al.* Effects of elastin haploinsufficiency on the mechanical behavior of mouse arteries. *Am. J. Physiol. Heart Circ. Physiol.* 289, H1209-17 (2005).

71. Lacolley, P., Regnault, V., Nicoletti, A., Li, Z. & Michel, J. B. The vascular smooth muscle cell in arterial pathology: A cell that can take on multiple roles. *Cardiovascular Research* vol. 95 194–204 (2012).

72. Lacolley, P., Regnault, V., Segers, P. & Laurent, S. Vascular Smooth Muscle Cells and Arterial Stiffening: Relevance in Development, Aging, and Disease. *Physiol. Rev.* 97, 1555–1617 (2017).

73. Sumpio, B. E., Timothy Riley, J. & Dardik, A. Cells in focus: endothelial cell. *Int. J. Biochem. Cell Biol.* 34, 1508–1512 (2002).

74. Jantzen, A. E. *et al.* Use of autologous blood-derived endothelial progenitor cells at point-of-care to protect against implant thrombosis in a large animal model. *Biomaterials* 32, 8356–63 (2011).

75. Che, J. *et al.* Endothelial FGF receptor signaling accelerates atherosclerosis. *AJP Hear. Circ. Physiol.* 300, H154–H161 (2010).

76. Tousoulis, D., Kampoli, A.-M., Tentolouris, C., Papageorgiou, N. & Stefanadis, C. The role of nitric oxide on endothelial function. *Curr. Vasc. Pharmacol.* 10, 4–18 (2012).

77. Hodgson, J. M. & Marshall, J. J. Direct vasoconstriction and endothelium-dependent vasodilation. Mechanisms of acetylcholine effects on coronary flow and arterial diameter in patients with nonstenotic coronary arteries. *Circulation* 79, 1043–1051 (1989).

78. Qi, Y.-X. *et al.* PDGF-BB and TGF-{beta}1 on cross-talk between endothelial and smooth muscle cells in vascular remodeling induced by low shear stress. *Proc. Natl. Acad. Sci. U. S. A.* 108, 1908–13 (2011).

79. Zhang, D. *et al.* Homocysteine activates vascular smooth muscle cells by DNA demethylation of platelet-derived growth factor in endothelial cells. *J. Mol. Cell. Cardiol.* 53, 487–96 (2012).

80. Lindner, V. & Reidy, M. A. Proliferation of smooth muscle cells after vascular injury is inhibited by an antibody against basic fibroblast growth factor. *Proc. Natl. Acad. Sci.* 88, 3739–3743 (1991).

81. Benetos, A., Waeber, B. & Izzo, J. Influence of age, risk factors, and cardiovascular and renal disease on arterial stiffness: clinical applications. *Am. J. Hypertens.* 15, 1101–8 (2002).

82. Schleicher, E. D., Wagner, E. & Nerlich, A. G. Increased accumulation of the glycoxidation product N(epsilon)- (carboxymethyl)lysine in human tissues in diabetes and aging. *J. Clin. Invest.* 99, 457–468 (1997).

83. Xu, B. *et al.* Impairment of vascular endothelial nitric oxide synthase activity by advanced glycation end products. *FASEB J.* 17, 1289–91 (2003).

84. De Caterina, R. *et al.* Nitric oxide decreases cytokine-induced endothelial activation. *J. Clin. Invest.* 96, 60–8 (1995).

85. Cheung, T. M. *et al.* Endothelial Cell Senescence Increases Traction Forces due to Age-Associated Changes in the Glycocalyx and SIRT1. *Cell. Mol. Bioeng.* 8, 63–75 (2015).

86. Fermini, B., Coyne, S. T. & Coyne, K. P. Clinical Trials in a Dish: A Perspective on the Coming Revolution in Drug Development. *SLAS Discov.* 23, 765–776 (2018).

87. Tagle, D. A. The NIH microphysiological systems program: developing in vitro tools for safety and efficacy in drug development. *Current Opinion in Pharmacology* vol. 48 146–154 (2019).

88. Mullard, A. *Parsing clinical success rates*. *Nature Publishing Group* (2016) doi:10.1038/nrd.2016.136.

89. Kudo, F. A. *et al.* Differential responsiveness of early- and late-passage endothelial cells to shear stress. *Am. J. Surg.* 190, 763–9 (2005).

90. Zhang, X. *et al.* Modeling early stage atherosclerosis in a primary human vascular microphysiological system. *Nat. Commun.* 11, (2020).

91. Salmon, E. E., Breithaupt, J. J. & Truskey, G. A. Application of Oxidative Stress to a Tissue-Engineered Vascular Aging Model Induces Endothelial Cell Senescence and Activation. *Cells* 9, (2020).

92. Gerhard, M., Roddy, M.-A., Creager, S. J. & Creager, M. A. Aging Progressively Impairs Endothelium-Dependent Vasodilation in Forearm Resistance Vessels of Humans. *Hypertension* 27, 849–853 (1996).

93. Alique, M. *et al.* Hypoxia-Inducible Factor-1α: The Master Regulator of Endothelial Cell Senescence in Vascular Aging. *Cells* 9, 195 (2020).

94. Fallis, A. . *Vascular Biology Protocols*. *Journal of Chemical Information and Modeling* vol. 53 (2013).

95. Salminen, A., Kauppinen, A. & Kaarniranta, K. Emerging role of NF-κB signaling in the induction of senescence-associated secretory phenotype (SASP). *Cell. Signal.*

24, 835–845 (2012).

96. Gorenne, I., Kavurma, M., Scott, S. & Bennett, M. Vascular smooth muscle cell senescence in atherosclerosis. *Cardiovascular Research* vol. 72 9–17 (2006).

97. Bennett, M. R., Sinha, S. & Owens, G. K. Vascular Smooth Muscle Cells in Atherosclerosis. *Circ. Res.* 118, 692–702 (2016).

98. Cheung, T. M., Ganatra, M. P., Fu, J. J. & Truskey, G. a. The Effect of Stress-Induced Senescence on Aging Human Cord Blood-Derived Endothelial Cells. *Cardiovasc. Eng. Technol.* 4, 220–230 (2013).

99. Halliwell, B., Clement, M. V., Ramalingam, J. & Lee Hua Long. Hydrogen peroxide. Ubiquitous in cell culture and in vivo? *IUBMB Life* 50, 251–257 (2000).

100. Yamazaki, Y. *et al.* Vascular Cell Senescence Contributes to Blood-Brain Barrier Breakdown. *Stroke* 47, 1068–77 (2016).

101. Wallace, C. S. & Truskey, G. A. Direct-contact co-culture between smooth muscle and endothelial cells inhibits TNF- ⎵ -mediated endothelial cell activation. *Am. J. Physiol. Heart Circ. Physiol.* 12, 338–346 (2010).

102. Fernandez, C., Yen, R., Reichert, W. & Truskey, G. *Human Tissue-Engineered Blood Vessels for in vitro Drug Response Testing*. (2013).

103. Fernandez, C. E. *et al.* A Human Vascular Microphysiological System for in vitro Drug Screening. *Sci. Rep.* (2016).

104. Ingram, D. A. *et al.* Identification of a novel hierarchy of endothelial progenitor cells using human peripheral and umbilical cord blood. (2004) doi:10.1182/blood-2004-04-1396.

105. Pfaffl, M. W. A new mathematical model for relative quantification in real-time RT-PCR. *Nucleic Acids Res.* 29, 45e – 45 (2001).

106. Bevilacqua, M. P. Endothelial-leukocyte adhesion molecules. *Annu. Rev. Immunol.* 11, 767–804 (1993).

107. Erl, W., Weber, C., Wardemann, C. & Weber, P. C. Adhesion properties of Mono Mac 6, a monocytic cell line with characteristics of mature human monocytes. *Atherosclerosis* 113, 99–107 (1995).

108. Ota, H. *et al.* Induction of endothelial nitric oxide synthase, SIRT1, and catalase by

statins inhibits endothelial senescence through the Akt pathway. *Arterioscler. Thromb. Vasc. Biol.* 30, 2205–11 (2010).

109. Saeed, M. *et al.* Low-dose doxycycline inhibits hydrogen peroxide-induced oxidative stress, MMP-2 up-regulation and contractile dysfunction in human saphenous vein grafts. *Drug Des. Devel. Ther.* Volume 13, 1791–1801 (2019).

110. Grenier, G. *et al.* Isolation and culture of the three vascular cell types from a small vein biopsy sample. *Vitr. Cell. Dev. Biol. - Anim.* 39, 131–139 (2003).

111. Sundaram, S. & Niklason, L. E. Smooth muscle and other cell sources for human blood vessel engineering. *Cells Tissues Organs* 195, 15–25 (2011).

112. Poh, M. *et al.* Blood vessels engineered from human cells. *Lancet* 365, 2122–2124 (2005).

113. Brown, M. A., Wallace, C. S., Angelos, M. & Truskey, G. A. Characterization of umbilical cord blood-derived late outgrowth endothelial progenitor cells exposed to laminar shear stress. *Tissue Eng. - Part A* 15, 3575–3587 (2009).

114. Moore, K. J. & Tabas, I. Review Macrophages in the Pathogenesis of Atherosclerosis. *Cell* 145, 341–355 (2011).

115. Virmani, R., Kolodgie, F. D., Burke, A. P., Farb, A. & Schwartz, S. M. Lessons From Sudden Coronary Death. *Arterioscler. Thromb. Vasc. Biol.* 20, 1262–1275 (2000).

116. Falk, E. Pathogenesis of Atherosclerosis. *Journal of the American College of Cardiology* vol. 47 (2006).

117. Parks, B. W. & Lusis, A. J. Macrophage Accumulation in Atherosclerosis. *N. Engl. J. Med.* 369, 2352–2353 (2013).

118. Hilgendorf, I. *et al.* Local proliferation dominates lesional macrophage accumulation in atherosclerosis. (2013) doi:10.1038/nm.3258.

119. Scicchitano, P. *et al.* The role of endothelial dysfunction and oxidative stress in cerebrovascular diseases. *Free Radical Research* vol. 53 579–595 (2019).

120. Victor, V. *et al.* Oxidative Stress, Endothelial Dysfunction and Atherosclerosis. *Curr. Pharm. Des.* 15, 2988–3002 (2009).

121. Chistiakov, D. A., Melnichenko, A. A., Myasoedova, V. A., Grechko, A. V. &

Orekhov, A. N. Mechanisms of foam cell formation in atherosclerosis. *Journal of Molecular Medicine* vol. 95 1153–1165 (2017).

122. Bäck, M. & Hansson, G. K. Anti-inflammatory therapies for atherosclerosis. *Nat. Publ. Gr.* 12, 199–211 (2015).

123. Skeoch, | July ; & Bruce, S. N. Atherosclerosis in rheumatoid arthritis: is it all about inflammation? *Nat. Rev. Rheumatol* 11, 390–400 (2015).

124. Carbone, F. *et al.* Atherosclerosis in Rheumatoid Arthritis: Promoters and Opponents. *Clinical Reviews in Allergy and Immunology* vol. 58 1–14 (2020).

125. Elshabrawy, H. A. *et al.* The pathogenic role of angiogenesis in rheumatoid arthritis. *Angiogenesis* vol. 18 433–448 (2015).

126. Ridker, P. M. *et al.* Antiinflammatory Therapy with Canakinumab for Atherosclerotic Disease. *N. Engl. J. Med.* 377, 1119–1131 (2017).

127. Coleman, P. R. *et al.* Stress-induced premature senescence mediated by a novel gene, SENEX, results in an anti-inflammatory phenotype in endothelial cells. *Blood* 116, 4016–4024 (2010).

128. Getz, G. S. & Reardon, C. A. Do the *Apoe* $^{-/-}$ and *Ldlr* $^{-/-}$ Mice Yield the Same Insight on Atherogenesis? *Arterioscler. Thromb. Vasc. Biol.* 36, 1734–1741 (2016).

129. Getz, G., VanderLaan, P. & Reardon, C. The Immune System and Murine Atherosclerosis. *Curr. Drug Targets* 8, 1297–1306 (2007).

130. Getz, G. S. & Reardon, C. A. Diet and murine atherosclerosis. *Arteriosclerosis, Thrombosis, and Vascular Biology* vol. 26 242–249 (2006).

131. Truskey, G. A. Human Microphysiological Systems and Organoids as in Vitro Models for Toxicological Studies. *Front. Public Heal.* 6, 185 (2018).

132. Rothbauer, M., Rosser, J. M., Zirath, H. & Ertl, P. Tomorrow today: organ-on-a-chip advances towards clinically relevant pharmaceutical and medical in vitro models. *Current Opinion in Biotechnology* vol. 55 81–86 (2019).

133. Atchison, L. *et al.* iPSC-Derived Endothelial Cells Affect Vascular Function in a Tissue-Engineered Blood Vessel Model of Hutchinson-Gilford Progeria Syndrome. *Stem Cell Reports* 14, 325–337 (2020).

134. Rubanyi, G. M. The Role of Endothelium in Cardiovascular Homeostasis and

Diseases. *J. Cardiovasc. Pharmacol.* 22, S1–S14 (1993).

135. Rumsey, S. C., Galeano, N. F., Arad, Y. & Deckelbaum, R. J. Cryopreservation with sucrose maintains normal physical and biological properties of human plasma low density lipoproteins. *J. Lipid Res.* 33, 1551–1561 (1992).

136. Chellan, B., Reardon, C. A., Getz, G. S. & Bowman, M. A. H. Enzymatically modified low-density lipoprotein promotes foam cell formation in smooth muscle cells via macropinocytosis and enhances receptor-mediated uptake of oxidized low-density lipoprotein. *Arterioscler. Thromb. Vasc. Biol.* 36, 1101–1113 (2016).

137. Prattichizzo, F. *et al.* Short-term sustained hyperglycaemia fosters an archetypal senescence-associated secretory phenotype in endothelial cells and macrophages. *Redox Biol.* 15, 170–181 (2018).

138. Long, A. N. & Dagogo-Jack, S. Comorbidities of Diabetes and Hypertension: Mechanisms and Approach to Target Organ Protection. *Journal of Clinical Hypertension* vol. 13 244–251 (2011).

139. Ridker, P. M. *et al.* Low-Dose Methotrexate for the Prevention of Atherosclerotic Events. *N. Engl. J. Med.* 380, 752–762 (2019).

140. Dolgin, E. Send in the senolytics. *Nat. Biotechnol.* 38, (2020).

141. Niedernhofer, L. J. & Robbins, P. D. Senotherapeutics for healthy ageing. *Nat. Rev. Drug Discov.* 17, 377 (2018).

142. Partridge, L., Fuentealba, M. & Kennedy, B. K. The quest to slow ageing through drug discovery. *Nat. Rev. Drug Discov.* 19, 513–532 (2020).

143. Li, J., Kim, S. G. & Blenis, J. Rapamycin: One drug, many effects. *Cell Metabolism* vol. 19 373–379 (2014).

144. Iorio, A. *et al.* Combined Treatment with Doxorubicin and Rapamycin Is Effective against In Vitro and In Vivo Models of Human Glioblastoma. *J. Clin. Med.* 8, 331 (2019).

145. Minghetti, P. *et al.* Sculptured drug-eluting stent for the on-site delivery of tacrolimus. *Eur. J. Pharm. Biopharm.* 73, 331–336 (2009).

146. Ruzicka, T., Assmann, T. & Homey, B. Tacrolimus: The drug for the turn of the millennium? *Archives of Dermatology* vol. 135 574–580 (1999).

147. Wang, Y. I., Carmona, C., Hickman, J. J. & Shuler, M. L. Multiorgan Microphysiological Systems for Drug Development: Strategies, Advances, and Challenges. *Adv. Healthc. Mater.* 7, 1701000 (2018).

148. Atchison, L., Zhang, H., Cao, K. & Truskey, G. A. A Tissue Engineered Blood Vessel Model of Hutchinson-Gilford Progeria Syndrome Using Human iPSC-derived Smooth Muscle Cells. *Sci. Rep.* 7, (2017).

149. Goy, C. *et al.* The imbalanced redox status in senescent endothelial cells is due to dysregulated Thioredoxin-1 and NADPH oxidase 4. *Exp. Gerontol.* 56, 45–52 (2014).

150. Haendeler, J. *et al.* Antioxidants inhibit nuclear export of telomerase reverse transcriptase and delay replicative senescence of endothelial cells. *Circ. Res.* 94, 768–75 (2004).

151. Martel, J. *et al.* Emerging use of senolytics and senomorphics against aging and chronic diseases. *Med. Res. Rev.* 40, 2114–2131 (2020).

Biography

Ellen Elizabeth Salmon (née Weburg) graduated cum laude with a Bachelor of Arts in Engineering Science and Bachelor of Engineering in Biomedical Engineering from Dartmouth College in 2014.

Upon acceptance to Duke University in 2014, she was awarded the Dean's Graduate Research Fellowship to begin her studies. From 2015-2017 she was supported by a National Institutes of Health T-32 training grant fellowship through the Center for Biomolecular and Tissue Engineering. In 2016 she was awarded a National Science Foundation Graduate Research Fellowship, which supported her research from 2017-2020. During her time at Duke University she was privileged to participate in two internship programs. In 2015 she served as an intern in the Education Department at the Montshire Museum of Science in Norwich, VT. In 2017 she completed an internship in the department of analytical development at KBI Biopharma. She also served as the program coordinator 9th grade curriculum developer for the S.E.N.S.O.R. Saturday Academy for 4 years.

1. E Salmon, J Breithaupt, G Truskey. "Application of Oxidative Stress to a Tissue-Engineered Vascular Aging Model Induces Endothelial Cell Senescence and Activation" *Cells*. May 2020. DOI: 10.3390/cells9051292

2. Xu Zhang, NO Abutaleb, E Salmon, G Truskey. "*In Situ* Fabrication and Perfusion of Tissue Enginered Blood Vessel Microphysiological System". Methods in Molecular Biology. September 2020

3. Xu Zhang, M Bishawi, Ge Zhang, V Prasad, E Salmon, J Breithaupt, Z Zhang, G Truskey. "Modeling Early Stage Atherosclerosis in a Primary Human Vascular Microphysiological System". Nature Communications. Issue 11. 2020.